Processing of Potato Spindle Tuber Viroids (PSTVd) RNAs in Yeast, a Nonconventional Host

---

A Dissertation

Presented to the Graduate Faculty of the University of the Sciences

in

Partial Fulfillment of the Requirements for the Degree of

DOCTOR OF PHILOSOPHY

by

Dillon R. Friday

June 23, 2017

UNIVERSITY OF THE SCIENCES

This is to certify that the Dissertation Prepared by

Dillon R. Friday

Titled

Processing of Potato Spindle Tuber Viroid (PSTVd) RNAs in Yeast, a Nonconventional Host

Complies with the Policies of the Graduate Faculty of the University of the Sciences and is approved by the Research Advisory Committee as Fulfilling the Dissertation Requirements for the Degree of

DOCTOR OF PHILOSOPHY

June 23, 2017

Dr. Michael Bruist
Research Advisory Committee
Chairman Member

Dr. John Tomsho
Research Advisory Committee
Member

Dr. Charles McEwen
Research Advisory Committee
Member

Dr. Matthew Farber
Research Advisory Committee
Member

Dr. Anil D' Mello
Reviewer

Dedication

To my unborn baby. Your family is your first true source of inspiration. I hope that your mother and I inspire you every day.

“All things are possible to him who believes”

(Mark. 9:23)

Acknowledgments

My journey began nearly 9 years ago while I was working at Campbell Soup Company. I reviewed the company's continuing education program information and decided to investigate further. I inquired about the program to my boss at the time, Dr. Bill Bangs. He was incredibly supportive and really pushed me to dive into this challenge head on. After his retirement, my new boss, Dr. Scott Keller was equally supportive (even sympathetic at times to my situation). They both allowed me to take time off to study for entrance exams, comprehensive exams, and pretty much gave me time off anytime that I needed to complete this degree. In retrospect, I couldn't have gotten a better deal than have Bill and Scott as my primary managers during this time. They are honestly the best mentors a young employee could have. I would like to thank both Bill and Scott and the Campbell Soup Company for their support and financial backing.

I would like to thank the University of the Sciences and more specifically the Department of Chemistry and Biochemistry for taking on a part-time PhD student. The University really does go out of their way to accommodate nonconventional students like myself. The graduate courses are all in the evening which really gives flexibility to a student trying to advance their education while working full time. Both Dr. McKee and Dr. Voki have been incredibly supportive to part time PhD students. I would like to thank my advisors: Dr. Baumstark and Dr. Bruist. While I was rotating, there were not too many PI's interested in taking a night and weekend student. Dr. Baumstark had both interesting research and was a night owl, so he had no problem taking me as a graduate student in 2010. Dr. Baumstark eventually left the University to follow additional career interests and Dr. Bruist was seemingly "voluntold" (can't confirm that…) to take on three new PhD students. He graciously took us in and became a very active advisor in all of our research. Not only that, he always made time on nights and weekends for me, and even read and

revised this dissertation while in a hospital bed. I will never forget his dedication and commitment to my journey. Both Dr. Bruist and Dr. Baumstark aided in my growth as a scientist and as a person. I am indebted to them for taking a chance on a part time PhD student that didn't know much/ any molecular biology when they started.

I would like to thank my advisory committee both past and present. Since it took me nearly forever to complete this degree, I have had several committee members retire. Those being Mr. Robert Smith and Dr. Julian Snow. I would like to thank them for their support early in my journey. I would like to especially thank my current committee. Dr. Charles McEwen has been with me since the beginning and Dr. Tomsho soon thereafter. Most recently, Dr. Matt Farber joined following Mr. Smith's retirement last year. This committee has pushed me, encouraged me, and guided me throughout my tenure. Lastly, I would like to thank Dr. Anil D' Mello for being my dissertation reviewer. He graciously accepted this responsibility and has been nothing but a pleasure to work with.

Previously, I spoke of three PhD students that Dr. Bruist took on. Those three were myself, Jess Zinksie, and Renee Salvo. I can honestly say that I would not have been able to complete this degree without both Jess and Renee. They were so amazingly helpful and often went out of their way to support me. Whether it be showing me a new method, checking my cells while I was at work, or coming in on a weekend to work with me. Not only that, they were so much fun and we got through this journey through hard work, and by having fun. I couldn't have asked for better lab mates.

I would like to thank my family. My parents, Wayne and Pat always pushed the importance of education. Not only that, they were truly a source of inspiration. My mom raised 9 children and my dad worked like a mad man to support us. Their dedication to our family really

pushed me to dedicate my time to something bigger than myself just as they did. Additionally, I would like to thank my brothers and sisters. They were just as supportive and instrumental to my journey. We are a very close-knit bunch and their encouragement and brutal honesty has helped me.

I would like to thank my wife, Courtneay. We just started dating when I decided to go back to school. I told her that this was going to be a tough path for us due to most of my nights and weekends being consumed. She didn't waiver and couldn't have been my biggest advocate. She sacrificed right alongside with me throughout this journey. She was patient, sympathetic, encouraging, and inspiring while I was taking on this challenge. I love her very much for who she is and for the mother that she is to become.

Biographical Sketch

Dillon Robert Friday grew up in Linwood, PA alongside his parents, Patricia and Wayne Friday as well as his 6 sisters: Danielle, Shannon, Kellie, Noelle, Dana, Devonne and his two brothers: Ryan and Shawn. Living quarters were tight, so Dillon preferred to be outside playing any sport: baseball, football, basketball, golf, and fishing. He and his Dad enjoy golf, he and his brothers enjoy fishing. Dillon, his sisters, and his Mom are huge movie fans, so they spend time reciting movie quotes and being "chuckle heads".

Dillon's parents stressed the value of education and really pushed Dillon to excel in his coursework. Dillon first grew fond of science in 1991 when he read a book containing all the amazing Voyager Images of our Solar System. From that year on, he was hooked on science. He eventually took honors biology and honors chemistry in his first two years in high school. Oddly enough, both his biology teacher; Mr. Donnelly and his chemistry teacher; Mr. Peterman were Usciences grads. They made science fun, but challenging and that is what made Dillon decide to purse a degree in biology.

Dillon eventually went on to pursue a BS in Biology at Gettysburg College in 2005. Following graduation and in large debt, Dillon decided to take a job as a contract technician at Campbell Soup Company. He didn't know a thing about food or food science, but he really needed the money and was up for a new challenge. After a year as a temp, Dillon was offered a full-time position as an Associate Technologist. He eventually considered Campbell's tuition reimbursement policy and decided to pursue his PhD in Biochemistry at Usciences. At about the same time of deciding to pursue a PhD, he made time to date another Associate Technologist at Campbell named Courtneay Cipolone. They would eventually wed in 2015. They reside in Old

City Philadelphia and enjoy everything the city has to offer. She would keep him “on track” with his studies and make sure that Dillon wasn’t having too much fun living in the city. Dillon and Courtneay both advanced their careers at Campbell Soup Company and are currently Sr. Technologists within R&D. They are expecting their first child in September 2017. Apart from science, Dillon has aspirations of learning Spanish and learning how to play the piano. His desire to learn new things and challenge himself will never diminish.

TABLE OF CONTENTS

List of Abbreviations

ASBVd- *Avocado sunblotch viroid*

BMV- *Brome mosaic virus*

BS- bundle sheath

BSPh- bundle sheath phloem

CCR- central conserved region

cDNA- complementary DNA

CEVd- *Citrus exocortis viroid*

circRNA- circular RNA

CSVd- *Chrysanthemum stunt viroid*

CVd-III- *Citrus viroid III*

DCL- dicer like

dim- dimer

dsRNA- double-stranded RNA

eEF1A- protein elongation factor 1 alpha

ELVd- *Eggplant latent viroid*

EM- extended middle

EPPO- European and Mediterranean Plant Protection Agency

HH- hammerhead ribozyme

HP- hairpin ribozyme

HPI- hairpin I

HPII- hairpin II

IVT- *in vitro* transcription

mon- monomer

ncRNA- non-coding RNA

NEP- nuclear encoded protein

nt- nucleotide

PAGE- Polyacrylamide gel electrophoresis

PEG- polyethylene glycol

Ph- phloem

PL- plasmodesmata

PLMVd- *Peach latent mosaic viroid*

Pol II- DNA- dependent RNA polymerase II

PSTVd- *Potato spindle tuber viroid*

RACE- rapid amplification of cDNA ends

rDrP- RNA-directed polymerase

RNA- ribonucleic acid

rRNA- ribosomal RNA

RT-PCR- reverse transcription polymerase chain reaction

snRNA- small nuclear RNA

ssRNA- single-stranded RNA

TBV- *Tomato bush stunt virus*

TGGE- temperature gradient gel electrophoresis

TL- tetra loop

triH- trihelix

tRNA- transfer RNA

ts- temperature sensitive

vd-sRNA- viroid small RNA

vsRNA- viroid specific small RNA

YE- yeast whole cell extract

ZF- zinc finger

List of Tables

List of Figures

Abstract

The discovery of viroids in 1971 opened the door to a whole new field of RNA biochemistry. Viroids subsequently became the first of many facets of RNA biochemistry: the first single stranded covalently closed RNA discovered in nature, the first subviral pathogen discovered, and the first pathogen of a eukaryotic system to have its genome sequenced. Viroids are the smallest known agents of infectious disease and they represent the borders of life. They replicate autonomously within their host and since they do not code for their own proteins, they act as scavengers of the host transcriptional machinery. By doing so, viroids find ways of trafficking, localizing, and replicating within their host based on the sequence and structure of the RNA alone. Once in their hosts, viroids are incredibly resilient and can cause economic damage on several commercial crops. Apart from controlling viroids for economic reasons, the more enticing feature of viroid study is the use of viroids as model systems to study essential underlying questions about the evolution of RNA pathogens, and to use viroids as models to study non-coding RNAs. The field of non-coding RNA research has surged within the past decade and viroids are becoming important vehicles to bring insight into this field of study. The study of viroids has been extensive through the years, but several questions remain: What structural conformations do viroids employ to recruit host enzymes, and what are the enzymes that cleave and ligate viroids into mature progeny. To answer some of these questions, we have looked at processing of the potato spindle tuber viroid (PSTVd) RNA in the budding yeast *Saccharomyces cerevisiae*. We found that one specific construct will process into a mature viroid circle in yeast and we also found that processing in this system is distinct from other plant and non-plant based host systems. This processing is a delicate interplay of ligation and degradation by host machinery. Yeast is a great system to study viroid processing as yeast allows for use of

the entire toolbox of temperature-sensitive and knockout protein mutants. By employing yeast, focus can be driven towards the mechanisms of host protein recruitment, viroid processing requirements, and degradation mechanisms from the host. We have ascertained insight into PSTVd processing using yeast. We have found methods to transform and process PSTVd, investigated enzymes that effect processing, and started to establish an *in vitro* yeast system. Through these studies, we have also developed a method to enrich viroid RNAs from total RNA extractives. This has been vital to assays specific around viroid transcription and cleavage. Overall, this research is further testament that viroids are minimalist scavengers of a very diverse array of cellular transcriptional machinery. They can process in higher eukaryotes (plants) and simple eukaryotes (yeast). They are shown to affect each host in distinct manners using fundamental RNA biology that all organisms share.

Preface

The discovery of viroids was a landmark event in RNA biochemistry and molecular biology. Viroids have provided insight into single-stranded RNA structure, RNA folding, and pathogenic RNA interactions within hosts. **Chapter 1** covers the history of viroid discovery, economic effects of viroids, viroid-host interactions, and viroid links to non-coding RNA research.

The goal of this research is to use yeast as a model system to study *potato spindle tuber viroid* (PSTVd) processing. Yeast is an enticing model system due to the toolbox of strains available for use. In **Chapter 2**, PSTVd expression systems were set up to express four different PSTVd conformations to monitor processing. We show that one conformation processes into a

mature viroid circle in yeast. The processing is distinct from that of other model systems, and host degradation machinery was shown to affect the production of circular progeny.

To utilize additional biochemical techniques to study transcriptions and cleavage of viroids in yeast, **Chapter 3** goes into methods of viroid enrichment from total RNA from yeast. Due to the high level of degradation of viroid RNA in yeast, enrichment of the viroid transcripts and processing intermediates is key to primer extension assays that provide additional processing details.

To garner additional processing data, an *in vitro* processing system could allow for the study structural and RNA- host protein interactions that would be difficult to study *in vivo*. **Chapter 4** covers the set-up of an i*n vitro* yeast whole cell extract assay to investigate PSTVd transcript processing.

Lastly, **Chapter 5** covers the cloning strategy of new PSTVd expression constructs for use in additional yeast knockout and temperature-sensitive mutant strains. This would unlock the entire library of yeast mutants to study PSTVd processing in greater detail.

Chapter 1: Introduction

Discovery of PSTVd and PSTVd Molecular Characteristics

The first description of a viroid infection was reported in the Irish Cobbler Potato plant in 1921. This disease was originally thought to be a virus that infects the tubers of potatoes and causes stunted plants with elongated tubers (1-3). Nearly 50 years later, Theodor Diener found that the causal nature of this agent was not that of a virus, but of a new class of subviral pathogen. Due to its small size and the fact that it's a non-encapsidated "naked" RNA, this pathogen did not fit under the definition of a virus, and hence the term "viroid" was created (4-6). The first viroid to be discovered was named Potato Spindle Tuber Viroid (PSTVd). Apart from being subviral and a "naked" RNA, it was found that viroids including PSTVd, do not have any translation products and, thus, do not behave like mRNAs (7, 8). In addition, viroids were the first covalently closed circular single-stranded RNAs ever detected in nature (9). The structure and sequence of PSTVd was soon determined, and this also became the first pathogen of a eukaryotic system to have its secondary structure and sequence determined (10). To this end, PSTVd was found to be a circular, non-coding, single stranded RNA of 359nt in length and, thus, the smallest known agent of infectious disease at this time.

Viroid taxonomy, host range, and symptoms

Since the discovery of PSTVd, approximately 32 viroid species have identified. Viroids are categorized within two families: *Pospiviroidae and Avsunviroidae* (Table1.1) (11, 12). The accession number for viroid species is available on GenBank.

Table 1.1: Viroid Species, abbreviations, sequence variants, genus and family (11)

Viroid species	Abbreviation	Accession	Size (nt)	Genus	Family
Potato spindle tuber	PSTVd	V01465	359	Pospiviroid	Pospiviroidae
Tomato chlorotic dwarf	TCDVd	AF162131	360	Pospiviroid	Pospiviroidae
Mexican papita	MPVd	L78454	360	Pospiviroid	Pospiviroidae
Tomato planta macho	TPMVd	K00817	360	Pospiviroid	Pospiviroidae
Citrus exocortis	CEVd	M34917	371	Pospiviroid	Pospiviroidae
Chrysanthemum stunt	CSVd	V01107	356	Pospiviroid	Pospiviroidae
Tomato apical stunt	TASVd	K00818	360	Pospiviroid	Pospiviroidae
Iresine 1	IrVd-1	X95734	370	Pospiviroid	Pospiviroidae
Columnea latent	CLVd	X15663	370	Pospiviroid	Pospiviroidae
Hop stunt	HSVd	X00009	297	Hostuviroid	Pospiviroidae
Coconut cadang-cadang	CCCVd	J02049	246	Cocadviroid	Pospiviroidae
Coconut tinangaja	CTiVd	M20731	254	Cocadviroid	Pospiviroidae
Hop latent	HLVd	X07397	256	Cocadviroid	Pospiviroidae
Citrus IV	CVd-IV	X14638	284	Cocadviroid	Pospiviroidae
Apple scar skin	ASSVd	M36646	329	Apscaviroid	Pospiviroidae
Citrus III	CVd-III	AF184147	294	Apscaviroid	Pospiviroidae
Apple dimple fruit	ADFVd	X99487	306	Apscaviroid	Pospiviroidae
Grapevine yellow speckle 1	GVYSd-1	X06904	367	Apscaviroid	Pospiviroidae
Grapevine yellow speckle 2	GVYSd-2	J04348	363	Apscaviroid	Pospiviroidae
Citrus bent leaf	CBLVd	M74065	318	Apscaviroid	Pospiviroidae
Pear blister canker	PBCVd	D12823	315	Apscaviroid	Pospiviroidae
Australian grapevine	AGVd	X17101	369	Apscaviroid	Pospiviroidae
Coleus blumei 1	CbVd-1	X52960	248	Coleviroid	Pospiviroidae
Coleus blumei 2	CbVd-2	X95365	301	Coleviroid	Pospiviroidae
Coleus blumei 3	CbVd-3	X95364	361	Coleviroid	Pospiviroidae
Avocado sunblotch	ASBVd	J02020	247	Avsunviroid	Avsunviroidae
Peach latent mosaic	PLMVd	M83545	337	Pelamoviroid	Avsunviroidae
Chrysanthemum chlorotic mottle	CChMVd	Y14700	399	Pelamoviroid	Avsunviroidae
Eggplant latent*	ELVd	AJ536613	333	Elaviroid	Avsunviroidae

Hosts for viroids include monocots and dicots. Vegetable crops, ornamentals, and woody perennials all are hosts to various species of viroid (3). Viroids can infect several economically

important plants including: potato, tomato, cucumber, hop, coconut, grapevine, avocado, peach, apple, pear, citrus, plum and chrysanthemum(11). Viroids can be transmitted mechanically through contact with contaminated farming tools, human hands and contact between plants. *Pospiviroidae* can be transmitted through infected seed, pollen, and insects. Symptoms of viroid infections vary according viroid type and species of plant infected. The symptoms can range from mild to severe and can include: stunting, epinasty, vein discoloration, leaf distortion, necrotic spots, tuber malformation, and in the most severe cases, plant death (3, 13-15). Infections by several viroids can result in little or no symptoms. In general, symptom expression is favored by high light intensity and higher temperatures (11). Chloroplastic abnormalities were also seen with some viroid infections. These chloroplastic symptoms included aberration of the thylakoid membrane and chloroplast discoloration (3, 11, 16, 17).

Economic implications of viroid damage and disease control

Viroid outbreaks can inflict serious economic damage if not treated in a timely manner. Coconut viroids are of concern since infected trees fail to produce nuts for many years before death. Since the discovery of coconut cadang viroid, approximately $4x10^7$ plants were destroyed. This accounts for roughly $20-50 million annually in losses. For potatoes, approximately 1% of crop losses are due to PSTVd infections. From 1988-1990, approximately 197,850 tons of potato losses were caused by PSTVd (18). Chrysanthemum stunt viroid (CSVd) accounted for $3 million in losses in Australia in 1987 (18). In Europe, its estimated that PSTVd causes over €10 million in damages to tomato and potato crops (19). PSTVd and Chrysanthemum stunt viroid (CSVd) are on the European and Mediterranean Plant Protection Organization (EPPO) quarantine pest list (20). This requires that seed stock be thoroughly tested for the presence of these pathogens (15).

Controlling viroid disease can be challenging due to the resiliency of viroids. PSTVd can survive in freeze-dried tomatoes for several years and can remain in potatoes for over 20 years. In addition, it has been shown that PSTVd can flourish symptomless in plants at subzero temperatures (21). The most effective measures of viroid control are prevention of infected plant material in the field or greenhouse, strict hygiene, and monitoring of crop symptoms (3).

To prevent and control viroid spread, detection of infected material is paramount. The earliest method of viroid detection was by poly acrylamide gel electrophoresis (PAGE) (22). From using PAGE, the electrophoretic migration of small RNA circles is distinct from that of linear RNA. The circular RNA can be extracted from the gel and subject to highly sensitive identification methods using reverse transcription PCR (RT-PCR) followed by sequencing. However, the PAGE method followed by extraction was time consuming. The first large scale screening programs were developed by Owens and Diener using recombinant DNA technology followed by dot blot hybridization (23). Since then, rapid and sensitive detection methods have been employed to essentially eradicate PSTVd in the US and Canada (3, 24-27).

To prevent viroid transmittance in the field, agricultural tools can be treated with various chemicals: sodium hypochlorite, hydrogen peroxide, sodium hydroxide, and formaldehyde (3, 28, 29). A combination of thermotherapy with meristem-tip culture resulted in efficient viroid elimination from infected plants (30, 31). Cryotherapy of shoot tips is also proving to be successful for eradication of pathogens from potato, sweet potato, grapevine, banana, raspberry and prunes (3, 32). Grafting has also proven to be an effective measure for eradication of pathogen from host plant. This technique has been applied for the elimination of *Citrus cachexia viroid* and *Citrus exocortis viroid* (3). Despite the best efforts of eradicating viroids, the problem persists in China where roughly 6.5% of the potatoes tested in 2015 were infected with PSTVd

(33). This indicates that designing more effective measures and rigor will need to be employed to eradicate PSTVd in China.

Viroid-host Interactions

Avsunviroidae Family

The 30 known viroid species are contained within two families: *Pospiviroidae* and *Avsunviroidae*. There are many similarities between viroids of both families. For instance, both families are subviral, circular, single-stranded RNA replicons that infect several species of plants. They are under 600nt in length, lack a protein coat, and do not code for proteins (34). There are also stark differences between the two families of viroids. A majority of viroids reside within the *Pospiviroidae* family, however; 4 viroids have distinct molecular characteristics and replication paths and these comprise the *Avsunviroidae* family (12). This section will go into detail on the molecular characteristics, replication and pathogen-host interactions of viroids within the *Avsunviroidae* family.

The type species for viroids of the Avsunviroidae family is the Avocado sunblotch viroid (ASBVd). This viroid was discovered in 1979 inducing sunblotch symptoms within avocados. It was found that this viroid was smaller than other viroids that were characterized at the time (35). ASBVd was sequenced and the secondary structure was determined. The results were somewhat confounding as this viroid only was only 247nt in length compared to PSTVd (359nt), and it only shared 18% sequence homology to PSTVd (36). The lack of sequence homology indicated that ASBVd was distinct of the PSTVd type viroid. The secondary structures of Avsunviroidae viroids are branched unlike the typical "rod-like" conformation of *Pospiviroids* (Figure 1.1) (37,

38). All members of the Avsunviroidae have been structurally mapped by *in vitro* and *in vivo* studies (39-42).

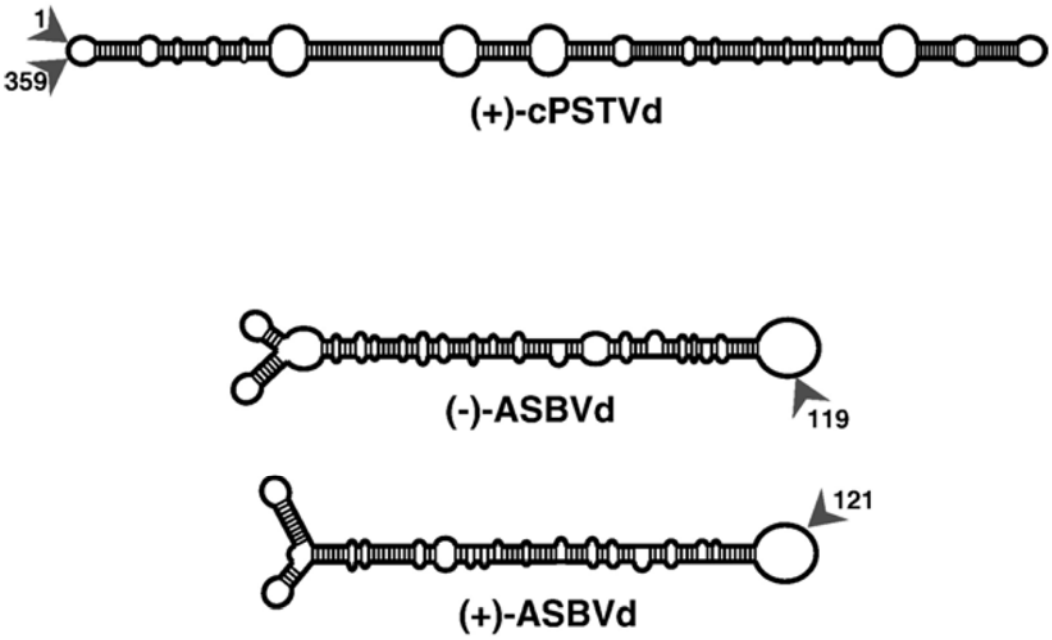

Figure 1.1: A. PSTVd secondary structure compared to B. ASBVd secondary structure (38)

One of the first unique features of ASVBd replication was that oligomeric forms of both (+) and (-) strand polarities were seen in roughly equal quantities during infection (43). A continuation of this work concluded that ASBVd replicates via a symmetric rolling circle

mechanism (44-46). The rolling circle replication cycles of *Avsunviroidae* (symmetric) and *Pospiviroidae* (asymmetric) are shown in Figure1.2 (46).

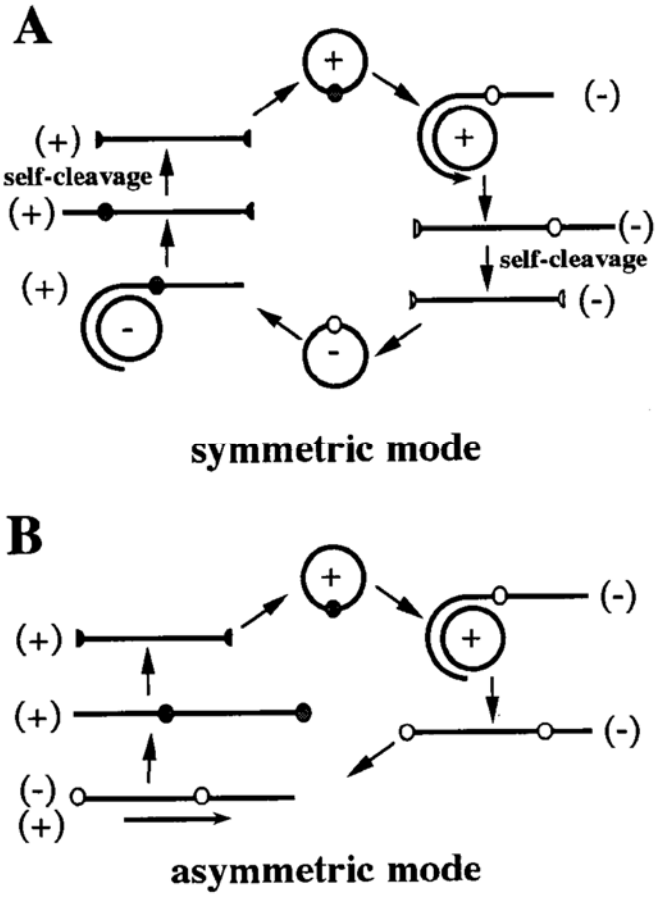

Figure 1.2: A. Symmetric rolling circle replication B. Asymmetric rolling circle replication (46)

A key feature of the symmetric rolling circle replication is that both (+) and (-) strand circles are formed within the cell. This replication cycle is carried out within the chloroplast of the cell and the nuclear encoded polymerase (NEP) is the polymerase responsible for making both (+) and (-)

strands (41, 47). Perhaps one of the most important discoveries in viroid research has been the cleavage mechanism of oligomeric strands of both the (+) and (-) strands. Hutchins *et al*. (48) showed that the cleavage is accomplished through a self-catalytic ribozyme. This ribozyme was 55 nt in length and was called the "hammerhead" (HH) ribozyme (49, 50). At the time of its discovery, this was the third self-catalytic RNA discovered. The ribozyme findings opened a whole discussion around RNA being the molecule to spark life (51). It was hypothesized that viroids and other circular RNAs were relics of pre cellular evolution (52).

Following cleavage unit length monomers, the viroid monomers rearrange themselves to form a highly base paired internal loop within the ribozyme that directs ligation (53, 54). After cleavage to (+) and (-) strands, it was shown that these strands fold differently from one another before ligation (55, 56).The RNA is then ligated by chloroplastic tRNA ligase (57). Apart from the tRNA ligase, the protein elongation factor 1-alpha (eEF1A) was shown to bind to Peach Latent Mosaic Viroid (PLMVd) (58). Movement and intercellular trafficking of viroids of *Avsunviroidae* is still being investigated. The proposed cellular trafficking for ASBVd and PSTVd is shown in Figure 1.3 (59). It was shown that the *Eggplant Latent Viroid* (ELVd, family Avsunviroidae) transports from the cytoplasm to the nucleus, then to the chloroplast for ligation(60). The reason for nuclear transport is unclear at this time.

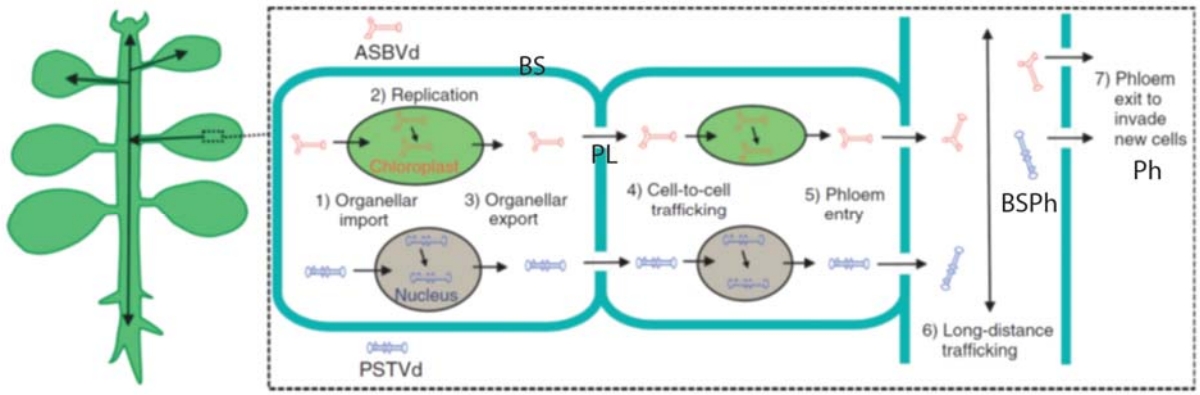

Figure 1.3: Systemic Infection, intracellular and cell to cell trafficking of ASBVd and PSTVd (59)

The movement of ASVd and PSTVd from either chloroplast or nucleus through the plasmodesmada (PL) and eventually through bundle sheath (BS). Following exit of the BS, the viroids travel through the bundle sheath phloem (BSPh) and the phloem (Ph).

Pospiviroidae

The type species for the *Pospiviroidae* family and the main target of our research is PSTVd. Unlike ASBVd, PSTVd adopts an unbranched rod like structure consisting of 5 domains: terminal left, pathogenicity modulating, central conserved region (CCR), variable, and terminal right (Figure1.4) (10, 61, 62). *Pospiviroidae* contain a region of high sequence homology the within the CCR. The *Avsunviroidae* family does not contain a CCR region within their sequence and thus does not share a region of high homology amongst its members. In the final stages of its replication, PSTVd forms a stable rod conformation, however; PSTVd can also adopt a variety of metastable structures that have been shown to be important within PSTVd replication (63, 64). From a molecular standpoint, a couple features of PSTVd are noteworthy. One of the most significant structures is the loop E motif within the CCR (65, 66). The loop E

motif is a sarcin ricin domain found in many different life forms (66, 67). The CCR was shown to be able to fold into a hairpin I domain (HPI) under various conditions (68). Within the variable region of PSTVd a hairpin II structure (HPII) can also form (69). The secondary structure of PSTVd and its structural transitions have been highly studied through the years using various biophysical and biochemical analysis (2, 41, 70, 71).

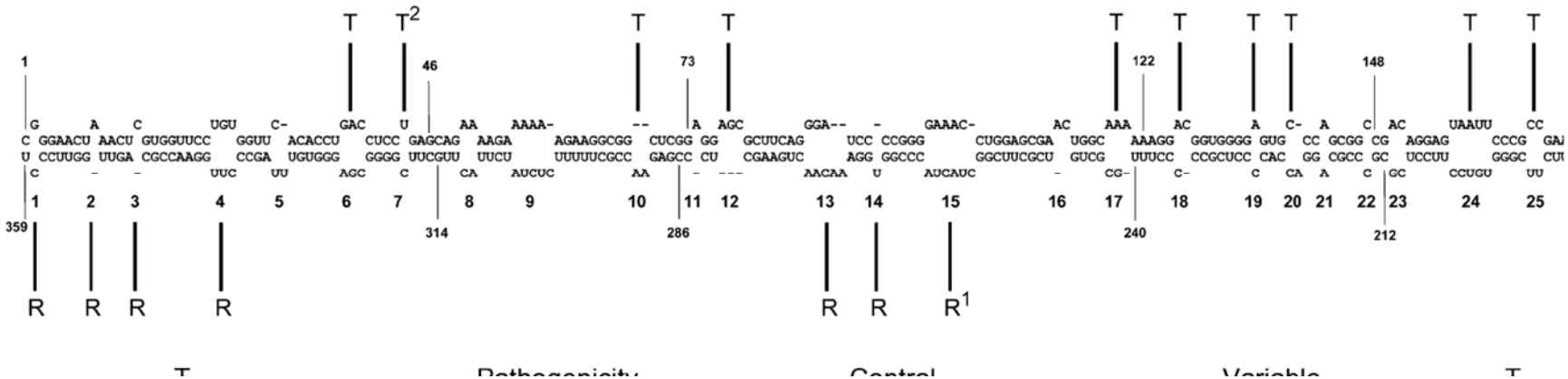

Figure 1.4: Secondary Structure, domains, and regions necessary for trafficking (T) and replication (R) of PSTVd (62)

The replication cycle (Figure 1.2) of PSTVd follows an asymmetric rolling circle path in the nucleus of infected cells (72). Both the replication cycle and replication site are different from ASBVd. Branch and Robertson (73) discovered that PSTVd follows the asymmetric rolling circle by northern blot analysis of replicative intermediates. They found that circles are only formed from (+) strand multimers. The synthesis of (+) and (-) strands is produced by DNA-dependent RNA polymerase II (Pol II) (74, 75). The Pol II finding is interesting in that a RNA-directed polymerase (rDrP) is not the RNA pathogen transcribing polymerase as seen in most plants (76). PSTVd redirects the Pol II into transcribing its RNA. Due to its small size, PSTVd does not require the whole series of host factors associated with typical Pol II transcription. However, the conversion of Pol II to transcribe RNA is associated with the canonical 9-zinc finger (ZF) transcription factor IIIA (TFIIIA-9ZF). Wang *et al*. (77) showed that suppression of this protein reduced PSTVd production. Furthermore, they showed direct evidence of Pol II interacting with (+) and (-) strands. Pol II interacts with both strands, however the formation and accumulation of the (+) strand is significantly higher than that of the (-) strand in PSTVd infected cells (78).

PSTVd does not contain a ribozyme sequence and cleavage of multimers to unit length monomers is accomplished by a host nuclease (79). For processing, PSTVd undergoes structural rearrangements to recruit host enzymes. The study of these structural rearrangements and recruitment of host enzymes and mechanism of infection has been investigated broadly since the discovery of PSTVd. To begin the study of this mechanism, the first infectious viroid cDNA was formed using a dimeric construct (80). Studies indicated that the CCR was important for PSTVd infectivity and replication. The research showed that short terminal duplications (8-11nt) of the CCR were highly infectious (81-85). Since the CCR can fold into a HPI motif upon exiting Pol

II, Diener (86) postulated that HPI domains can align oligomers into a thermodynamically stable and highly base paired structure containing three stacked helices termed the "trihelix". Due to its high level of base pairing and thermodynamic stability, the trihelix was the top candidate to act as the recognition site for the host nuclease. Apart from the trihelix, a CCR containing duplications can fold into multiple metastable structures. An *in vitro* study showed that RNase T1 could cleave and ligate a CCR with duplication, but the exact substrate was still not known (87).

To elucidate the exact structural requirements needed for viroid processing, a PSTVd transcript containing a 17nt duplication of the CCR was studied in potato nuclear extracts (88). This transcript could adopt four possible secondary structures and the structure formation was controlled by temperature, ionic strength and structure-directing complimentary RNA oligonucleotides. Only one of these structures could form wild-type PSTVd circles. Interestingly, one of the structures that this transcript could fold into was the trihelix, and this was not the structure that ligated into a circle. From this study, the only structure to ligate properly was the "extended middle" structure. Using UV crosslinking, chemical mapping, temperature gradient gel electrophoresis (TGGE) and thermodynamic calculations, it was concluded that the CCR of the "extended middle" folds into a GNRA tetraloop (TL) (63, 89). The trihelix and TL structures are shown in Figure 1.5. After cleavage, the TL switches to the extended rod that contains the loop E motif that stabilizes the structure to dictate ligation.

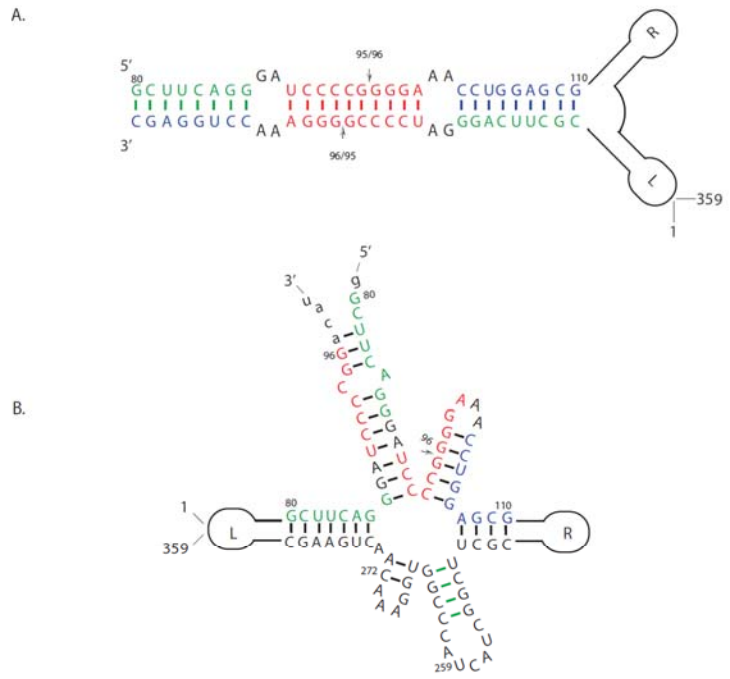

Figure 1.5: A. Trihelix structure (triH) containing two copies of the CCR and B. Tetraloop (TL) structure containing 17nt duplication (80-96)

The nucleotides of the upper CCR are given explicitly. Green (nucleotides 80-87), red nucleotides 90-99) and blue (nucleotides 102-110). L (terminal left) and R (terminal right) represent the remaining viroid structure. The arrowheads mark cleavage sites.

A later study conducted by Gas *et al*. (64) suggested that cleavage is not controlled by the TL, rather that cleavage was directed by the triH. The system that they used to show cleavage and ligation was an *in vivo* transgenic *Arabidopsis thaliana* model. They proposed that two HPI

motifs interact by kissing loops in sequential arrangement on a dimeric RNA, or on different monomers, to initiate the formation of the trihelix. Specifically, they introduced mutations on a dimeric *Citrus exocortis viroid* (CEVd) that were expected to abolish the formation of a GNRA tetraloop. These mutations had no adverse effect on cleavage. They also observe that not all members of the *Pospiviroidae* family can form GNRA tetraloops within the CCR. All of these factors led them to conclude that the trihelix is in fact the structural intermediate necessary for cleavage and ligation in all members of the *Pospiviroidae* family (90).

The structural debate was further convoluted by experiments performed on members of the *Pospiviroidae* family whose CCR may adopt an alternative form of the tetraloop. Biophysical and chemical mapping of the citrus viroid III (CVd-III) indicated that the CCR of this viroid rearranges differently than PSTVd to allow for cleavage and ligation (91). Lastly, work using PSTVd infected *Nicotiana benthamiana* showed that mutations that disrupt HPI, the sequence that forms the trihelix, have a strong effect on viroid trafficking, but little effect on replication. They concluded that both HPI and HPII are not essential for PSTVd replication (Figure 1.4) (62).

Identifying the necessary host processing enzymes has been a growing area of study for viroid research. Knowing the processing enzymes can give insight into the structural intermediates by knowing the preferred substrates of these enzymes. In the past decade, significant advancements have been made in the identification of the polymerases, nucleases and ligases involved with viroid processing. One of the first processing enzyme discoveries was that of Pol II being the protein to transcribe (+) and (-) strands. This was already covered within this introduction and extensively reviewed in Flores *et al*. (92). An RNaseIII was initially identified as the nuclease involved in processing. This proposed enzyme postulated by a series of mutational studies conducted in transgenic *Arabidopsis* (64). From this study, the researchers

concluded that 3' protruding nucleotides in each strand showed the signature cleavage of an RNaseIII. This work was followed up by another study investigating the ends left after cleavage and before ligation. Gas *et al*. (93) showed that a dimeric CEVd transcript leaves a 5' phosphoester and a 3' hydroxyl in *Arabidopsis*. This provided additional evidence of an RNase III /Dicer-like enzyme being involved in cleavage. To study Dicer involvement in PSTVd processing, Dicer knockdown plants of *Nicotiana benthamiana* were created and infected with PSTVd. The researchers were able to show that Dicer-Like 4 was involved in PSTVd processing (94, 95). For the ligation step, surprisingly, a DNA ligase and not an RNA ligase was shown to circularize PSTVd linear monomers. Nohales *et al*. (96) were able to show that a DNA ligase I cloned from Arabidopsis was able to ligate a PSTVd transcript when containing a 5' phosphoester and 3'OH. The site of ligation was also very specific, as the ligase only circularized between G95 and 96. A review of all of the known viroid-protein interactions are summarized in Katsarou *et al*. (97).

PSTVd Trafficking

For a systemic infection, viroid RNAs must transport individually from infected cells to neighboring cells, and eventually distant organs. Cell to cell trafficking of PSTVd occurs through the plasmodesmata (98) and long distance trafficking occurs through the phloem (99). The overall movement of the viroid RNA is mediated by RNA motifs within the viroid sequence. The phloem was shown to have a mechanism to recognize and traffic PSTVd. Phloem entry and exit appear to be regulated differently according to PSTVd variant (100, 101). A bipartite RNA motif is required to move PSTVd from bundle sheath to the mesophyll and this requirement only applies to young leaves (101). A genomic map of PSTVd sequences and regions of importance for trafficking and replication have been identified (Figure 1.3 and Figure1.4) (62). Certain loops

within the extended rod of PSTVd are critical to systemic trafficking. A mutational study showed that Loop 19 mediates traffic from palisade mesophyll to spongy mesophyll in *Nicotiana benthamiana*. The A135 and C227 within this loop were the bases critical to the movement of PSTVd (102).

RNA Silencing and Viroid Pathogenesis

Post-transcripitonal gene silencing (RNA silencing) is a multilayer defenese mechansim of plants which normally protects the plants from invasion by pathogenic RNA replicons (103). However, since viroid RNA is not translated, this defense has no value against viroids. Rather the viroids co-opt this stystem against plantsin order to produce their pathogenicity. Double-stranded RNA (dsRNA) and single-stranded RNA (ssRNA) with self-complementary regions trigger silencing in plants. These RNAs are recognized and processed by class III RNases termed Dicer-Like (DCL) (92, 104). The DCL cleaveage produces silencing RNAs (siRNA) of 20-25 nt in length (105). One strand of the DCL generated RNAs are incorporated into the RNA-induced silencing complex (RISC) in the cytoplasm to cause RNA degradation, translation arrest, or DNA methylation through transciptional gene silencing (101, 106). Pathenogenic DCL-produced 21-22 nt RNAs derived from the viroid that accumlate in plants are called vd-sRNAs. Wassenegger *et al*. (107) reported that PSTVd vd-sRNAs direct methylation of cDNA sequences found within the tobacco genome (92). This was one of the first reported cases of PSTVd being involved in RNA silencing.

Plants use RNA silencing as as a defensee against viroid infection, however; viroids also use this RNA silencing machinery for replication. With PLMVd, it was shown that a vd-sRNA can base-pair to an mRNA enoding the chloroplasitc heat-shock protein 90. The binding results

in cleavage of the mRNA. The degradation of this RNA may favor viroid accumulation. preventing the proper folding of many critical proteins (108). Adkar-Purushothama *et al*. (109) discovered that a region of PSTVd processed by host DCLs generate a vd-sRNA that modulates host gene expression to benefit the viroid. The vd-sRNA produced mimics a miRNA that targets host callose sythesis mRNA. This results in a lowering of the mRNA and thus a reduction in callose production. Callose synthesis at the plasmodesmata is a host defense known to restrict virus trafficking (92, 110); the viroid has used mRNA silencing to counter this defense. In addition, and as previously discussed, data shows that Dicer-Like 4 is is the cleavage nuclease repsonsible for viroid processing (94). Lastly, Minoia *et al*. (111) were able to show that additional degradation pathways exist with a viroid infection and that degradation may procede during replication. The decay pathways could be part of an overall mRNA degradation pathway.

Saccharomyces cerevisiae and Other Nonconventional Hosts Used as Model Systems to Study Viroids

Yeast is a highly studied, highly characterized and convenient molecular biology tool for *in vivo* and *in vitro* studies (112). Yeast was the first eukaryotic organism to have its genome completely sequenced and the yeast genome consists of only ~6000 genes. Over 5780 of these genes have been functionally characterized (113, 114). Due to extensive study following the sequencing of its genome, knockout strains for every nonessential gene in yeast have been created (115, 116). As for the essential genes, knockdown or temperature sensitive mutant collections have also been created (117). Thus, there are tools in yeast to examine all of the genes within its genome and this over 18 million gene-gene combinations (118) among these.

The study of plant viruses and viroids in their native host plants can be challenging. Plants have relatively large genomes (~20-30,000 genes) and most genes have not been thoroughly studied. In addition, because of the high level of redundancy gene function in plants, deconvoluting virus-host interactions can prove time consuming and tedious (119). The Ahlquist lab pioneered the use of yeast as a model system to study RNA plant pathogens. They were able to express the brome mosaic virus (BMV) in the yeast strain YPH500 (120, 121) and get reproduction of a (+)-strand RNA virus. Following the ability to process a plant virus in yeast, Ahlquist *et al*. took full advantage of the yeast collections to start identifying the proteins and host factors that were essential for (+)-strand virus processing in yeast (122-124).

The Nagy lab has also explored what yeast can offer scientists studying the replication of other (+)- strand viruses, particularly tomato bushy stunt virus (TBV) They were able to screen entire temperature sensitive (ts) libraries of yeast to identify host factors needed for virus replication (124) that included enzymes for nucleotide metabolism, phospholipid and sterol synthesis, as well as protein chaperones, translation factors, cyclophilins, and RNA helicases each of which has a relevant mammalian homolog (125, 126). Another screen revealed a set of host factors needed for recombination among viral genomes (125). Apart from plant viruses, animal viruses have also been shown to process in yeast. Host factors for replication of the influenza virus have been identified using yeast as a model system (127). Following this trend, viroids have also been shown to process in yeast. ASBVd was shown to process in yeast and the researchers were able to investigate some viroid degradation pathways using yeast mutants (128).

One of the first nonconventional hosts used for *Pospiviroid* studies *in vivo* studies was transgenic *Arabidopsis thaliana* (129). Daros *et al*. (64) were able to transform *Arabidopsis* with

a dimeric transcript and conduct a multitude of mutational studies to investigate processing intermediates. Using the same model system, Daros *et al*. (93) conducted 5' and 3' RACE (rapid amplification of cDNA ends) to map viroid termini. Using *Nicotiana benthamiana*, Daros *et al*. (57) were able to show that a tRNA ligase is responsible for ligation of viroids of the *Avsunviroidae* family. Quickly following that research, the Daros lab was able to use a DNA Ligase I knockdown gene in *Nicotiana benthamiana* to indicate that DNA ligase I was the enzyme responsible for circularizing PSTVd (96). The cleavage enzyme (DCL4) of PSTVd was also identified in *Nicotiana benthamiana* knockdown plants (95). Lastly, eggplant has been used to study viroid turnover and decay. Interestingly, the study showed that eggplant tends to decay PSTVd to a higher extent compared to that of nicotiana or tomato (111).

With the sequencing of their genomes, some of the plant systems are catching up to yeast with respect to knockout or knockdown strains, but plants are still hugely limiting due to the availability and growth of plant knockout/knockdown strains. As discussed, entire libraries of ts mutants have been employed to study host factors for various plant viruses. A similar approach can be used for viroid study. To date, some of the proteins identified as being critical to viroid processing have homologs in yeast Table1.2. Not only is there a homolog, but also most of the homologous proteins have been well-studied RNA metabolism enzymes.

Table 1.2: Plant proteins and Their Yeast Homologs

Plant Protein	**Yeast Homolog (reference of study)**
tRNA Ligase	TRL/RLG (130-132)
DNA Ligase I	CDC9 (133, 134)
DCL-4	RNT1-RNaseIII (135, 136)

Viroids and the RNA World

The "RNA world" is a hypothesis stating that RNA was the primordial molecule that started life on this planet. This hypothesis was initially postulated in the 1960's and the proposal is somewhat implicit to the name of the hypothesis: If RNA had some functionality as a protein (RNA polymerase and nuclease capability), RNA could be the molecule that started start life (137). The discovery of ribozymes in the early 1980's seemed to further strengthen the notion of a protein-less biological world (137, 138). Following this discovery, the term "RNA World" was first coined by Gilbert (51). Once ribozymes were discovered within ASBVd (48), suddenly, viroids became relevant members of the RNA World.

Following this, Diener suggested that viroids were more likely candidates than introns as being living fossils of the RNA world (52). Viroids have several characteristics that indicate that they are from an old origin. These characteristics of viroids being: small genomes, circular structure negating the need of genomic tags to complete replication, structural periodicities facilitating modular assembly, no protein coding capacity, and the presence of ribozymes (52, 139). To summarize, it is generally accepted that the simplest is the oldest, and viroids have simple small genomes. Viroids are G+C rich and more thermodynamically stable compared to A+U. Circularity allows for replication without genomic tags or initiation start sites. Since viroids do not code for proteins, they came before ribosomes. Most importantly, viroids of the Avsunviroidae family contain ribozymes to complete their replication (139).

From a phylogenic standpoint, plastids derive from primitive cyanobacteria, which emerged before eukaryotic cells. These cyanobacteria could have hosted Avsunviroidae before plants emerged (139, 140). Recently, it was reported that ASVBd can process and maintain their

presence in cyanobacteria (141). Viroids are simple, small, adaptive, circular, RNAs that contain self-catalytic regions, and mutate at high rates (Figure 1.6).

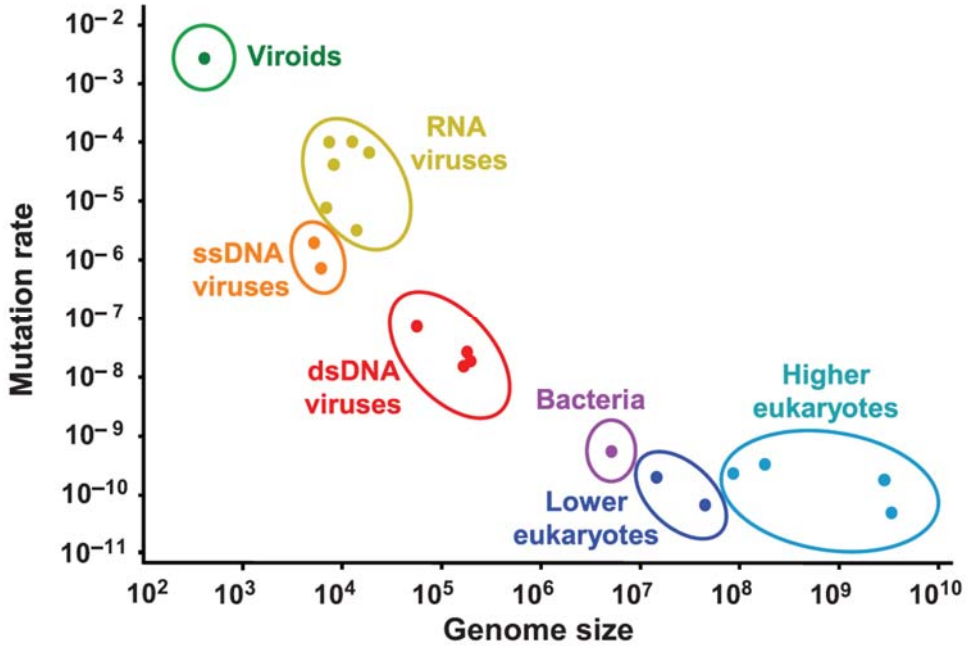

Figure 1.6: Mutation Rate vs. Genome Size of Viroids to Higher Eukaryotes (142)

The study of Non-coding RNA and Its Link to Viroid Studies

Less than 2% of the human genome is known to code for proteins. Until recently, the other 98% of genome not coding for protein was considered by many to be "junk" (143). With the advent of deep RNA sequencing techniques and high throughput screening methods, tens of thousands of RNAs were recognized to originate from these non-coding region (144). Of the non-coding RNA found in the human genome, roughly 1% is circular (circRNA) (145). A well-studied circular RNA important for human disease studies is the hepatitis delta virus (HDV).

This virus encodes for single protein and is a subviral satellite of hepatitis B virus (146). HDV also replicates via a rolling circle and recruits host DNA-dependent RNA polymerase to initiate replication similarly to how viroids transcribe within their host.

Viroids constitute a class of long non-coding RNA (lncRNA). In animals, lncRNA have been studied extensively due to their link to disease development through regulation of gene transcription (147). Regulation of gene transcription is also seen in viroids as part of the RNA silencing recruitment with viroid infection. Intriguingly, viroid replication suggests an amplification path for lncRNAs.

With advanced RNA-seq combined with computational approaches (148) larger numbers of circRNAs are being discovered. The functionalities of these circRNA are still being elucidated. Cellular stress (149), cancer (150), Crohns disease (151), and Alzheimers disease (152). have all been linked to circRNA and lncRNA. Because of the importance of circRNA in human disease, model systems such as viroids are needed to drive research into structure-host mechanisms. Viroids are the best studied circRNAs ever discovered, and the nuances of viroid replication can bring insight into what these circular RNAs are doing in our bodies for cellular regulation and disease control. Viroids use deception to entice host RNA Pol II and DNA Ligase I into bringing about pathogenic replication. The mechanism of how viroids trick host machinery is not well understood, but deriving insights into the mechanism would be of great value for studying all circRNAs. There is a vast amount of circRNA in our own cells, however little is known about how this RNA functions. Are these RNAs malevolent like viroids, or cellular protectors, or both? As non-coding RNA research advances, the answers to these questions will likely be uncovered.

Goals of Research

The main goal of this thesis work was to use yeast as a model system to study PSTVd processing. From doing so, we wish to study the structural requirements for cleavage and ligation of PSTVd, but also derive insight into processing proteins responsible for cleavage, ligation and degradation in of PSTVd in yeast. To accomplish this goal, the project consisted of three aims:

1. Establish a PSTVd yeast expression system to study structural intermediates for PSTVd processing *in vivo.*
2. Establish an *in vitro* processing system to study cleavage and ligation in a whole cell yeast extract system.
3. Using the toolbox of yeast molecular biology, to investigate the processing proteins of PSTVd using knockout and ts mutants.

Chapter 2: Processing of Potato Spindle Tuber Viroid (PSTVd) RNAs in Yeast, a Nonconventional Host

Abstract

Potato spindle tuber viroid (PSTVd) is a circular, single-stranded, noncoding RNA plant pathogen that is a useful model for the processing of noncoding RNA in eukaryotes. Infective PSTVd circles are replicated via an asymmetric rolling circle mechanism to form linear multimeric RNAs. An endonuclease cleaves these into monomers; a ligase seals these into mature circles. All eukaryotes may have such enzymes for processing noncoding RNA. As a test, we investigated the processing of four PSTVd RNA constructs in the yeast *Saccharomyces cerevisiae.* Of these, only one form, the construct that adopts a previously described tetraloop-containing conformation (TL), produces circles. TL has 16 nucleotides of the 3' end duplicated at the 5' end and a 3' end produced by self-cleavage of a delta ribozyme. The other three constructs, an exact monomer flanked by ribozymes, a trihelix-forming RNA with requisite 5' and 3' duplications, and a tandem dimer, do not produce circles. The TL circles contain non-native nucleotides resulting from the 3'-end created by the ribozyme and the 5'-end from an endolytic cleavage by yeast at a site distinct from where potato enzymes cut these RNAs. RNAs from all four transcripts are cleaved in places not on path for circle formation, and are likely RNA decay. We propose that these constructs fold into distinct RNA structures that interact differently with host cell RNA metabolism enzymes, resulting in varying susceptibility to degradation versus processing. We conclude that PSTVd RNA is opportunistic and may use different processing pathways in different hosts.

Introduction

Viroids are subviral, circular, single-stranded RNA replicons that infect many different species of plants. They are small in size (240-600 nt), lack a protein coat, are highly structured and there is no evidence of any viroid translation product (5, 153-155). Due to this lack in a translation product, viroid replication and pathogenesis depends on the RNA itself, host factors, and host enzymatic machinery (156). Additionally, viroids have high rates of *in vivo* mutation compared to other nucleic acid based pathogens (157, 158). These attributes make viroids enticing models to study RNA structure-function relationships.

The 34 known viroid species are categorized in two families: *Pospiviroidae* and *Avsunviroidae*. Members of the *Avsunviroidae* family exist as (-) and (+) strand RNAs in infected tissue. They replicate via symmetric rolling circles in chloroplasts using the nuclear encoded polymerase (NEP) (159, 160). Production of monomeric linear RNAs relies on self-cleavage by hammerhead ribozymes encoded in the (+) and (-) viroid RNAs. A host ligase is presumed to circularize the viroids (161-164).

The replication of viroids within the *Pospiviroidae* family differs from viroids of the *Avsunviroidae* family in several main aspects: 1. their plus-strand dominates the cells; 2. they are replicated through an asymmetric rolling circle mechanism in the nucleus, using host RNA Polymerase II (Pol II); and 3. they do not contain a ribozyme sequence for self-cleavage (1, 75, 78, 165, 166) and therefore rely on a host nuclease. Specifically, plus-circular RNAs enter the nucleus and are transcribed by Pol II into linear minus-strand multimeric RNA, serving as templates for Pol II to create the plus-strand multimeric linear RNAs. The plus-strand multimers are then cleaved and ligated into plus-viroid circles (79, 167, 168).

Potato spindle tuber viroid (PSTVd), the representative viroid of the *Pospiviroidae* family, adopts an unbranched, highly base paired rod-like conformation (169) that has five domains: terminal left, pathogenicity modulating, central conserved region (CCR), variable, and terminal right (170). The CCR is a region of high homology among member of the *Pospiviroidae* family, and it was found that linear RNA transcripts with short terminal duplications (8-11 nucleotides) in this region were highly infectious (81-85, 171). Thermal denaturation studies indicated that the native secondary structure of PSTVd is disrupted upon exiting Pol II and the CCR folds into a stable hairpin called HP1, this hairpin may be involved in the processing of oligomeric plus-PSTVd to mature circles (172). Diener (86) proposed that two HP1 motifs can align oligomers into a position for cleavage/ligation by forming a thermodynamically stable, highly base paired structure termed the "trihelix" (Figure 1C, green, red, and blue) (173-175) . In addition, it was shown that PSTVd RNAs that contain CCR duplications can fold into a number of metastable conformations (88, 176).

Multiple structural studies soon followed to elucidate the exact structural elements required for viroid processing. Using transcript processing in potato nuclear extracts, a PSTVd RNA containing a 17 nt duplication of the CCR was found that converts into wild-type circles. Processing required that this transcript adopt one specific fold of the four possible secondary structures. Access to each secondary structure was controlled by temperature, ionic strength, and structure-directing complementary RNA oligonucleotides. Interestingly, one structure had the trihelix, which encompasses the proposed cleavage site (Figure 1 C), but it did not process into a mature viroid circle (88). The only structure to get cleaved and ligated was the "extended middle" structure. Additional work using UV crosslinking, chemical mapping, temperature gradient gel electrophoresis (TGGE), and thermodynamic calculations showed that the CCR of the "extended

middle" structure folds into a GNRA tetraloop (Figure 1B). After cleavage, the tetraloop region switches into the extended rod conformation containing a loop E motif that dictates ligation (63, 89).

Contrary to the tetraloop model, an *in vivo* study by Gas *et al.* in transgenic *Arabidopsis thaliana* suggested that cleavage is controlled by the trihelix structure (64). They proposed that kissing loop interactions by HP1 structures in sequential arrangement on a dimeric RNA or on different monomers initiate the formation of the trihelix. Specifically, they introduced mutations in citrus exocortis viroid (*Pospiviroidae* family) that are expected to abolish the formation of the GNRA tetraloop. These mutations had no adverse effect on cleavage. They also observe that not all members of the *Pospiviroidae* family are capable of forming GNRA tetraloop motifs within the CCR. All these factors led them to conclude that the trihelix is the substrate for cleavage *in vivo* in all members of the *Pospiviroidae* family (168). Both the trihelix and tetraloop model postulate that formation of a loop E motif promotes ligation in *Pospiviroids*.

The structural debate is further complicated by results from additional experiments on members of the *Pospiviroidae* family whose CCR may adopt an alternate form of the tetraloop. Thus, multiple options exist by which the CCR rearranges to allow cleavage and ligation(91). Lastly, work using PSTVd infected *Nicotiana benthamiana* showed that mutations that disrupt HP1, the sequence that forms the trihelix, have a strong effect on viroid trafficking, but little effect on replication (62, 177).

To further understand the structural requirements for PSTVd processing, we used the nonconventional-host *Saccharomyces cerevisiae* as a model system that has become a convenient molecular biological tool (112, 178) to study RNA processing and replication *in vivo*. Specifically, yeast contains the cellular machinery to replicate several plus-strand RNA viruses(179, 180), and

recently was shown to support replication of avocado sunblotch viroid (ASVd, *Avsunviroidae* family) (128). Here we report that PSTVd RNAs under the control of a galactose regulated expression vector can effectively be processed. This system allows us to investigate the structural requirements for viroid cleavage and ligation in yeast. In addition to a dimeric PSTVd RNA analog to the CEVd dimer used by Gas *et al*., we created DNA constructs that produce three RNA transcripts of exact or slightly larger than monomeric length designed to preferably adopt 1) an exact monomer with an unbranched rod-like structure, 2) the extended CCR that forms a tetraloop-containing conformation (TL), and 3) a complete duplication of the UCCR that folds into the trihelix (triH). When these were tested for processing *in vivo*, the only construct that cleaved and ligated into mature circular progeny was the TL-forming construct. Consistent with thermodynamic data, these subtle changes in the extent of duplication have a strong effect on the processing of these RNA. In this yeast system, only the tetraloop-containing construct is processed to circles; the other constructs fold into structures that are not efficiently recognized by the processing enzymes and instead are targeted for degradation. The evidence of PSTVd processing in a non-plant system is further testament to viroids utilizing fundamental RNA biology that all organisms share.

Materials and Methods

Yeast strains, cell growth and transformation. The yeast strain YPH500 (*MAT*α *URA*3-*52 LYS2*-801 *ADE2-101 TRP1*-Δ*63 HIS3*-Δ *LEU2*-Δ*1*) was used throughout the study. Yeast cultures were grown at 30˚C in synthetic media containing either 2% glucose or 2% galactose for suppression or stimulation of the promoter. Tryptophan was not added to the media for plasmid

maintenance. Transformations were carried out using the Frozen-EZ yeast transformation II kit from Zymo Research (T2001). A *RAT1* mutant strain was also used in this study. The plasmid for creation of the *RAT1-107* allele (A661E) was a gift from Dr. Eric Phizicky (181). The *RAT1-107* gene along with a *URA3* fragment of plasmid pIC115 was digested with AatII and BamHI, run on an agarose gel and excised. The excised fragment was transformed into YPH500. Colonies that grew on uracil drop out medium were screened for *RAT1-107* by PCR and confirmed by sequencing (Supplemental Table 1 and Appendix)

Oligonucleotides and plasmids for yeast *in vivo* expression and *in vitro* transcripts.

Oligonucleotides were obtained from Invitrogen and are listed in Supplemental Table 1. Each yeast construct has a plasmid used to make a PCR template for *in vitro* transcripts (IVTs) and a plasmid for expression of the PSTVd RNA in yeast. Plasmids are listed in Supplemental Table 2. Plasmid TBO110 contains the TL PSTVd construct and has been described previously (88). Plasmids pTBO112 and p15-14 were made in the same manner except that they contain the triH and dimer PSTVd sequences shown in Figure 1C. IVT PSTVd RNAs and probes for northern blots were made by PCR amplifying templates using primers and plasmids indicated in Supplemental Table 3. The template for RNA TBO_triH was cut with EcoRI prior to T7 transcription.

The PSTVd yeast expression constructs were all cloned into the yeast /*E. coli* shuttle plasmid pB3RQ39 (*TRP1*, *CEN4*, *GAL1* promoter), which expresses Brome mosaic virus (BMV) RNA (182). The BMV sequence was excised using restriction enzymes SnaB1 and PshA1 and replaced with PSTVd sequences such each sequence is under control of the *GAL1* promoter and followed by the hepatitis delta ribozyme. This allows galactose to induce the RNA; ribozyme cleavage creates a precise 3' end after the PSTVd sequence (180). Insertion of the tetraloop

sequence from pTB110 (36), the trihelix sequence from pTB112, and the tandem dimer sequence from p15-14 gave pTBO_TL, pTBO_triH, and pTBO_DIM respectively. For the monomer, the exact 95/96 opened monomer flanked by the 5' hammerhead ribozyme and a 3' hairpin ribozyme was subcloned from pCR2.1-TOPO.4 (167) into pB3RQ39 so as to replace both BMV and delta ribozyme.

RNA extraction

Yeast containing the appropriate plasmid was grown in the selective media to an OD of 0.6-1.0. Total RNA was extracted from 10 OD /mL of cells using the hot phenol extraction method (183)

Reverse transcription PCR for detection of plus-PSTVd and PSTVd circles.

One microgram aliquots of total RNAs were treated with DNase I (Invitrogen). The RNA was then phenol chloroform extracted and ethanol precipitated. 3 ng of DNase-treated total RNA was subject to reverse transcription (Invitrogen superscript III) using 20 pmol of the primer 259R in 10 µl (Table 1). One tenth of this product was used for PCR amplification. The amplifications were carried out in 12.5 µl of 2x Go Taq (Promega) with 25 pmol of the following primers: 259R/112F for plus-PSTVd and 259R/2F for circles. The following program was run on an Eppendorf thermocycler: 5 mins at 95˚C, 30 cycles of 30s at 95˚C, 40 s at 64˚C, 60s at 72˚C followed by 5 mins at 72˚C and a 4˚C hold. Amplification products were separated on a 5% polyacrylamide(PAA)-8M urea gel and visualized by silver staining (184).

Gel purification of linear and circular PSTVd.

A total of 5 µg RNA was run on a 5% denaturing PAA along with RNA from infected tomato to provide migration markers for linear and circular plus-PSTVd RNA. RNAs corresponding to linear and circular molecules were cut out from the gel, the RNAs were eluted by soaking the excised band in gel elution buffer (500 mM Tris-HCl, pH 7.0, 0.1 mM EDTA, 1 mM $MgCl_2$, 0.1% SDS). The samples were then frozen, thawed and incubated with shaking overnight at 4C. The supernatant was then removed and another aliquot of gel elution buffer was added and allowed to shake for 2 hours. The combined supernatants were phenol-chloroform extracted and then precipitated by ethanol. The gel extracted RNAs were then subject to RT-PCR for detection of plus-PSTVd and PSTVd circles. After 5% PAA gel detection and confirmation, the RT-PCR products were cleaned using the Promega PCR clean up kit. The resulting DNA was sent to the Yale Sequencing Center for final sequencing. The primers used for sequencing of the ligation junction were 2F and 259R (Supplemental Table 1).

RNA detection by northern blotting.

Total RNAs (5 µg) were separated on a 5% PAA-8M urea gel and were semi-dry electroblotted to a Hybond N+ membrane (GE Healthcare). The membranes were incubated in UltraHyb solution (Ambion) overnight at 65°C with the appropriate riboprobe and washed with 2x SSC (1x SSC is 0.15M NaCl + 0.015M sodium citrate) and 0.1% SDS. Four 65°C washes were performed (2x 10 minutes and 2x20 minutes). The membranes were imaged using phosphorimager screens measured with a Storm 840 Phosphorimager (GE Healthcare). IVT PSTVd controls and riboprobes for detection of PSTVd, actin, and SCR1 (185) were generated as described in Supplemental Table 3. Radioactive labeling used [α-^{32} P] UTP or [α-^{32} P] CTP (PerkinElmer).

Manganese chloride treatment of total yeast RNA to enrich small RNAs.

For enrichment of viroid linear intermediates, total RNAs from yeast were treated with $MnCl_2$ according to Semancik and Szychowski (186). RNA solutions (100ng/µl) were treated with 50mM $MnCl_2$ in 0.1XTE. After incubation at 4°C, the solution was centrifuged at 15K rcf for 5 minutes. The supernatant containing the small RNA fraction was then ethanol precipitated.

Primer extension.

Oligonucleotide M1BR (Supplemental Table 1) binds PSTVd (+) strand positions 150-133. The primer was 5'-end-labeled with [γ-^{32}P] ATP using T4 polynucleotide kinase (Invitrogen). Approximately 10^6 cpm of this primer was annealed to 25 µg of total RNA from yeast, 12.5 µg of manganese treated RNA from yeast, and to 0.5pmol of viroid *in vitro* transcript. The extension was conducted using 100 units of reverse transcriptase (Superscript III) kit, Invitrogen). After extension for 90 minutes at 52°C, the reaction was stopped and the products were ethanol precipitated. A DNA sequencing ladder was generated using primer M1BR and PCR fragment encompassing the PSTVd sequence from the plasmid harboring the trihelix sequence. The ladder was formed using Sequitherm cycle sequencing kit (Epicentre Technologies). The products from the primer extension and the ladder were separated on 8% (19:1) PAA, 8M urea sequencing gels.

Results

Proper cleavage of a longer-than-unit length viroid RNA in plants depends upon the length and border sequence of the duplications around the monomer(63, 64, 88, 89). Furthermore, efficient ligation requires compatibility of the ends generated by the RNA endonuclease and the

ligase that joins them (111, 187) and a structural context that puts the ends in close proximity and paired with complementary RNA.

We created four PSTVd RNA constructs representing the major conformations recognized in previous studies: 1) an exact monomer (mon), which should ligate to form the mature rod-like RNA (Figure 1A); 2) a monomer with duplications (tetraloop TL) containing a 3' 17 nt duplication in the upper central conserved region (UCCR), which should fold into the metastable tetraloop (Figure 1B); 3) a trihelix (triH) with the full 30-nucleotide UCCR duplication (i.e. the TL 5' end and 13 more nucleotides added to the 3' end), which is the sequence required for adopting the complete trihelix structure (Figure 1C); and 4) a full PSTVd dimer (Figure1C), corresponding to the CEVd construct utilized in the experiments by Gas *et al*. (64). This dimer has the potential to form the trihelix, among other stable and metastable conformations.

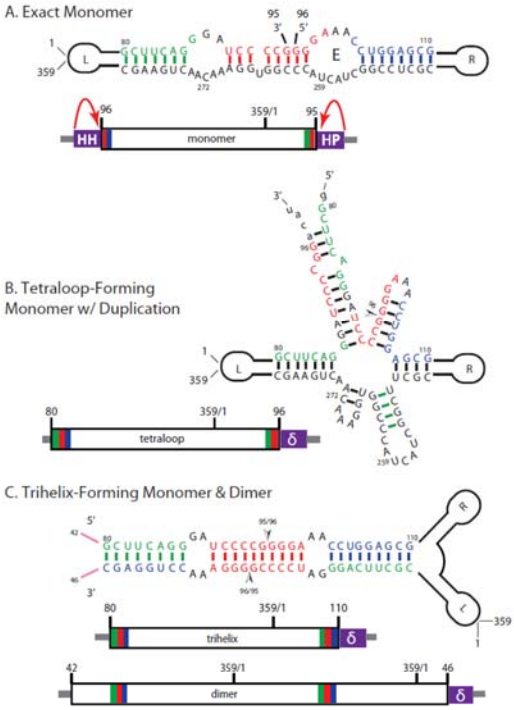
A. Exact Monomer
monomer
HH
HP
B. Tetraloop-Forming
Monomer w/ Duplication
tetraloop
C. Trihelix-Forming Monomer & Dimer
trihelix
dimer

Figure 2.1: *In vivo* constructs and corresponding structural motifs used to express PSTVd in yeast.

In vivo constructs and corresponding structural motifs used to express PSTVd in yeast. The left and right arms of PSTVd are indicated schematically, while the nucleotides of the CCR upper and lower strands are given explicitly. Nucleotides shown in green (80-87, red (90-99), and blue (102-110) comprise the upper CCR (UCCR), which is duplicated to different extents in each construct. The lower CCR (LCCR) nucleotides are shown in black. (A) Monomer construct. The construct is flanked by a 5' hammerhead (HH) and a 3' hairpin (HP) ribozymes, which cleave at the curved arrows. Upon ligation, the construct should fold into the wild-type extended rod containing a loop E motif. (B) The GNRA tetraloop (TL) construct. 3'-Duplication of the UCCR nucleotides 80-96 (green) allows formation of a metastable structure in which nucleotides 93-106 form a stem capped by the tetraloop; this stem contains the 95/96 processing cleavage site (arrowhead). This construct contains a 3' delta ribozyme (δ). (C) The trihelix-forming monomeric (triH) and dimer constructs. The triH RNA has the same 5'-end as the TL; its 3' end duplicates nucleotides 80-110 (green, red, blue). The two complete copies of the UCCR hybridize to form the trihelix (top), which has two potential 95/96 cleavage sites (arrowheads). The dimer construct (bottom) contains two complete copies of the viroid arranged as a monomer flanked by duplications on each side, i.e. nucleotides 42-79 on the 5' end and nucleotides 1111 (through 359/1) to 46 on the 3' end. The duplications enable the complete trihelical element to form in the trihelix; the pink lines on the trihelix structure indicate the flanking duplications.

Construction of PSTVd-Yeast Expression Systems

These PSTVd sequences were cloned into a yeast expression vector under the control the *GAL1* promoter and transformed into yeast strain YPH500 for growth and expression under galactose induction. All four RNAs will be transcribed by RNA pol II and are expected to be 5' capped. The plasmid for transcription of the PSTVd monomer has a DNA cassette containing the 359 viroid nucleotides flanked by sequences for the hammerhead and hairpin ribozymes at the5' and 3' ends respectively. The resulting PSTVd monomer starts at base 96 and continues via bases 359/1 to base 95, the same as the RNA that is ligated into a circle in plants (Fig. 1A). The three other constructs (dimer, TL, and triH) contain a single ribozyme, delta ribozyme 3' to the viroid sequences. These three constructs have duplications at the 5'-(pre nt 96) and 3'-ends (post nt 95)

as described above and in Figure 1. All ribozymes self-cleave to generate 5'-hydroxyl (monomer only) and 2'-3'-cyclic phosphate termini.

Reverse Transcription PCR indicates expression and PSTVd processing

RT-PCR was employed to confirm the expression of plus-strand viroid-specific RNA in total RNA preparations from these cells and to detect the possible presence of PSTVd circles that would result from processing linear precursors. This RT-PCR scheme is shown in Figure 2. The inward primer set, 112F and 259R (see Figure 1 for numbering), should always yield a PCR product of 148bp as long as there is plus-sense PSTVd RNA present with an intact right half. RNAs transcribed from all four constructs will be templates for synthesis of this fragment. The outward primer set, 2F and 259R, will only yield an amplification product when ligation unites the two halves of the UCCR or when they are already sequential in a dimer or higher multimer. Thus, only circular RNA products and the dimer RNA will give rise to a 240 bp DNA fragment with the outward primers.

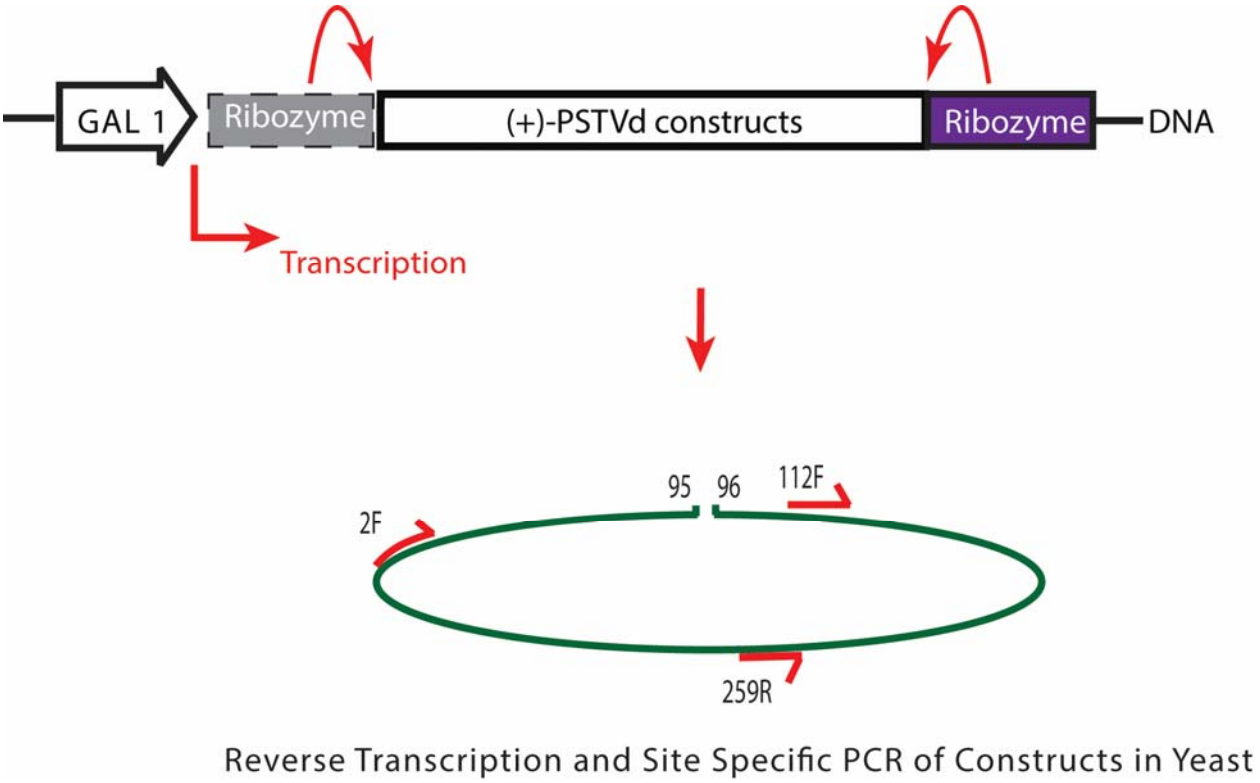

Figure 2.2: Transcription of constructs in yeast and corresponding ligation-monitoring RT-PCR scheme.

Transcription of constructs in yeast and corresponding ligation-monitoring RT-PCR scheme. Once transformed into yeast, galactose induces the transcription of the PSTVd RNA. Upon induction and transcription, the RNA will fold into the structures seen in Figure 1 for processing and ligation within the UCCR; the example shown here is the exact monomer transcript open at the 95/96 site. For analysis, the RNA is extracted, reverse transcribed and then PCR amplified using primers 112F and 259R (inward) to screen for all (+) PSTVd or primers 2F and 259R (outward) across the UCCR region specifically for processed circles. The grey dashed box represents the hammerhead ribozyme, which undergoes self-cleavage in the monomer construct. All constructs contain a 3' ribozyme; only the exact monomer construct contains the 5' ribozyme;

Figure 3 provides the results for the RT-PCR detection of plus-PSTVd expression in yeast. YPH500 containing the TL (+), triH (+), and mon (+) cassettes showed galactose-induced transcription as evidenced by the presence of the expected 148bp product from the inward primer set (Figure 3A, lanes 8, 10, 12). To our surprise, in contrast to the *in vitro* dimer transcript (lane

14), total RNA from YPH500 transformed with the dimer construct did not yield a 148 bp RT-PCR product (lane 6), raising the question whether this was an indication of possible problems with the DNA plasmid, pol II transcription of the cassette, or transcript stability for this particular construct. The integrity of the dimer expression cassette was confirmed through PCR and restriction digestion, and this is also the plasmid that was PCR-amplified to generate the T7 template for the dimer IVT. These results rule out a faulty expression plasmid as the reason for a lack of full-length dimer RNA detection.

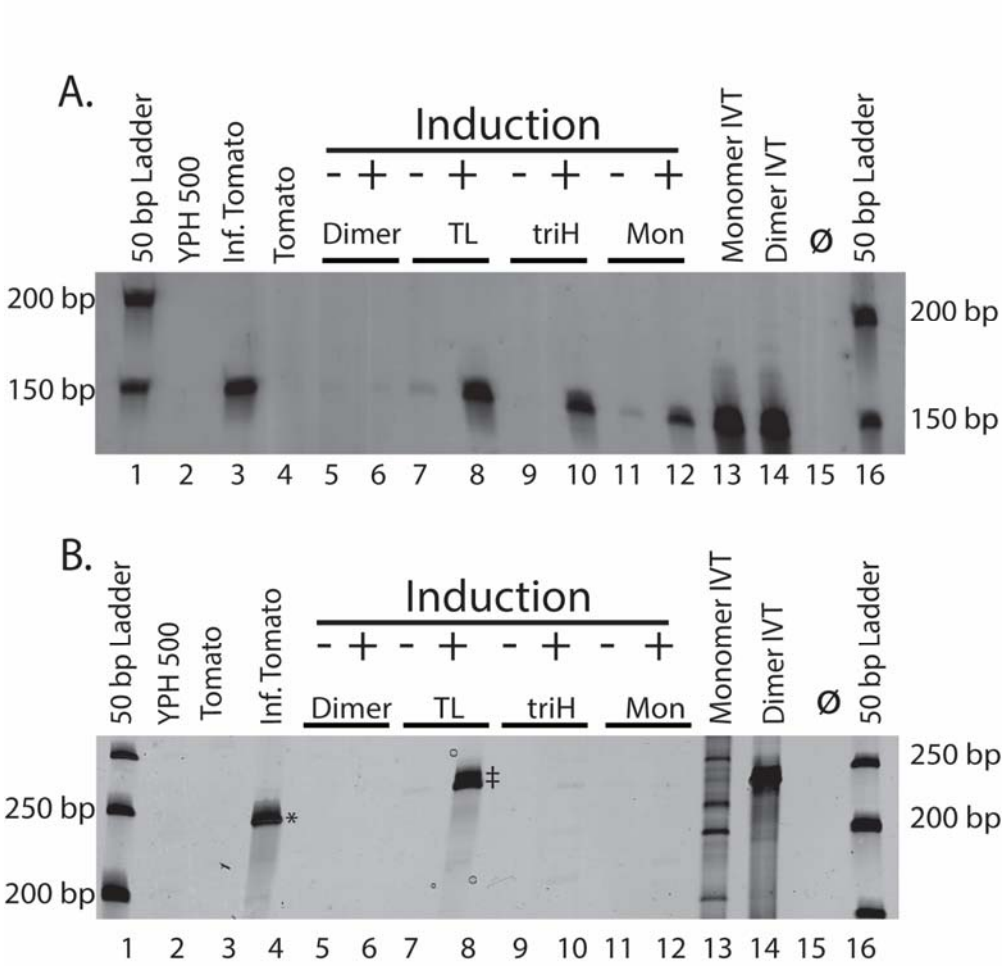

Figure 2.3: Detection of plus-PSTVd and PSTVd circles from total RNA of induced yeast using RT-PCR.

Detection of (+) PSTVd and PSTVd circles in total RNA from induced yeast using RT-PCR. (A) RT-PCR with inward primer set 112F/259R reveals that all PSTVd RNAs tested produce a 148 bp DNA fragment. Lanes are: (2) empty yeast strain, (3) PSTVd-infected tomato, (4) healthy tomato, (5-12) RNA from the yeast strain YPH500 transformed with plasmids containing the PSTVd constructs listed in Figure 1. Positive controls were *in vitro* transcripts of PSTVd monomer (13) and dimer (14). Lane 15 is a transcript-free RT-PCR control. RNAs were extracted from yeast grown in inducing galactose media (+) and non-inducing dextrose media (–). The molecular weight marker is a 50 bp DNA ladder. (B) RT-PCR with outward primer set 2F/259R reveals the presence of circular PSTVd RNA as a 240bp (tomato, *) or 248 bp (yeast, ‡) DNA duplex. The lane order is the same as (A) with the exception of the infected and healthy tomato samples. The different migration behavior of the marker bands in lanes 1 and 16 is due to an electrophoretic ‘smile’.

Circle/multimer detection using the outward primer set gave rise to the expected 240 bp band for the infected tomato (Figure 3B, lane 4) and the dimer *in vitro* transcript (lane 14) controls. Of the four constructs, only TL (lane 8) yielded a similar band. This band migrates slightly slower, indicating a size slightly larger than 240 bp. Importantly, expression of the triH construct did not direct the formation of a 240 bp fragment in this assay (lane 10), even though the inward primer pair demonstrated strong expression of the precursor plus-strand triH RNA (Figure 3A, lane 10). The lack of a 240 bp band from the *in vivo* dimer construct is consistent with the lack of a 148bp band for detection of plus-PSTVd (Figure 3A/B lanes 6).

Northern Blot detection of PSTVd primary transcripts, degradation products and circles

Expression of TL (+), triH (+), and mon (+) was confirmed by northern blotting (Figure 4). Total RNA isolated from yeast containing the expression plasmids and grown under inducing (+) or non-inducing (–) conditions was separated by electrophoresis, transferred to a membrane, and probed using a radiolabeled minus-sense full-length viroid RNA. As expected, PSTVd-derived RNA species for all four constructs could only be detected after induction (lanes 5, 7, 9, 11). RNA from PSTVd-infected tomato provided both linear and circular migration standards (lanes 1, 2, 15). The monomer *in vitro* transcript (lane 12) shows four bands. From top to bottom these are: the primary transcript with both ribozymes still attached (547 nt), two intermediate products in which either only the hairpin or the hammerhead ribozyme have cleaved (482 and 424 nt, respectively), and the proper monomer released by cleavage of both ribozymes (359 nt). The corresponding double-ribozyme *in vivo* construct only yielded a weak monomer band, indicating low efficiency cleavage of the two ribozymes (lane 11). The most prominent RNA band in this lane results from cleavage by the hammerhead, but not the hairpin ribozyme

cleavage. Both TL and triH RNA *in vivo* constructs displayed an RNA band in the range of linear molecules slightly larger than the unit length linear molecule (lanes 7, 9; marked by red arrowheads), in good agreement with the expected size with the UCCR duplication and matching the size of the *in vitro* transcript (lane 13). Multiple repeats of this northern blotting assay displayed clearly and consistently that the TL had the highest level of RNA accumulation *in vivo* of all constructs tested. The dimer construct did not yield a detectable band in the dimeric RNA range established by the *in vitro* transcript (lanes 5, 14 red arrow) in our northern blot analysis. However, induction did produce a viroid specific RNA *in vivo* (lane 5, open arrow head) similar in size to the monomer-hammerhead-ribozyme fusion, and a little larger than the TL and triH RNAs expressed *in vivo*, but significantly smaller than the dimer *in vitro* transcript control (lane 14), whose band migrates just below the viroid circles (lane 16). The identity of this band is uncertain. The RT-PCR results indicate it cannot contain continuous RNA between the inward primer set binding sites. In both the TL (+) and triH (+), there are signs of smaller RNAs below the primary transcript. For example, the TL construct consistently yields at least one shorter RNA species (lane 7, open arrowheads) that closely migrates with exact linear monomeric RNA (lanes 2, 12, 15). Numerous northern blots indicate this band is slightly smaller than an exact linear monomer.

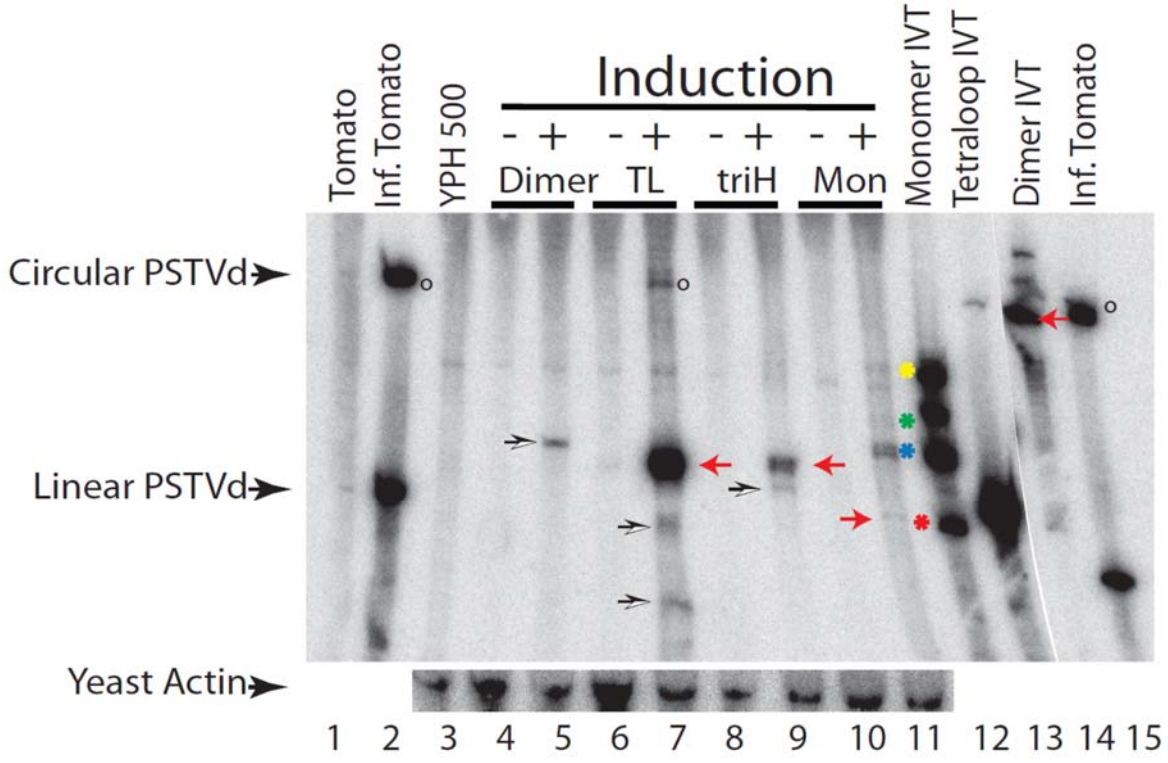

Figure 2.4: Northern blot analysis of total RNA from PSTVd infected yeast.

Total RNAs from healthy tomato (lane 1) infected tomato (lane 2), empty YPH500 (lane 3) and YPH500 transformed with the constructs as indicated (lanes 4-11) were separated on a 5% PAA and blotted onto positively charged nylon. Induction conditions are represented by dextrose (–) and galactose (+). *In vitro* transcripts corresponding to mon, TL, and dimer were used as positive loading controls (12-14). The ribozymes of the monomer IVT (lane 12, see Figure 1A) did not cleave to completion, resulting in four bands: HH-PSTVd-HP (547 nt, yellow asterisk), PSTVd-HP (482 nt, green asterisk), HH-PSTVd (424 nt, blue asterisk), and linear PSTVd (359nt, red asterisk). The blot was probed with an α^{32}P- (–) PSTVd transcript. Linear and circular PSTVd are marked. For a loading control, the yeast actin gene (1537 nt) was probed in a second hybridization. Actin migrates above circular PSTVd. Red arrows indicate primary transcripts from the *in vitro* transcripts prior to any yeast cleavage/ligation events (*in vivo*). The open circle denotes circular products resulting from processing of the TL construct *in vivo* (lane 7).

Gel Extraction of linear and circular PSTVd followed by RT-PCR and sequencing

In the previous experiments, northern blots and RT-PCR amplifications were performed on separate RNA preparations. Figure 5 directly confirms that the circles observed in northern blots are responsible for the 240 bp RT product amplified across the circle junction. Total RNA from induced and uninduced cells containing plasmids with the TL or triH expression cassettes were separated on a 5% PAA denaturing gel in duplicate. One duplicate was subjected to northern blotting using minus-PSTVd RNA as probe (Figure 5A). The other was stained with ethidium bromide, enabling gel regions corresponding to standard linear and circular RNA species from infected tomato to be cut out (5A dashed lines). RNA extracted from these bands was used as substrate for RT-PCR; each sample was tested with both inward and outward facing primer pairs.

The results are presented in Figure 5A. As before, the northern blot showed linear longer-than-unit-length RNAs in both the induced TL and triH samples. A band co-migrating with PSTVd circular RNA from infected tomato is only seen in the induced TL lane (Figure 5A, lane 3) and not in the triH-induced lane (lane 4). RT-PCR analysis with the inward primer set gave rise to the 148 bp band from RNA extracted from both the TL and triH RNA linear regions, as expected. Importantly, outward RT-PCR with RNA extracted from the area of expected circular species only resulted in a 240-bp-like product for the TL RNA (Fig. 5B, lane 10, double dagger) and positive controls, not for the triH (lane 11).

The DNA product obtained through RT-PCR analyzed in Figure 5B, lane 10, was sequenced using the primers for outward PCR to confirm circularization of the RNA template. Unexpectedly, this revealed that eight additional nucleotides had been inserted at the ligation junction, corresponding to a 4 nt duplication of PSTVd sequence (nt 93-96) and four vector-

derived nucleotides (acau) located directly upstream 5' of the delta ribozyme cleavage site (Figure 5C). This same sequence was observed in three independent analyses of yeast circular RNAs. The sequence of events best able to explain this outcome is a yeast endonuclease-driven cleavage of the 5’ end between nucleotides 92 and 93, and a 3’-cleavage at the expected location upstream of the delta ribozyme, followed by ligation of the two heterogeneous ends, as described in more detail in the Discussion.

Based on this model, we would expect to find a linear 367-nt RNA with nucleotide 93 at its 5’ end. Other longer intermediates could be possible. The northern blots, e.g. Figure 4, lanes 5, 7, and 9 and Figure 5A, lanes 3 and 5, show possible candidate bands (open arrowheads) for TL, TriH, and dimer constructs expressed *in vivo*. These putative intermediates do not appear on every blot. However, in every case where we have seen them and mapped their size, they were not consistent with an exact monomer, with or without the eight-base insert indicated by the circle sequence. Only the dimer produces an extra band longer that 359 nt.

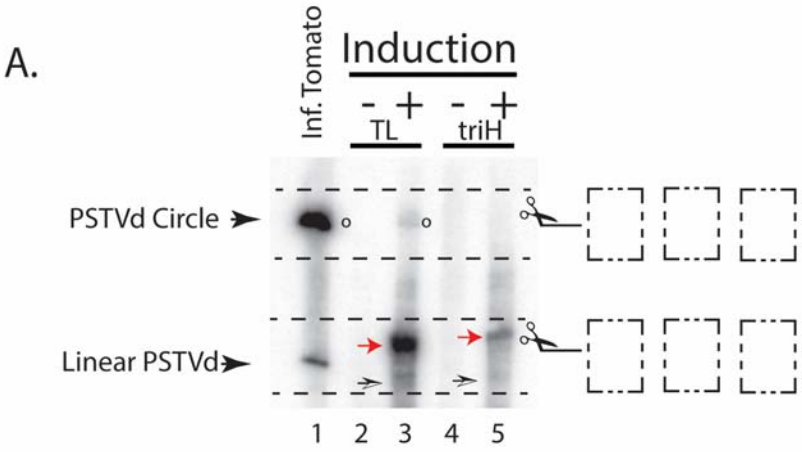
A.
Inf. Tomato
Induction
-
+
TL
-
+
triH
PSTVd Circle
Linear PSTVd
1 2 3 4 5

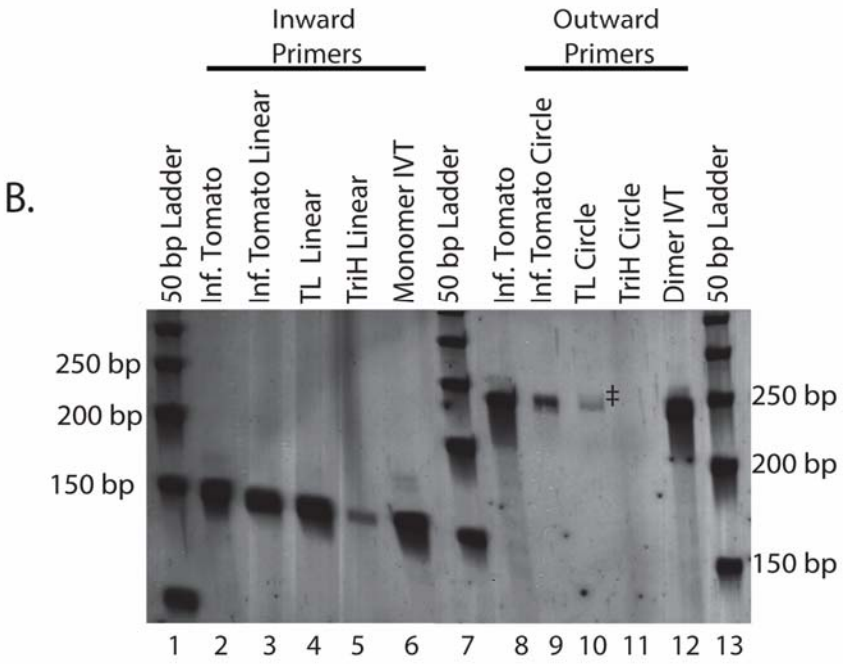
B.
Inward Primers
Outward Primers
50 bp Ladder
Inf. Tomato
Inf. Tomato Linear
TL Linear
TriH Linear
Monomer IVT
50 bp Ladder
Inf. Tomato
Inf. Tomato Circle
TL Circle
TriH Circle
Dimer IVT
50 bp Ladder
250 bp
200 bp
150 bp
250 bp
200 bp
150 bp
1 2 3 4 5 6 7 8 9 10 11 12 13

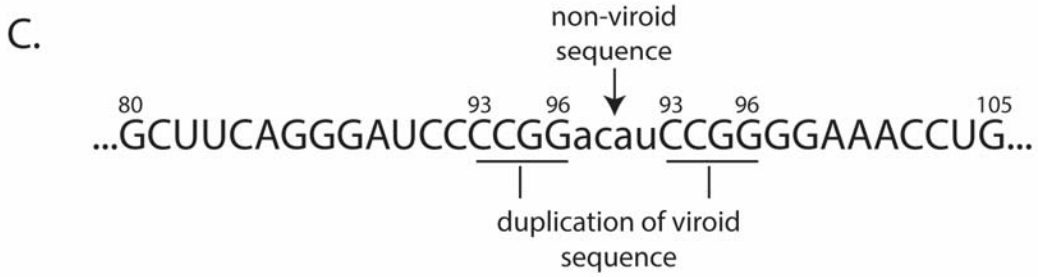
C.
non-viroid sequence
80
93
96
93
96
105
...GCUUCAGGGAUCCCCGGacauCCGGGGAAACCUG...
duplication of viroid sequence

Figure 2.5: RT-PCR of gel excised linear and circular PSTVd, northern blot confirmation and sequence data.

A denaturing 5% polyacrylamide gel with duplication of five lanes was run and cut in half. (A) The left half was used for a northern blot. Lane 1 is a positive control of infected tomato, lanes 2-3 are yeast total RNA from the TL construct, and lanes 4-5 are yeast total RNA from the triH construct. Red arrows indicate primary transcripts, open arrows indicate cleavage products of viroid RNA, and circles designate circular PSTVd products. (B) Regions indicated by the scissors and dashed boxes in (A) were excised from the right half of the gel; the RNA was extracted and used as templates for RT-PCR. Lanes 2-6 use the inward primer set 112F/259R to reveal plus-PSTVd. Lanes 8-12 use the outward primer set 2F/259R to reveal circular PSTVd RNA. Lanes 2,6,8, and 12, are positive controls from RT-PCR of RNAs that were not gel extracted; lanes 3/9 use gel-extracted linear/circular RNA from infected tomato. The template RNA for lanes 4 /10 and lanes 5/11 were the extracted linear/ circular bands from induced TL and triH RNA. (C) Sequence results of gel extracted circle from TL in yeast. The lowercase letters represent non-viroid vector sequence and the bars indicate duplications of viroid sequence.

Mapping of 5' cleavage sites by primer extension

Primer extension is a more precise method for mapping 5' ends of linear RNA molecules. Initial experiments could not even reproducibly detect the primary transcript in different total RNA preparations, prompting us to search for ways to enrich and possibly stabilize the transcript and its processing intermediates. Two different approaches were explored. For the first, Semancik and Szychowski (186) have shown PSTVd RNA can be enriched using 50 mM Mn^{2+}. This precipitates single-stranded RNAs greater than ~300 nt, but does not precipitate PSTVd RNA. For the second, knocking down RNases *in vivo* might stabilize intermediates. *RAT1* is an essential nuclear 5' to 3' exoribonuclease. Cells with a nonlethal allele, *RAT1-107*, display reduced RNA degradation (181). Levels of linear transcripts from our various PSTVd cassettes, as well as circles from the TL construct, were elevated in a strain with this allele (Supplemental Figure 1). With the combination of Mn^{2+} precipitation and the *RAT1-107*

mutation in YPH500, primary and putative processed RNAs were reproducibly observed in primer extensions. Figure 6 presents an autoradiogram of a primer extension with a major band at the -3 position (black arrow) when the TL construct is induced (lane 7, solid arrow), indicating the transcription start within the *GAL1* promoter. The triH construct should produce the same band, as its 5' end is equivalent to that of the TL construct; yet, this band was not detected, despite the use of both *RAT1-107* and Mn^{2+} precipitation (lane 5). This result was in agreement with the northern blots where the TL construct always produced more primary transcript than the triH.

The TL primary transcript does show processing of the primary transcript, with major bands at positions 110 and 106, and a minor band at position 91. None of these is consistent with the circle sequence, which indicates cleavage at position 92/93, or with the cleavage at 95/96 seen in plants(64, 89). If the 3' end of the RNAs with cleavage after 106 or 110 were the expected cleavage site of the delta ribozyme, these bands would be consistent with the near monomer-sized bands that appear with TL and triH primary constructs (Figure 5A, lanes 3 and 5). Possible processed bands were also seen in the Mn^{2+}-precipitated RNA from the trihelix construct. These are lighter, more numerous, and at positions distinct from those seen for the TL RNA (Figure 6, lane5, vertical bars). These lanes should be compared to the control (lane 3) with YPH500 *RAT1-107* strain Mn^{2+}-precipitated RNA without plasmid. The band seen in northern blots of RNA from the dimer construct (Figure 4, lane 5, open arrow) is also relevant to this section. All of these shorter-than-primary-transcript bands could arise from multiple 5' ends created during the degradation or other processing of the triH transcript. This indicates that all of our primary transcripts face degradation in yeast and that any change in sequence, full duplication or the addition of just a few bases, changes the degradation pattern significantly.

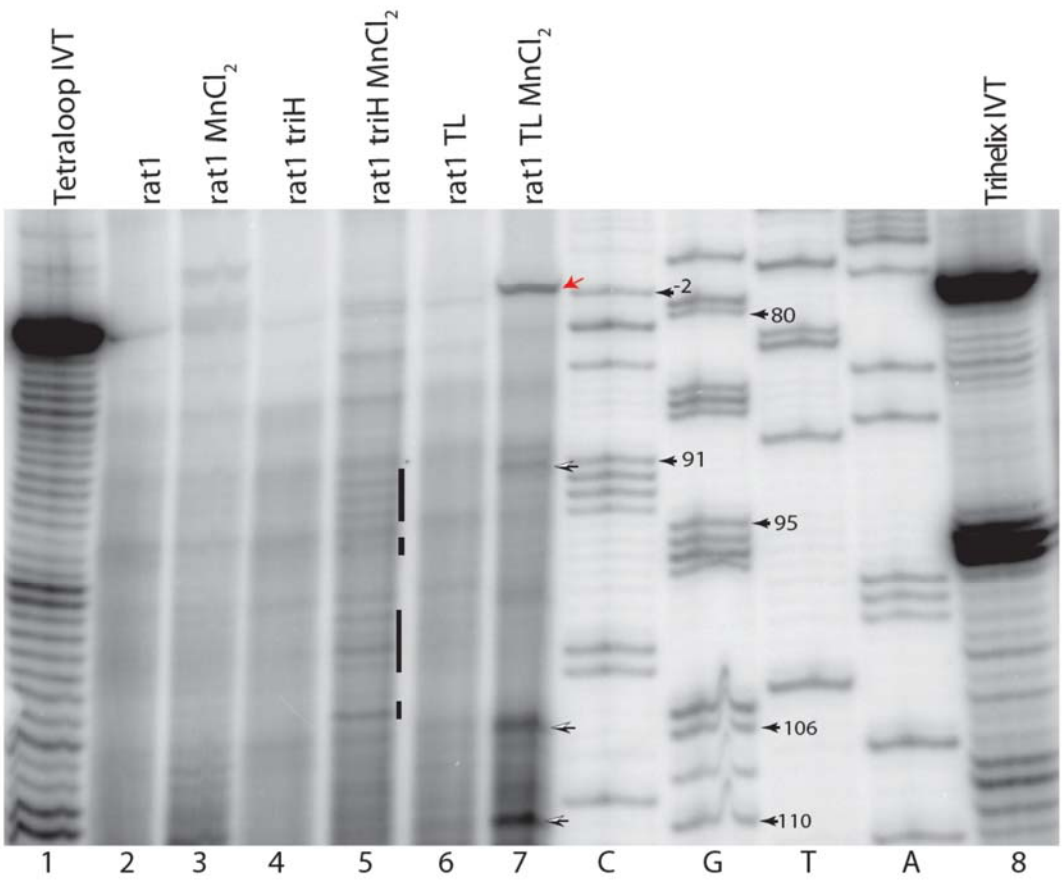

Figure 2.6: Determination of RNA 5'-ends for viroid species detectable *in vivo*.

Total RNA was prepared from a yeast RAT1-107 mutant expressing PSTVd TL and triH constructs. Untreated (25 µg) and $MnCl_2$-treated RNA (12.5 µg) were then analyzed by primer extension. *In vitro* transcripts (0.5 pmol) of TL and triH (1 and 8) were used as controls. The 5' ends of both *in vitro* transcripts are identical and transcription starts at position G80. Lanes 2 and 3 are plasmid-free strains of the *RAT1-107* mutant without and with $MnCl_2$ treatment. Lanes 4 and 5 contain RNA from triH transformed RAT1-107 without and with $MnCl_2$ treatment. Lanes 6 and 7 contain TL transformed RAT1-107 without and with $MnCl_2$ treatment. Position -2C (red arrow) marks the yeast transcription start sites in constructs harboring a GAL1 promoter. Position G80 marks the first PSTVd base. Open arrows indicate additional 5' ends/degradation products detectable in the $MnCl_2$-enriched TL RNA (lane 7). The bars in lane 5 indicate the high level of additional 5' ends/degradation products seen in the triH variant compared to the TL variant.

Discussion

Viroid replication initiates with rolling circle replication on a plus-RNA utilizing a host RNA-directed RNA polymerase that generates a multimeric minus-RNA. *Avsunviroidae* process this strand directly; *Pospiviroidae* copy this strand to a multimeric plus-RNA before processing. For processing, an endonuclease produces monomers, which are then ligated into mature RNA circles. In *Avsunviroidae*, the endonuclease activity is provided by ribozymes encoded by both the plus- and minus-RNAs. However, *Pospiviroidae* rely on a host endonuclease. It has been speculated that viroids may have originated in the RNA world (188). If so, the RNA replicating and maturing activities should have been present in the last universal common ancestor of all life, and cells in all kingdoms of life would be expected to support viroid replication. Currently, viroids are only known to occur natively in plants, while a close relative, hepatitis delta, a satellite RNA to hepatitis B virus, is found in animals. Viroid replication has been introduced into non-host plants such as *Nicothiana* and *Arabidopsis* (167, 189) through adaptive changes or transgenic constructs. Beyond plants, the Maurel and Torchet labs have recently shown that ASBVd can be propagated in the nonconventional hosts *S. cerevisiae* or cyanobacterium *Nostoc*, supporting the notion that both eukaryotes and bacteria support viroid replication (128, 141). Here, we investigate the processing of RNA polymerase II transcripts containing PSTVd in yeast. Such a system opens the toolbox of yeast molecular biology to study the processing pathway, possible structural requirements to the formation of intermediates and end products, as well as the enzymes involved.

In contrast to the work published on ASBVd in yeast, the challenges at the outset of this work were two-fold: First, for PSTVd as a member of the *Pospiviroidae*, in addition to pol II, we also have to assume that a yeast endonuclease instead of the viroid-encoded ribozyme in

Avsunviroidae is available to cleave RNA multimers to monomers that can be circularized by a suitable yeast ligase. Second, in order to address the question of whether there are structural requirements for processing in yeast as there appear to be in host and non-host plants, we needed to design constructs that would fold into distinct RNA conformations *in vivo*. From prior work involving TGGE analysis of *in vitro* transcripts, it was clear that both small differences in the number of nucleotides duplicated between the 5- and 3'-end of larger-than-unit length PSTVd as well as the rate of folding have a large influence on the structures available to this RNA (88, 176).

We chose two constructs related to the ones shown to be active in previous processing studies, the tetraloop-forming larger-than monomer RNA active in potato nuclear extracts, as well as a dimeric PSTVd RNA corresponding to the CEVd construct processed in transgenic *Arabidopsis*. In addition, we included a perfect linear monomer RNA generated by two flanking ribozymes to interrogate the yeast system for ligation in case cleavage of the other RNAs was inhibited, as well as a new larger-than monomer RNA that was designed to favor a trihelical element. This latter construct adds an important dimension to the previous processing approaches: in comparison to the RNAs used by Steger *et al.* (176) and Baumstark *et al*. (63, 88), this transcript contains a full duplication of the entire UCCR, which is able to form a perfect trihelical element. TGGE analysis indicates this structure is the thermodynamically favored one; it can form directly during or after transcription, as well as after thermodynamic pretreatments under equilibrium conditions (data not shown.) Secondly, in contrast to transcripts such as our PSTVd RNA dimer or the CEVd dimer used by Gas *et al*., we do not have to take into account the possibility of multiple combinations and permutations of structural elements available between two complete units (190). Lastly, we do not have to rely on a mechanism for trihelix

formation via refolding of hairpin 1 elements through kissing-loop interactions as postulated by Gas *et al*.(64, 187).

All of these four constructs showed various degrees of expression; yet only the TL construct was active in forming circles. However, these were of aberrant length: they contained four non-viroid, vector-derived nucleotides and a four-nucleotide viroid duplication (Fig 5, 7). For the other three constructs, the primary transcript accumulation *in vivo* was consistently lower than the TL construct. The triH RNA allowed detection in northern blots as the 390nt primary transcript length. The full-length dimer RNA was very unstable in yeast cells; no signal was seen by RT-PCR and only a faint ~420 nt degradation product appeared on northern blots. Similarly, the exact monomer released from the double-ribozyme cassette was barely detected in northern blots. The monomer transcript with a 5'-end uncleaved HH ribozyme did accumulate to noticeably higher levels, indicating a stabilizing effect of this initial, 5'-capped pol II product (Fig. 4).

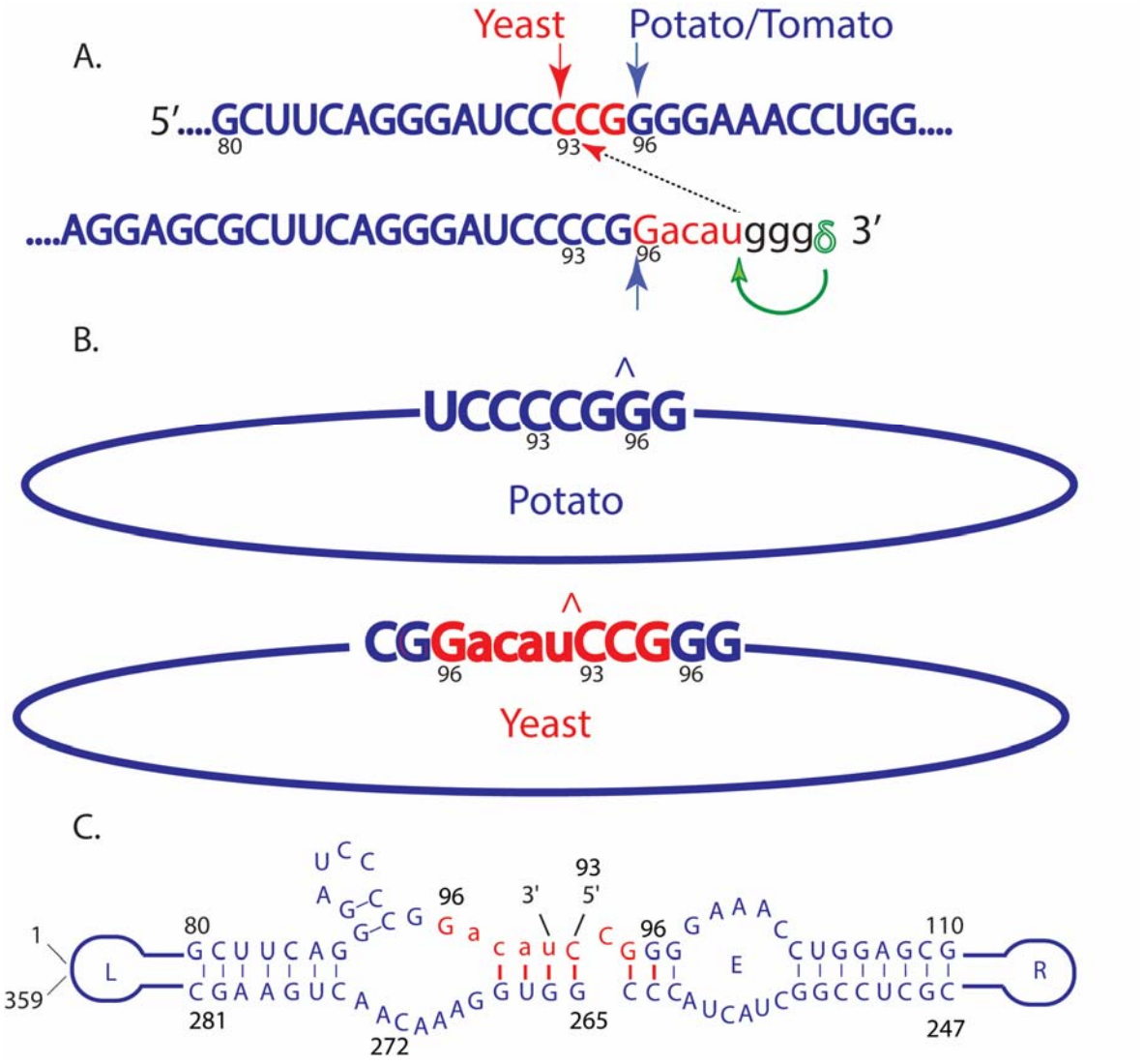

Figure 2.7: The cleavage and ligation sites for PSTVd in yeast total RNA extractives containing the TL construct.

Letter coloring and upper/lowercases indicate the same nucleotides throughout. The lowercase red letters are vector nucleotides added during plasmid construction. (A) The sequence of the 5' and 3' ends of TL transcribed in yeast. Uppercase blue and red letters are wild-type PSTVd sequences. The blue arrows (95/96) indicate the known cleavage sites of PSTVd processed in potato or tomato. The downward red arrow indicates (92/93) the 5' cleavage site of processing in yeast. The lowercase black letters are the 5' end of the delta ribozyme. The green arrow indicates cleavage by the delta ribozyme. The dotted line with the red arrow marks the sites for ligation in yeast. (B) Sequences of ligation junctions in potato and yeast. The caret (^) marks the ligation sites. Sequences shown were determined from RT-PCR of gel extracted RNA circles from yeast and tomato. The proposed ligation scheme results in an additional 8 nt in yeast (red). (C) Ligation substrate in yeast. The marked 3' and 5' ends are ligated to form the yeast circle. The additional 8 nt (red) comprise nt 96, the four vector nt and nt 93 through nt 95.

Of the shorter, viroid-specific RNA species detected in cells expressing the TL or triH constructs, none was of the size expected for processing into unit-length molecules. Primer extension confirmed that the 5'-ends of these RNAs varied (Fig. 6), consistent with them being the result of degradation rather than a specific viroid processing pathway in replication. Our observations are in line with results by Delan-Forino *et al*. (128), who determined that successful processing of ASBVd plus-RNA into circles is accompanied in parallel by degradation of linear ASBVd RNA via the yeast RNA surveillance pathway. This competition between processing and degradation is not unique to yeast, as recent studies have shown the presence in PSTVd-infected plants of subgenomic-length RNA species a that appear to be products of endonucleolytic cleavage leading to degradation (111). The concentration of these subgenomic fragments varies considerably from one host to another.

Based on our results, four factors influence the balance between degradation and processing in yeast. These appear to be applicable to the other systems able to replicate viroids. 1) Specific structural motifs must be recognized by the endonuclease(s). 2) The chemical nature of the ends produced by cleavage must be compatible with the ligase. 3) These ends must be presented in a suitable orientation to the relevant ligase, for example by being base paired to a continuous complementary strand; and finally, 4) there must be a thermodynamically feasible pathway to arrive at that base pairing through refolding from a transient, kinetically favored nascent structure. A fast forming intermediate is recognized by the endonuclease, which upon cleavage refolds towards a lower free energy structure recognized by the ligase, akin to a riboswitch sensitive to the context and transcriptional age of an RNA sequence. In the following, these factors will be discussed in more detail below.

Dimer, triH and TL RNAs all provided structural context for endonuclease cleavage as indicated by the production of distinct shorter RNA species detected in the northern blots. In the case of the dimer and the triH, those species were still larger than monomeric length, implying that either they would require further cleavage before being able to yield mature circles, which we did not observe, or that in fact they were degradation products similar to the subgenomic PSTVd RNAs observed by Minoia *et al*. (111). The shorter fragments derived from TL RNA also did not correlate with productive processing, as they were shorter than monomeric length. Since the TL RNA did, however, give rise to circles in yeast without detectable accumulation of the precise linear intermediates determined by sequencing of the circular products to be 367 nt long (5'-C93-359/1-G96-acau-3'), as shown in Fig. 7, we conclude that these intermediates are extremely short-lived, and that they either get converted immediately to circles or degraded rapidly in yeast. The acau insertion is not present in the trihelix RNA; thus, the traditional trihelix structure is maintained. If the 92/93 cleavage site were used in the trihelix, a double-stranded cleavage would still occur within a properly paired RNA double helix and produce a four-base 5' overhang. Rapid ligation of the ends from the trihelix cleavage cannot explain the lack of a productive intermediate in this construct, as no circles are observed. Thus, we conclude that yeast has an endonuclease that recognizes and cleaves a structure specific to TL RNA, but this endonuclease does not recognize and cleave triH RNA at the same location. Presumably, these two sequences fold into different tertiary structures.

The chemical nature of the ends produced by cleavage of the RNA constructs in this study is a direct consequence of the type of endonuclease recognizing them as substrates. RNA endonucleases can produce either a 2'-3' cyclic phosphate and a 5'OH or a 3' hydroxyl and a 5' phosphate. Cleavage site recognition typically relies on RNA secondary and tertiary structure,

rather than exact sequence (191). The work of Gas *et al*. (64, 187) provided evidence implicating dicer-like RNase IIIs as the endonucleases that process CEVd in *Arabidopsis thaliana* to generate 5'-phosphate and 3'-OH termini.

RNase III endonucleases are involved in rRNA, snRNA and snoRNA processing, mRNA maturation, RNA silencing and transcriptome surveillance(192, 193) . They interact with their RNA target via a dsRNA binding domain, and typically recognize dsRNA in a sequence non-specific manner. Many RNA III endonucleases rely on additional protein components in a complex to create specificity (194). Such protein factors could be responsible for recognition changes from one host to another. In yeast, the sole RNase III enzyme is the Rnt1 protein, which prefers substrates with a variety of RNA hairpins capped by tri-, tetra-, or pentaloops over long RNA double-strands (135, 195, 196). We note that the GAAA tetraloop that caps the PSTVd TL RNA structure does not conform to the most preferred AAGU or NGNN tetraloop substrates of Rnt1p (197). Furthermore, the 92/93 cleavage site is closer to the capping loop than the expected 12-14 nt; yet, the new site is farther from the loop than the site utilized in potato, and this site is at the bottom of the stem predicted by RNA folding programs (88). Given the wide range of targets for Rnt1p in RNA yeast cell metabolism, it cannot be ruled out that Rnt1p is responsible for generating the 5'-cleavage in the TL RNA at position 92/93 in the TL RNA leading to the processing into circles. Taking into account the lack of specific processing products for the triH RNA expressed in yeast (Fig. 3, 4) as well as the distribution of 5'-ends detected in the primer extension, we conclude that the imperfectly double-stranded trihelix is not an appropriate target for the *Saccharomyces* Rnt1p. While it is possible that RNase III counterparts in other eukaryotic systems recognize this structure, in yeast it is most likely that enzymes from degradative pathways cleave the triH RNA into successively smaller products. In a *RAT1-107* background,

the concentration of linear products increased for both the TL and the triH constructs, but this did not result in circle production in case of the trihelix RNA.

The ends generated by the endonuclease have to be compatible with the ligase that closes the circle, and for our system that poses the question as to why those ends generated from the TL construct are suitable, while those from the exact monomer RNA are not. Nohales *et al*. showed that DNA ligase 1, which, like T4 RNA ligase, requires 5'-phosphate and 3'-OH ends, catalyzes circle formation of PSTVd RNA and other *Pospiviroidae* in the host plant tomato; furthermore, it does so with rather high selectivity for the position along the rod-like secondary structure (96). Correspondingly, the monomeric linear CEVd RNA transgenically expressed and processed in *Arabidopsis thaliana* with normal cleavage at 95/96 was determined to contain 5'-phosphate and 3'-OH termini (187). However, the same work showed that monomeric linear CEVd isolated from infected gynura contained 5'-OH and 2'-3' cyclic phosphate termini. Also, viroid RNA molecules recently shown to accumulate as subgenomic species in tobacco, tomato and eggplant had 5'-OH and 3'-phosphate termini; these were proposed to be products of developmentally regulated plant endoribonucleases (111). Finally, Feldstein *et al*. (167) were able to infect *Nicotiana benthamiana* by expressing an exact minus-PSTVd monomer within a double ribozyme cassette that, fully cleaved, was open at position 91/92 with 2'-3'cyclic phosphate and 5'-OH ends. This RNA was found to be infectious and give rise to detectable levels of minus-sense unit-length circles, presumably sealed by a tRNA ligase rather than the DNA ligase proposed for natural PSTVd infection (96).

RNA ligases use two different mechanisms: a 5'-phosphate may be joined to a 3'-OH (5—3 mechanism) or a 2'-3'-cyclic-phosphate may be joined to a 5'-OH (3—5 mechanism); the latter mechanism is restricted to archaea and vertebrates and is not found in yeast or plants (198).

Yeast and plant tRNA ligases follow the 5—3 mechanism, but are able to utilize substrates with 2’-3’ cyclic phosphates and 5’ hydroxyls because their multidomain structure allows them to open the cyclic phosphate and phosphorylate the 5’ OH before ligation. A separate enzyme removes the 2' phosphate (199).

In our case, the ability of the TL RNA to be processed into circles and the sequence environment around the ligation site lead us to conclude that the 2'-3' cyclic phosphate generated by the delta ribozyme is ligated to the 5'-end generated by a host nuclease cleaving between C92 and C93. Presumably, this is a 5'OH to complement the cyclic phosphate. This raises the question: why does the monomer RNA released from the double-ribozyme cassette, which contains the exact same end groups, not ligate? The ligation position in yeast is a few bases downstream from the site in potato (G95/G96), making it possible that the difference in the local sequence and secondary structure environment may account for the differential activity of the ligase on both substrates. Indeed, Nohales *et al.* have shown that 1) recombinant eggplant tRNA ligase acting on eggplant latent viroid with 2'-3' cyclic phosphate and 5'OH ends (164) and 2) DNA ligases from tomato and tobacco acting on PSTVd RNA with 3'-OH and 5'-phosphate ends (96) ligate at the wild-type positions *in vitro*, but not at other positions along the native structure of the respective viroid RNAs.

It is also possible that the 5'-end generated by the host nuclease on TL RNA in fact carries a 5'-phosphate rather than a 5'-OH. If so, then a DNA ligase similar to the one in *Arabidopsis* is responsible for circle formation, then the 2'-3' cyclic phosphate would first have to be hydrolyzed into 3'-OH and 2'-phosphate. This extra step may be highly inefficient, if it has to occur separately from the cleavage, which would explain the relatively low amounts of circles currently produced in our yeast system. In this scenario, the monomer might not be a substrate

for ligation because either the conversion of the 2'-3' cyclic phosphate is inhibited by the particular base pairing of the G95/G96 ends, or the requirement for phosphorylation of the 5'-end in addition to the potentially slow hydrolysis of the 2'-3' cyclic phosphate renders the overall efficiency too low to compete with destructive degradation. Our observation that *in vivo* the fully cleaved monomer RNA accumulates at lower levels than the intermediate with the 5'-ribozyme still attached, in contrast to similar band levels from *in vitro* transcription (Figure 4, lanes 11 and 12), supports this interpretation.

In this regard, ligation of the TL construct can be interpreted as utilization of an "end of convenience" provided by the delta-ribozyme. Figure 7C presents a particular pairing of the upper and LCCR of the proposed linear TL processing intermediate, containing the two four-nucleotide additions, that that would provide a reasonable substrate for an RNA ligase. Here, the 3' cau from the vector acau sequence as well as the 5'-C93 pair with G268 through G265 of the LCCR. This local conformation is stabilized by further base pairing of 5'-upper strand G95 through G97 with lower strand C264 through C262, requiring that C94 be unpaired as an extra-helical base. The ends consisting of 3'-U and 5'-C93 would be held in place for ligation by pairing with G266 and G265. Importantly, this arrangement keeps the upper and lower strands of Loop E in register, so that it could still contribute to a stable conformation required for ligation. With the current constructs, it is unresolved as to whether an exact monomer with open ends between C92 and C93 and no extra sequence would be ligated similar to the TL RNA, or degraded similar to the monomer G95/G96. However, the incorporation of extra sequence into aberrant circles is not unique to the TL construct expressed in yeast. Earlier processing experiments in which *in vitro* transcripts of TL Nearest pre-formed into different structures and incubated with potato nuclear extracts also showed that larger-than-unit length circles were

produced. This was explained as the result of a premature switch into the "extended left" loop E-containing conformation (63). The sequence of the aberrant circles revealed a duplication of 16 viroid nucleotides, which were generated with comparable efficiency to the production of correct 359 nt viroid circles.

Taken together, our results from PSTVd expression in the nonconventional host yeast continue to expands our understanding of how viroids have adapted and thrived in a variety of natural and non-traditional hosts. Viroids have shown a unique plasticity to present themselves as substrates for the cell's promiscuous RNA metabolism and begin to replicate where they encounter the appropriate types of RNA polymerase, endonuclease and DNA or tRNA ligase. Members of the *Avsunviroidae* provide their own ribozyme for cleavage to match the required ligase end requirements. At the same time, all viroids have to overcome the challenge of evading the cell's RNA degradation processes while potentially having to rely on enzymes such as endonucleases that may be part of those very same decay pathways they have to avoid. Even here viroids are ingenious, as some of the products of these degradation pathways may be utilized to act as viroid-specific small RNAs (vsRNA) to subvert the plant defense systems via transcriptional and post-transcriptional gene silencing, which is most likely how viroids exert their pathogenicity (158, 200).

The evolutionary success of viroids appears to be a variation of two strategies: offering recognition elements such as hairpins and other local structures that direct the appropriate nuclease to a preferred location, and applying RNA refolding between cleavage and ligation steps such that kinetically formed metastable intermediates rearrange to thermodynamically stable end products that are no longer an efficient substrate for further cleavage or degradation. From one host cell to another, a particular structure that contributes productively towards

generation of circular progeny in one host may not find a favorable use in a different host and be channeled towards degradation instead of productive processing. The precise sequence of most suitable structures for both cleavage and subsequent ligation and the type of host enzymes involved in their recognition may vary from system to system. The fact that this has been demonstrated for a growing number of viroids and hosts such as *Arabidopsis*, tobacco, potato, eggplant, Cyanobacteria, and now for the second time in yeast, underscores the underlying power and adaptability of the viroid RNA replication strategy.

Supplemental Information

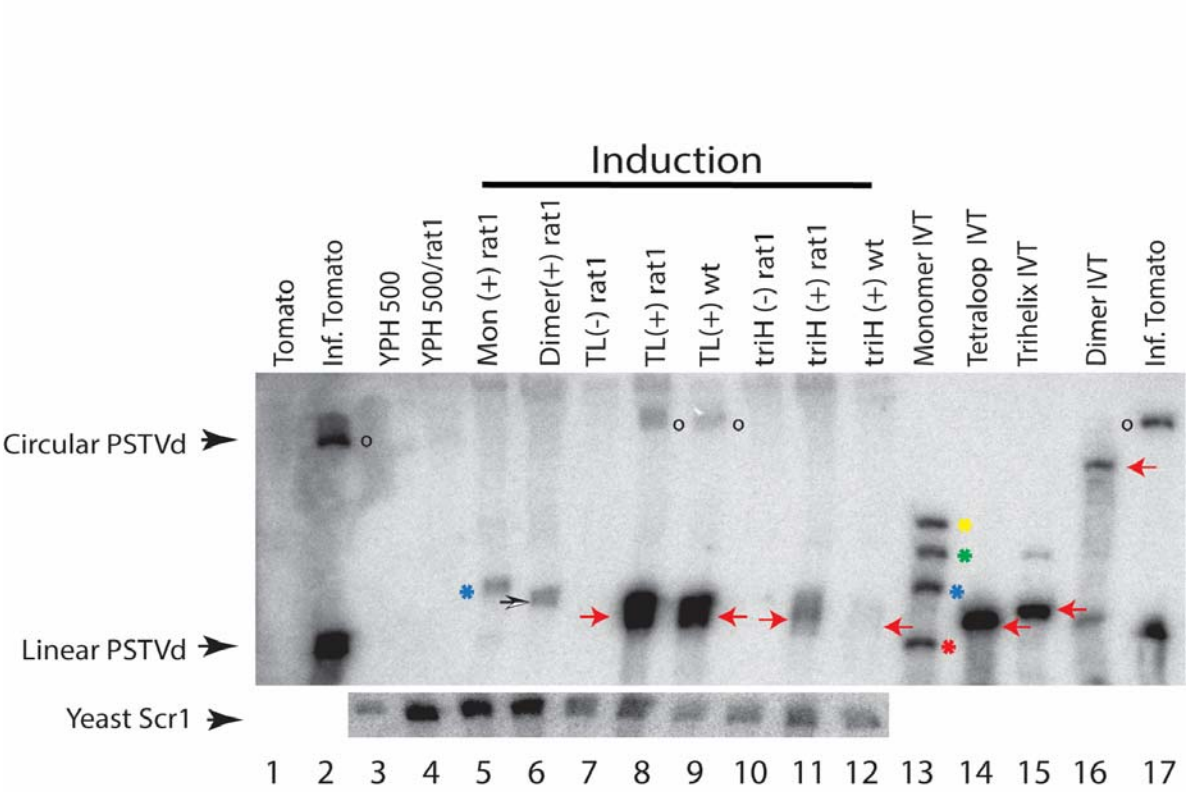

Supplemental Figure 2.1: Northern blot analysis of total RNA from PSTVd infected wild-type and *RAT1* YPH500 yeast strains.

Total RNAs controls include: healthy tomato (lane 1) infected tomato (lane 2), empty YPH500 (lane 3), empty *rat1* (lane 4). Lanes (5-6) represent galactose induction (+) of the *RAT1* stain transformed with the monomer and dimer construct. Lanes (7-8) represent the *RAT1* stain transformed with the TL construct under dextrose (-) and galactose (+) induction. Lanes (10-11) represent the *RAT1* stain transformed with the triH construct under dextrose (-) and galactose (+) induction. Lanes 9 and 12 are the YPH500 strain with gal induction of the TL and triH transformants. *In vitro* transcripts corresponding to each *in vivo* construct were used as positive loading controls (13-16). The ribozymes of the monomer IVT (lane 13, see Figure 1A) did not cleave to completion, resulting in four bands: HH-PSTVd-HP (547 nt, yellow asterisk), PSTVd-HP (482 nt, green asterisk), HH-PSTVd (424 nt, blue asterisk), and linear PSTVd (359nt, red asterisk). The blot was probed with an α-^{32}P minus-PSTVd transcript. Linear and circular PSTVd are marked. For a loading control, the yeast scR1 gene (522 nt) was probed in a second hybridization. Red arrows indicate primary transcripts from the *in vitro* transcripts or prior to any yeast cleavage/ligation events (*in vivo*), blue asterisk HH-PSTVd, open arrowheads indicate viroid RNA cleavage products, the open circle denotes circular products resulting from processing of the TL construct *in vivo* (lanes 8-9).

Supplemental Table 1.1: Oligonucleotides used in this study

Oligonucleotide	Sequence (5'-3')
112F[a]	ACTGGCAAAAAGGACGGTGGGGA
259R	GTAGCCGAAGCGACAGCGCAAAGG
2F	CCTGTGGTTCACACCTGACCTCC
MB1R	TCGGCCGCTGGGCACTCC
ActF	GGTATTCTCACCAACTGGGACG
M13 F	GTAAAACGACGGCCAG
M13 R	CAGGAAACAGCTATGAC
T7 prom F[b]	*GAAATTAATACGACTCACTATA*
TB110 down R	AATTCCGGGGATCCCTGAAGCGCTCC
T7 prom F	*GAAATTAATACGACTCACTATA*
TB112 down R	GCCACCTGACGTCTAAGAAACC
T7ActR	*GTAATACGACTCACTATAG*GCGACGTAACATACTTTTTCCT GATGT
SCR1F	TGGCCGAGGAACAAATCCTT
T7ScR1R	*GTAATACGACTCACTATAG*TTAAACCGCCGAAGCGATCA
T7 PSTVd dim F	TAATACGACTCACTATAGGTACGTACTG
PSTVd dim R	GGGACAGAGGTCCTCAG

[a]Forward primers (ending in F) have the same sequence as the transcribed RNA.

[b]Italicized letters indicate the introduced T7 promoter sequence.

Supplemental Table 1.2: Plasmids used in this study

Plasmid	Construct[b]	RNA	Reference
p13/119	PSTVd Monomer	Mon IVT	This work
p15/14	PSTVd dimer	Dimer IVT	This work
pB3RQ39	P_{GAL1}-BMV-RNA3-δ	BMV-RNA3	(180)
pCR2.1_TOPO.4	HH-95/96 monomer-HP	Mon	(167)
pTB110	parent pRH701	TL IVT	(88)
pTB112	PSTVd trihelix	triH IVT	This work
pTBO_dim	P_{GAL1}-PSTVd dimer-δ	TBO_Dim	This work
pTBO_mon	P_{GAL1}-HH-PSTVd monomer-HP	TBO_Mon	This work
pTBO_TL	P_{GAL1}-PSTVd tetraloop-δ	TBO_TL	This work
pTBO_triH	P_{GAL1}-PSTVd trihelix-δ	TBO_triH	This work
pIC115	*RAT1-107*::*URA3*	RAT1-107::URA3	(181)

[a] *pGAL1*=full *GAL1* promoter; *pGAL1'=GAL1* promoter without *UAS1*.

[b] δ=delta ribozyme; HH=hammerhead ribozyme; HP=hairpin ribozyme; PC=paperclip ribozyme

Supplemental Table 1.3: Templates for IVT PSTVd RNAs and riboprobes

RNA	Template	Forward Primer	Reverse Primer
TL IVT	pTB110	T7 prom F	TB110 down R
triH IVT	pTB112	T7 prom F	TB112 down R
Dimer IVT	p14/15	T7 PSTVd dim F	T7 PSTVd dim F
Mon IVT	p13/119	M13 F	M13 R
(-)PSTVd riboprobe	p13/121	M13 F	M13 R
(-)Actin	YPH500 genome	ActF	T7ActR
(–)SCR1	YPH500 genome	SCR1F	T7ScR1R

Chapter 3: Enrichment of RNAs below 400 nucleotides with Manganese Chloride Precipitation

Abstract

Enrichment of specific RNAs is of importance for the type of RNA analyses being conducted. Several methods and commerical kits can be utlized according to the the RNA of interest. $MnCl_2$ has been used previously to enrich viroid RNA fractions from total RNA from infected plants. We have expanded upon this method to show that $MnCl_2$ can enrich single-stranded RNAs of 400 nt and below from a total RNA preparation. We have applied this method to map the transcription start sites of a PSTVd transcript from total RNA from yeast under conditions where the RNA was previously undetectable. This underscores the ability of $MnCl_2$ enrichment to enable 5' mapping of low copy number RNAs of 400 nt and below in a total RNA extract.

Introduction

RNA biochemistry requires that *in vivo* RNA of interest be separated from proteins, especially RNAases. This can be achived using several commerical kits and by use of phenol-chloroform extraction (201). In addition, enrichment of specific RNAs with regard to type and size within a total RNA extract is essential. Several methods have been used for this additional downstream RNA purification. The PEG (polyethylene glycol) method selectively precipitates plasmid DNA from *in vitro* transcripts as well higher molecular weight species of rRNA and mRNA (202). A simple and under utilized method uses $MnCl_2$ precipiation to enrich 371 nt potato spindle viroid (PSTVd) RNA from total RNA from infected plant tissues (186). The

ressearchers who designed the method were able to clearly demonstrate the enrichment of linear and circular viroids by use of 50 mM $MnCl_2$ with an incubation at 4^0C for 1 hour. Additionally, they showed that these enriched viroid fractions were still effective at infecting plants.

The $MnCl_2$ method is simple and effective at enriching viroid RNAs. We have expanded upon this method to enrich modified viroid RNAs from total RNA of yeast and shown that the range for RNA enrichment is roughly 400 nt. With $MnCl_2$ precipitation, we were able to map transcription start sites of the yeast transcripts through primer extension, which was not possible without enrichment.

Materials and Methods

Oligonucleotides

Oligonucleotides were obtained from Invitrogen and are listed in Appendix Table1.

Yeast Strains, Plasmids and Transcripts

The strain YPH500 (*MAT*α *ura*3-*52 lys2*-801 *ade2-101 trp1*-Δ*63 his3*-Δ *leu2*-Δ*1*) was used throughout the study. Yeast cultures were grown at 30˚C in synthetic media containing either 2% glucose or 2% galactose for suppression or stimulation respectively of the vector's promoter. *In vivo* yeast transcripts of PSTVd were directed by plasmids pTBO TL or pTBO triH are described in Chapter 2/Appendix. These encode PSTVd monomers with 5' and 3' duplications that support the folding of tetraloop and trihelix conformations of PSTVd RNA respectively (5). Both of these transcripts have a 3' delta ribozyme, which cleave efficiently in yeast to give a defined 3' end of the RNA.

The T7 viroid transcripts contained a PSTVd monomer flanked by two ribozymes, produced according Feldstein *et al*. (167). Transcription substrates were produced by PCR from plasmid p13/119 using primers ActF and T7ActR (Appendix). The opposite strand (without ribozymes) was copied to produce the template for minus-PSTVd, used as a riboprobe. The TL i*n vitro* RNA was transcribed from a template copied from pTB110 as described (88). The triH *in vitro* RNA template was formed by PCR amplification of plasmid pTB112 using a primer containing the T7 promoter sequence (T7 prom F) as well as sequences needed to form a complete trihelix using the primer TB112 down R (Appendix Table 3). An additional digestion using EcoR1 to remove extra 3' sequences is needed to make an exact trihelix.

RNA Extraction

Yeast containing the appropriate plasmid was grown in the selective media to an OD of 0.6-1.0. The cells were then harvested. Total RNA was extracted from 10 OD/mL of cells using the hot phenol extraction method (183). This procedure provides ethanol precipitated RNA, which has had DNA digested and proteins extracted.

RNA Enrichment

RNA was enriched by the $MnCl_2$ method (186). $MnCl_2$ enrichment was conducted with a total RNA concentration of 100ng/µl in 50 mM Tris, 1 mM EDTA (TE). In a standard precipitation, $MnCl_2$ was added to 50 mM, vortexed and incubated for 60 min at 4°C followed by centrifugation for 5 min at 15K rcf. Pellets were dissolved in 50 mM Tris, 10 mM EDTA. Supernatants were ethanol precipitated (70% EtOH, 0.3 M Na acetate) and re-dissolved in TE.

RNA was also enriched by PEG precipitation (202). Polyethylene glycol 6000 (Sigma) was first introduced to 6% with 0.42 M NaCl. PEG pellet 1 (P1) was precipitated by

centrifugation at 15K rcf for 5 min. The supernatant was removed and PEG and NaCl were brought to 20% and 0.52 M respectively. PEG P2 was precipitated by centrifugation as before. These conditions were optimal for this methodology. Slight modifications of each protocol were made as described in specific figure legends.

Electrophoresis

Size-distribution of RNAs were determined by gel electrophoresis. Samples were heat denatured at 90°C in formamide loading solution (95% formamide, 0.025% bromophenol blue, 0.025% xylene cylanol) and run on a 5% polyacrylamide (29:1 acrylamide: bisacrylamide) 1x TBE, 8 M urea denaturing gel at 55°C. Samples were visualized by silver staining (184) or dried and exposed to phosphorimaging screen when labeled with ^{32}P. Yields were determined by beta counting radioactive decay from respective samples.

RNA Detection by Northern Blotting and Riboprobes

Total RNAs (5 μg) were separated on a 5% polyacrylamide-8M urea gel and were semi-dry electroblotted to a Hybond N+ membrane (GE Healthcare). The membranes were incubated in UltraHyb solution (Ambion) overnight at 65 °F with the appropriate riboprobe. The membranes were washed with 2x SSC (1x SSC is 0.15M NaCl + 0.015M sodium citrate) and 0.1% SDS. Four washes were performed (2 x10 minutes and 2 x 20 minutes) at 65 °F. The membranes were exposed to a phosphorimaging screen and the signals were measured using a Storm 840 Phosphorimager.

The riboprobes for detection of PSTVd, and actin, were generated by *in vitro* transcription of PCR products either obtained from a plasmid (PSTVd) or from yeast genomic DNA. The PCR

fragments were produced using the primers listed in the Appendix Table 3. The label was [α-^{32} P] UTP.

Primer Extension

Oligonucleotide M1BR (Appendix Table 1) binds plus-strand nucleotides 150-133. The primer was 5'-end-labeled with [γ-^{32} P] ATP using T4 polynucleotide kinase (Invitrogen). Approximately 10^6 cpm of this primer was annealed to 25 µg of total RNA from yeast or 18 µg of $MnCl_2$-treated RNA from yeast. Primer extension used 100 units of reverse transcriptase (Superscript III kit, Invitrogen) at 52°C for 90 minutes. The reaction was stopped and the products were ethanol precipitated. A DNA sequencing ladder was generated with the Sequitherm cycle sequencing kit (Epicentre Technologies) using primer M1BR and a PCR fragment containing the PSTVd sequence from pTBO triH. The products from the primer extension and the ladder were run on 8% (19:1) polyacrylamide (PAA), 8M urea sequencing gels.

Single-Stranded RNA $MnCl_2$ Enrichment Study

A Century Plus ™ single stranded RNA ladder (Ambion, 100-1,000 nt) was transcribed in the presence of [α-^{32}P] CTP. Approximately 10^6 cpm of this ladder was used in 300 µl reactions containing 100 ng/µl total RNA from yeast, 50 mM Tris-HCl, pH 8.0, and 1 mM EDTA. The reactions were incubated at 4°C for 60 minutes. After incubation, four-10 µl samples were taken and counted. Four-50 µl aliquots were then taken and spun at 15K rcf for 5 minutes. The supernatant was transferred and four 10µl samples were counted. The pellets were taken up in 50 µl of 10 mM Tris-HCl, pH 8.0, and 10 mM EDTA and four 10 µl samples counted. For gel analysis, 5 µl of each sample were analyzed on 5% PAA-8M urea gels. The gels were dried and

exposed to phosphorimaging screens. Signals were measured using a Storm 840 Phosphorimager.

Results and Discussion

Enrichment of RNAs of different sizes, functions and structures is of importance for tailored analysis and assays of specific RNAs. Several methods have been employed for enrichment of viroid RNA (4, 5). We have built upon the use of $MnCl_2$ for viroid enrichment by showing clear size specificity using modified viroid transcripts of various sizes. The optimized $MnCl_2$ enrichment has allowed the 5'-end mapping of *in vivo* plasmid-transcribed viroid primary RNA in yeast as well as enhanced detection of these transcripts and their processing intermediates via northern blot analysis.

We have investigated the size dependence of $MnCl_2$ precipitation of various sized viroid RNAs utilizing the double-ribozyme PSTVd monomer described in Chapter2, 5'-hammerhead (HH)-PSTVd monomer-hairpin (HP)-3'. *In vitro* tanscription of this construct produces four bands due to incomplete digestion by the ribozymes: HH-PSTVd-HP (547 nt) PSTVd-HP (482 nt), HH-PSTVd (424 nt), and linear PSTVd (359 nt) (Figure 3.1, lane1). 50 ng of viorid transcript was mixed with 1 μg of total RNA from yeast in 100 μl total volume. The standard conditions of 50 mM $MnCl_2$, incubation at 4°C for 60 minutes, and spinning five min at 15K rcf, gave a supernatant that was depleted in the 547 and 482 nt fragments, lane 4. The pellet fraction showed all four bands; the two smaller bands did not show noticeable depletion. Increasing the centrifugation time or agitating the reaction during incubation did not alter the results (lanes 7-10). Changing the $MnCl_2$ concentration to 100 mM (lane 6), even with a 10-min centrifugation time (lane 10), resulted in only partial depletion of the two larger bands. $MgCl_2$ at 50 and 100

mM at 4^0C for 1 hour of incubation (lanes 11-14) precipitated RNA, but did not show utility in enriching small viroid RNAs. From this experiment, an optimal condition for enrichment of smaller viroid RNAs (< 480 nt) was 50 mM $MnCl_2$ with incubation at 4°C for one hour with a 5-minute centrifugation at 15K rcf.

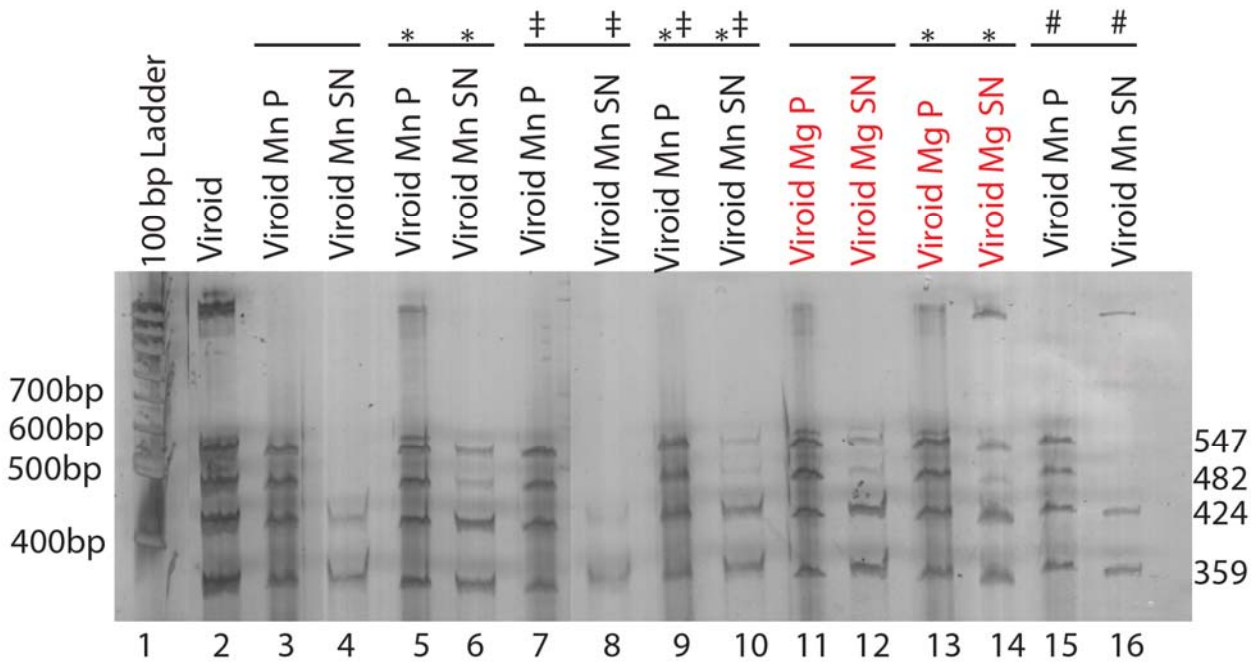

Figure 3.1: Enrichment of Viroid RNAs of under various conditions.

An *in vitro* transcript of a construct containing monomeric PSTVd with 5'-hamerhead and 3'-hairpin ribozymes was added to total RNA from yeast and then treated under various conditions to enrichment specific RNA fragments. Incomplete digestion by the ribozymes gives rise to four RNA fragments: HH-PSTVd-HP (547 nt), PSTVd-HP (482 nt), HH-PSTVd (424 nt), and monomeric linear PSTVd (359 nt) (lane 2). 50 ng of the fragments were spiked into 1 µg of total RNA from yeast. The fragments were treated with MnCl2 (Lanes 3-10, 15-16) or MgCl2 (lanes 11-14), spun at 15K rcf, and resuspended pellets (P) and ethanol-precipitated supernatants were run on a 5% polyacrylamide-8M urea gel and silver stained. Lane 1 is a 100bp DNA ladder. An asterisk (*) indicates the use of 100 mM MnCl2 or 100 mM MgCl2 (all others are 50 mM). The double dagger (‡) indicates the reaction was spun for 10 minutes instead of 5 minutes. The pound symbol (#) represents shaking while incubating at 4°C.

Viroid enrichment by PEG 6000 or $MnCl_2$ precipitation was compared. ^{32}P UTP-labeled PSTVd TL IVT (described in Chapter 2), 381 nt, (Fig 3.2A) or unlabeled transcripts (Fig 3.2 C)

were spiked into 10 μg of total RNA from yeast and enriched using the $MnCl_2$ precipitation (Figure 3.2 A lanes: 3,4; part C: lanes 5,6) or PEG precipitation (Figure 3.2 A lanes: 5,6; part C: lanes 3,4). The PEG protocol and $MnCl_2$ protocol were similar regarding the enrichment of viroid RNA, however; comparisons of the two methods revealed that $MnCl_2$ enrichment of the TL transcript gave a slightly better yield (part B) and efficiency as seen by the more prominent band above the background RNA in Fig 3.2C lane 6.

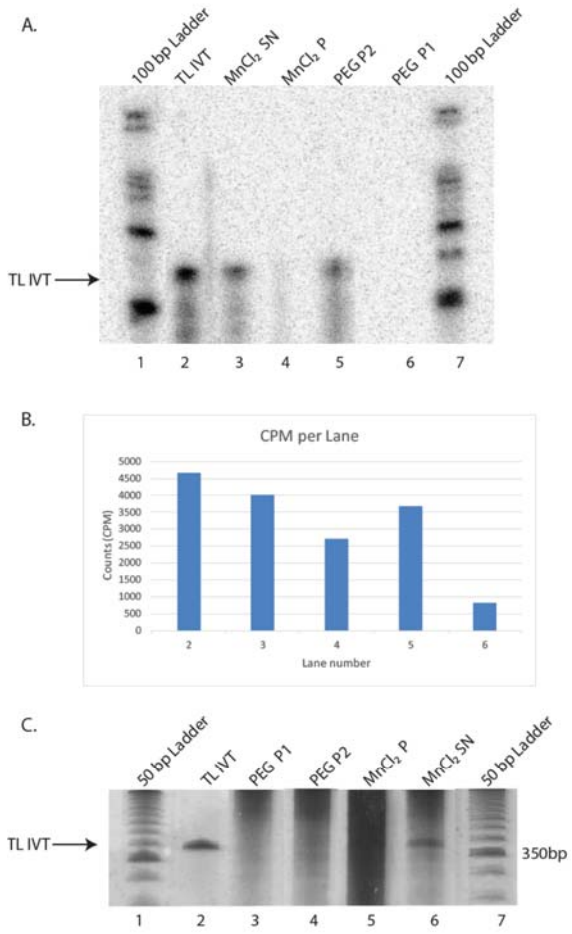
A.
100 bp Ladder
TL IVT
MnCl2 SN
MnCl2 P
PEG P2
PEG P1
100 bp Ladder
TL IVT
1 2 3 4 5 6 7
B.
CPM per Lane
Counts (CPM)
5000
4500
4000
3500
3000
2500
2000
1500
1000
500
0
2 3 4 5 6
Lane number
C.
50 bp Ladder
TL IVT
PEG P1
PEG P2
MnCl2 P
MnCl2 SN
50 bp Ladder
TL IVT
350bp
1 2 3 4 5 6 7

Figure 3.2: Assessment of PEG viroid enrichment compared to $MnCl_2$ enrichment

A. A viroid transcript of 381 nt in length (TL) was transcribed in the presence of ^{32}P-UTP. This transcript ($1.1x10^4$ counts) was then spiked into 10 µg of total RNA from yeast. The system was treated with PEG (lanes 2,3) or $MnCl_2$ (lanes 4,5). The letter "P" is the pellet fraction and "SN" is the supernatant fraction. The pellets were taken up in 5 µl FLS and the SN were ethanol precipitated and then taken up in 5 µl FLS prior to gel loading. The full-length transcript is shown in lane 6 (arrow). **B.** Graph of cpm per lane from Figure A. C. The same TL IVT (200ng) was transcribed with non-labeled ribonucleotides and spiked into 10 µg of total RNA from yeast. The system was treated with PEG (lanes 3,4) or with $MnCl_2$ (lanes 5,6) followed by ethanol precipitation. Samples were run on a 5PAA-8M urea gel and silver stained. The full-length transcript (arrow, 100 ng) is shown in lane 2. A 50 bp DNA ladder was used as a marker (lanes 1 and 7). The sample prep prior to gel loading was identical to that of A with the exception of the labeling of the transcript.

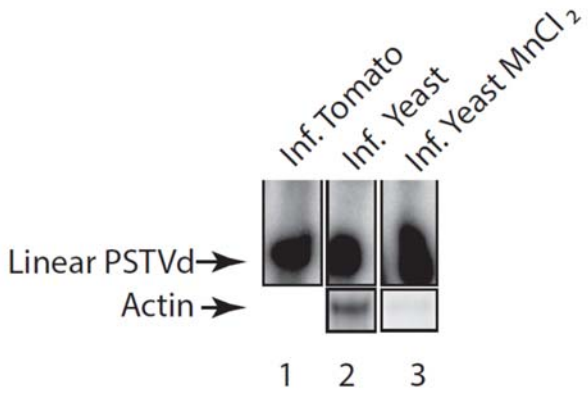

Figure 3.3: Northern blot analysis of PSTVd infected tomato, PSTVd infected yeast, and PSTVd infected yeast followed by $MnCl_2$ enrichment

Total RNA from PSTVd infected tomato (Lane 1), PSTVd infected yeast (Lane2) and PSTVd infected yeast followed by $MnCl_2$ enrichment were separated on a 5% PAA and blotted onto positively charged nylon. Lane 1 contains 1 µg of PSTVd RNA; lanes 2 and 3 contain 5 µg of PSTVd infected total RNA from yeast. Linear PSTVd (359 nt Inf. Tomato/ 375 nt Inf. Yeast) The blot was probed with a ^{32}P-minus-PSTVd transcript. For a loading control, the yeast actin gene (1537 nt) was probed in a second hybridization.

$MnCl_2$ enrichment of *in vivo*-transcribed linear and circular PSTVd is compared in Figure 3.3. Total RNA from yeast was extracted and a portion of the RNA was then treated with $MnCl_2$ to obtain an enriched portion of linear PSTVd transcript. This RNA was then analyzed by

northern blotting and probed with ^{32}P-minus-PSTVd and ^{32}P-minus-actin transcripts (Figure 3.3). The PSTVd infected tomato gives the expected band for linear PSTVd (lane 1). PSTVd infected yeast also gives linear PSTVd (lane 2). Lane three shows the yeast RNA after $MnCl_2$ precipitation. This enrichment produced a stronger signal for linear PSTVd, and very little signal for the yeast actin (1537nt)

To determine whether or not the secondary structure of RNA affects its precipitation by $MnCl_2$, the Century Plus RNA ladder template (Ambion) was transcribed with (Figure 3.4A, lane 1) or without (Figure 3.4 C Lane 5) α -^{32}P-CTP present. Yeast total RNA (100ng/µl) was spiked with radiolabeled single-stranded RNA ladder and subjected to $MnCl_2$ enrichment using 0, 15, 30, and 50 mM $MnCl_2$, with a 60-min 4°C incubation. The pellet fraction and supernatant as well as a pre-spin fraction of these RNAs were run on a gel. The untreated ladder serves as a marker (Figure 3.4, A: lanes 1, 11). Total radioactivity in each fraction is presented in Figure 3.4 B. Without the addition of $MnCl_2$, almost all of the RNA is in the supernatant fraction (SN) (A: lane 4, B: 0 mM). With 15 mM $MnCl_2$ there is an increase in precipitation of RNA up to 500 nt; however, most RNA still resides within the SN fraction (A: lanes 5 and 6, B: 15 mM). At the 30mM $MnCl_2$ level, roughly 70% of the ssRNA ladder resides in the SN and 30% is in the pellet (B: 30mM); however, the gel result indicates that there is an increase in the larger RNA's in the pellet (A: 7-8). Lastly, at the 50 mM concentration of $MnCl_2$, there is nearly an equal split of RNA in the pellet to the supernatant (B: 50 mM). There is also a more intense signal of larger RNA (400 and 500 nt) in the pellet fraction (A: lane 9). These results are corroborated by radioactivity measurements, as with increasing $MnCl_2$ concentration there seems to be an increase in larger RNA in the pellet fractions as well as an increase in total counts in the pellets. 30 mM $MnCl_2$ seems optimal with the cut off being around 300-400 nt. Quantitation of the

radioactivity in each lane supports this conclusion (Figure 3.4B). Figure 3.4C displays a silver-stained gel of the ssRNA ladder with no radioactive label provided by Paul Freidhoff. This gel indicates that the cut off for single-stranded RNA that remains in the supernatant is approximately 500 nt. It also shows that precipitation is the same at pH's of 7.5 and 8.5 (lanes 1-4). Thus, similar molecular weight dependencies were seen for modified viroid RNA and ssRNA. However, for RNAs in the range of 400 - 500 nt, the precipitation behavior should be checked for each individual species.

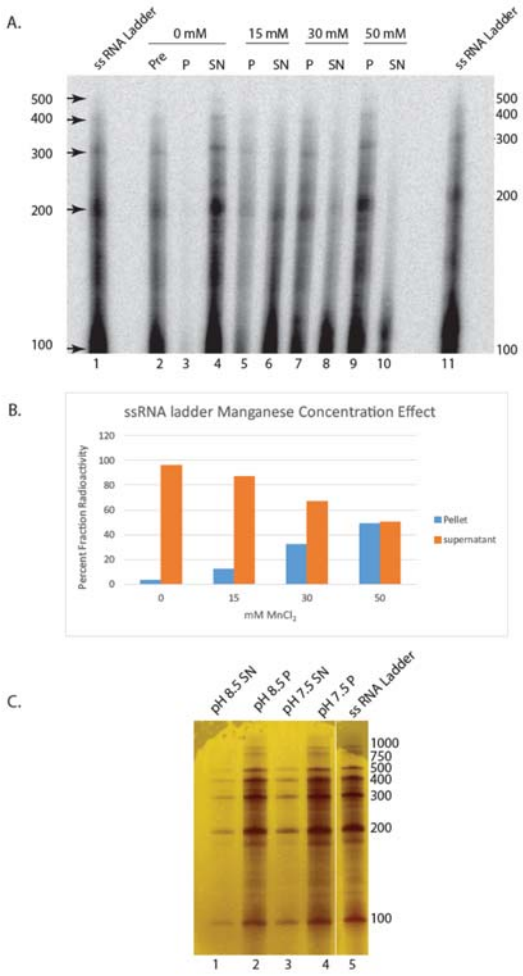
A.
ss RNA Ladder
0 mM
15 mM
30 mM
50 mM
Pre
P
SN
P
SN
P
SN
P
SN
ss RNA Ladder
500
400
300
200
100
1
2
3
4
5
6
7
8
9
10
11
B.
ssRNA ladder Manganese Concentration Effect
Percent Fraction Radioactivity
120
100
80
60
40
20
0
0
15
30
50
mM MnCl2
Pellet
supernatant
C.
pH 8.5 SN
pH 8.5 P
pH 7.5 SN
pH 7.5 P
ss RNA Ladder
1000
750
500
400
300
200
100
1
2
3
4
5

Figure 3.4: Single-stranded RNA ladder subject to various concentrations of $MnCl_2$

A. A single-stranded (ss) RNA ladder was transcribed in the presence of ^{32}P CTP, dosed into total RNA from yeast, treated with various levels of $MnCl_2$ (lanes 2-10) and separated on a 5% PAA gel. Lanes (1, 11) are untreated ssRNA ladder. Lane 2 is an untreated ssRNA ladder spiked into total RNA from yeast (Pre). The letter "P" represents pellet fraction and "SN" represents supernatant fraction following $MnCl_2$ addition. The 0, 15, 30, and 50 mM are doses of $MnCl_2$. **B.** Percent fraction of total tube counts for the pellet and supernatant of a radiolabeled ssRNA ladder spiked into total RNA from yeast following various treatments of $MnCl_2$. Four replicates of the pellet fraction and supernatant fraction were beta counted for each concentration of $MnCl_2$ (0, 15, 30, and 50 mM). The pellet and supernatant fractions correspond to the RNAs separated by the gel on part A. **C.** 6% PAA gel of ss RNA ladder treated with $MnCl_2$ at varying pH's. For lanes 1 and 2, the $MnCl_2$ treatment was carried out at pH 8.5 and Lanes 3 and 4 the $MnCl_2$ treatment was carried out at 7.5. (Data from Paul Freidhoff as personal communication.)

Lastly we demonstrate the power of this $MnCl_2$ precipitation method in combination with primer extension to map the 5' ends of viroid RNA being processed in yeast. Identifying specific transcripts or processing intermediates by primer extension can be challenging when analyzing total RNA. These challenges include nonspecific primer binding or failure of primer binding due to low levels of transcripts. Our results (Figure 3.1-3.3) indicate that MnCl2 can enrich RNA fractions of 422 nt and below, therefore MnCl2 enrichment could be of value for primer extensions mapping the 5' ends of tetraloop or trihelix PSTVd transcripts (381 and 390 nt respectively). To test this, we doped 60 μg of total RNA from yeast with 1000, 100, 10 fmol of a viroid transcript of 390nt in length (triH). The fractions were then split and 30 μg was directly analyzed by primer extension for detection of the PSTVd transcript. The other 30 μg was treated with $MnCl_2$, ethanol precipitated and then anlayzed by primer extension. Figure 3.5 presents the results. The 5' end of the initial triH transcipt should be at position G80 (lane 1). RNA from yeast that were not doped with trasncript, with and witout $MnCl_2$ enrichment were used in lanes 2 and 3. Lanes 4 and 5 present total RNAs spiked with 500 fmol of triH RNA. There is a clear

signal at G80 (lane 4) for the RNA that was $MnCl_2$ treated. This signal does not appear in the non-$MnCl_2$ treated fraction (lane 5). When the dose of the transcript was dropped to 50 or 5 fmol no signal was seen at G80 regardless of $MnCl_2$ enrichment (lanes 6-9).

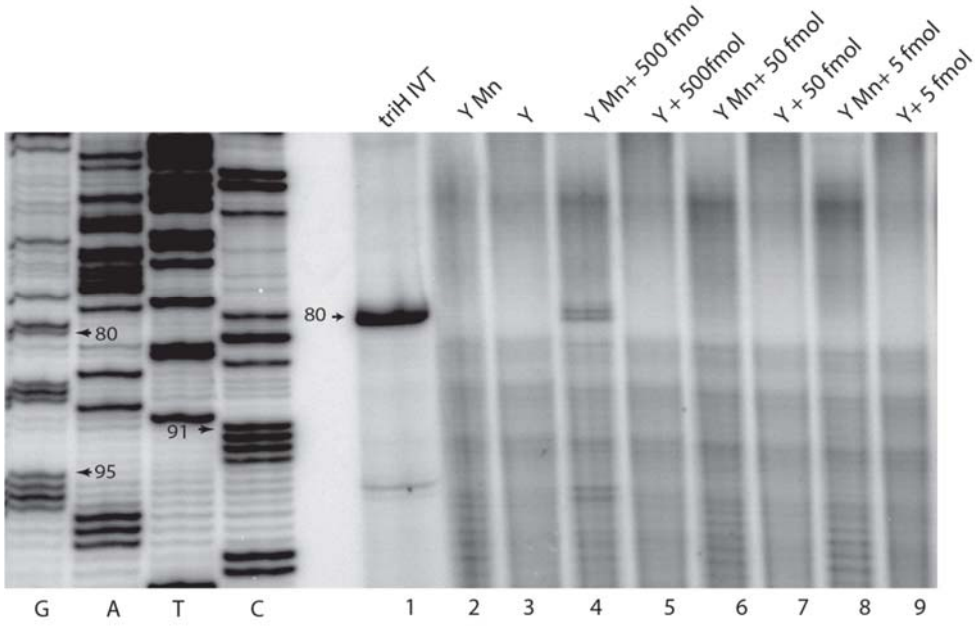

Figure 3.5: Primer Extension of total RNA from yeast spiked with viroid transcript

Total RNA was prepared from the yeast strain YPH500 (Y). The RNA (60μg) was dosed with 1000, 100, and 10 fmol of viroid trasncript of 390 nt (triH IVT). From this, 30 μg was taken and analyzed by primer extension. The other 30 μg was treated with $MnCl_2$, ethanol precipiated and then subject to primer extension (Mn). The 5' end of the triH IVT begins at position 80 of PSTVd sequence. For numbering refer to Gross *et al*. (169). Lane 1 is the triH IVT alone (0.5 pmol) . Lanes 2 and 3 are undosed YPH500 RNA, untreated and treated with $MnCl_2$ respectively. Lanes 4-9 are dosed with the indicated amounts of transcript. Lanes 4, 6, and 8 are all treated with $MnCl_2$. Lanes 5, 7, and 9 are not treated with $MnCl_2$.

To analyzie the utility of $MnCl_2$ enrichment of a transcript produced *in vivo*, the yeast strain rat1-107 was transformed with a PSTVd expression construct (pTL) to yield linear PSTVd transcripts. The initial transcript from TL is the same as triH on the 5' end. RNAs were then extracted from yeast and one subset was $MnCl_2$ enriched an the other was not. A primer

extension to map the 5’ of the PSTVd transcript (Figure 3.5) was performed. An *in vitro* transcribed TL was used asva size marker (lane 1). Total RNA from yeast rat1-107 trasnformed with TL was used as template for lanes 2 and 3, which have 25 µg of untreated and 18 µg of $MnCl_2$-treated total RNA respectively. The transciption start site (red arrow lane 3) was seen only in the RNA that was treated with $MnCl_2$, additional 5'-processed bands may be seen below it.

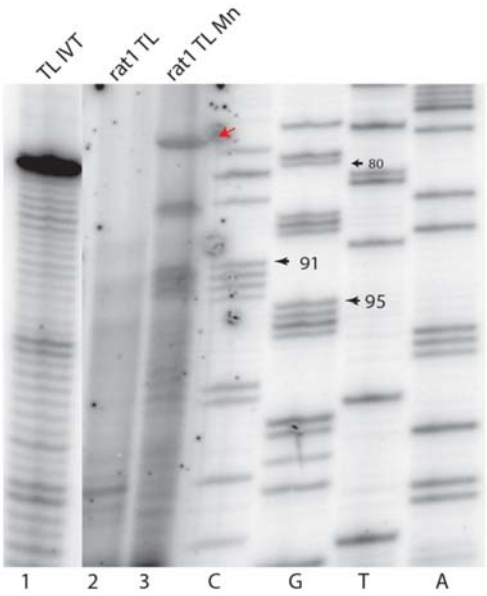

Figure 3.6: Determination of RNA 5’- ends for viorid species detectable *in vivo*

Total RNA was prepared from a yeast rat1-107 mutant expressing a PSTVd TL construct. Untreated (25µg) and $MnCl_2$ -treated RNA (18µg) were analyzed by primer extension. An *in vitro* transcript (0.5 pmol) of TL (Lane 1) was the control. The 5’ ends of the *in vitro* transcript starts at position G80. Lanes 3 and 3 represent TL transformed into rat1-107 without and with $MnCl_2$ treatment. Position -2C (red arrow) is the yeast transcription start sites in constructs harboring a *GAL1* promoter. Position G80 marks the first PSTVd base.

The enrichment of specific RNAs is of critical importance to studies of *in vivo* RNAs. Several methods are already employed toward enrichment of certain RNA types/sizes (186, 202-205). We have optimized a reported methodology for the specific enrichment of viroid sized

RNA fragments (186). Specifically, we have demonstrated the specific sizes of modified viroid and single-stranded RNA enriched by this method. We have demonstrated the utility of the method by showing increased sensitivity for primer extensions of low quantity transcripts from total RNA in yeast (Figure 3.5 and 3.6). $MnCl_2$ enrichment is a simple and effective way to enrich non-coding RNAs of 420 nt and below from a total RNA extractive.

Chapter 4: Investigation into the Processing of PSTVd in a Yeast Whole Cell Extract

Abstract

Yeast is a very robust and viable model system used for many types of RNA studies. Knockout strains and temperature sensitive mutants have been created for both essential and non-essential genes in yeast. This allows for very thorough and fast screening of proteins required for RNA processing studies. To further streamline the use of yeast, a yeast whole cell extract provides even more agility with RNA-protein interactions. Studies have shown that viroids are capable of processing in yeast *in vivo* systems however; this process is time consuming and unpredictable. Using yeast whole cell extracts to study viroid processing, allows us to obtain important information before moving to an *in vivo* system. In this study, we present evidence that a yeast whole cell extract is capable of cleaving PSTVd to unit length monomer. We do not have concrete evidence that this whole cell extract can ligate to mature PSTVd circles; however not all processing condition studies have been exhausted, so further study is warranted.

Introduction

The use of yeast whole cell extracts to monitor RNA processing is not a new concept or a new experimental system for studying RNA. Starting in the early 1980's yeast whole cell extracts were used for *in vitro* transcription and splicing assays (206, 207). Recently, it was shown that yeast whole cell extracts can be used to study the structure and replication of a plant virus (208). However, the use of yeast whole cell extracts in studying viroid processing is a new

concept. In this work, we have shown that yeast is capable of processing PSTVd *in vivo*. Thus, we have reason to believe that viroids can process in an *in vitro* yeast system.

The processing of PSTVd in a yeast whole cell extract has many benefits. From previous studies, we have shown that processing of PSTVd *in vivo* is not an efficient process and one where degradation occurs quickly. Also, the expression of PSTVd in an in *vivo yeast* system is a fastidious and time-consuming process. Not all yeast expression vectors are suitable for launching viroids in yeast and require careful selection of a suitable promoter. The use of an extract allows for increased sensitivity when using radioactive transcripts. In addition, we have previously showed that the use of manganese chloride enriches viroid RNA, this enrichment would have even more utility in a whole cell extract where the spiking of the transcript is controlled and not dependent on a promoter.

By using an *in vitro* system while controlling the levels of transcripts entered into the processing, we could enrich processing intermediates as well. The *in vitro* system allows manipulation of the transcript ends to obtain insight into the ligase involved in processing. Identifying the proper conditions for yeast whole cell processing of PSTVd allows us to have access to the yeast knockout strains and temperature-sensitive mutants without having to transcribe PSTVd *in vivo* (115). This system to quickly screen processing proteins before moving to an *in vivo* system

Previously, Baumstark, *et al*. (63, 88, 89) demonstrated that PSTVd processes in a potato nuclear extract. Yeast whole cell extracts have benefits over potato nuclear extracts as well. For one, maintenance of a potato callus requires additional facilities and expertise to maintain. Secondly, the process of making the potato nuclei is more time consuming and tedious compared

to yeast whole cell extracts (88, 209). The growth and maintenance of yeast is magnitudes easier than that of callus maintenance and protoplast formation.

The potato nuclei however were a very robust and reliable system for PSTVd studies. Using these nuclear extracts, Baumstark *et al*. (88) discovered that the only one of four possible structures of a specific IVT were capable of processing into a circle. Using various conditions, they were able to manipulate the transcript to adopt four possible structures. The structure responsible for processing exhibited a tetraloop structure within its central conserved region (TL IVT) (63) . We have the same exact transcript and have prior *in vivo* data that would support that this transcript can process in a yeast whole cell extract. We also have a complete monomer that only required ligation in yeast, but did not circularize *in vivo.* The 5' and 3' ends of the transcripts is vital to the ligation and we can test ligation effects by changing the 5' and 3' transcript ends and assaying for circle formation. Setting up the *in vitro* system will save significant time in the screening process for viroid-protein interaction studies. Apart from RNA-protein studies, the *in vitro* system will allow for structural studies that cannot be performed *in vivo*. To date, *in vivo* structural analysis is limited to SHAPE (selective 2'-hydroxyl acylation analyzed by primer extension), DMS modification, and structure-seq (210, 211).

Materials and Methods

Transcript Formation

The plasmid used throughout this study was the TB110 (TL IVT/ Appendix Table 3) transcript that was produced according to Baumstark *et al*. (63, 180). Linearization of the plasmid by EcoR1 followed by *in vitro* transcription in the presence of ^{32} P-UTP yields 5' vector-

derived pppG and a vector-derived AAUU at the 3' end. The transcript was purified using a G50 spin column.

Yeast whole cell Extract

The yeast whole cell extract was a gift from Dr. Beate Schwer. This extract was produced using a method adapted from Umen and Guthrie (209). The extracts are stored at -70^{0}C and are stable for at least 6 months (207).

Processing Reaction

Processing reactions were performed in 50 µl volumes and incubated at room temperature for various times (see figure legends). Various volumes of yeast whole cell extract to transcription buffer (20 mM HEPES-KOH, 50mM KCl, 10mM $MgCl_2$, 5mM EGTA, .05 mM EDTA, 2.5 mM DTT, 10% glycerol) were used throughout the study and these conditions are outlined within the figure legends. Each reaction contained between 10^5-10^6 cpm of ^{32}P labeled TL IVT. Each reaction also contained 40 units of Riboguard RNase Inhibitor (Epicentre). The reactions were stopped using 150 µl of stop mix (27mM EDTA, 0.5% SDS). Following this, the RNA was extracted by phenol-chloroform and ethanol precipitation. Approximately 10^3-10^4 counts of RNA were loaded and analyzed on a denaturing 5% polyacrylamide-8M urea gels. The gels were dried and the signals were measured using a Storm 840 Phosphoimager.

Results

The TL IVT cleaves *in vitro* in a yeast whole cell extract

The RNA substrate used throughout this study was the same RNA substrate shown to process in yeast nuclear extracts (88). We were able to demonstrate that the TL IVT follows a similar cleavage pattern in a yeast whole cell extract (Figure 4.1 and 4.2). Figure 4.1 indicates that the TL IVT will undergo multiple cleavages to start of the processing cycle as previously shown in potato nuclear extracts (63, 88).

To fully investigate the cleavage process, we conducted semi-log plotting of the bands (Supplemental Figure 4.1). The viroid cleavage pattern was similar to Baumstark *et al*. (88). Using the semi-log plotting, we see signs of full length product (FL), cleavage 1 (L1), and cleavage 2 (L2).

We varied multiple conditions to monitor both the cleavage and possible ligation of TL transcript. The first variables that were manipulated were ratios of yeast whole cell extract (YE) to buffer. The reactions were carried out at multiple incubation times. (Fig 4.1). Figure 4.1 shows that cleavage is seen in all cases (Lanes 2-8). Qualitatively, lower incubation times may be favorable (Lanes 2-3, 6-7) as seen by visual band intensities. These conditions still needed refinement as no circle progeny were detected under the conditions listed within Figure 4.1. According Baumstark *et al*. (88) the circle would migrate above 1631 base pairs.

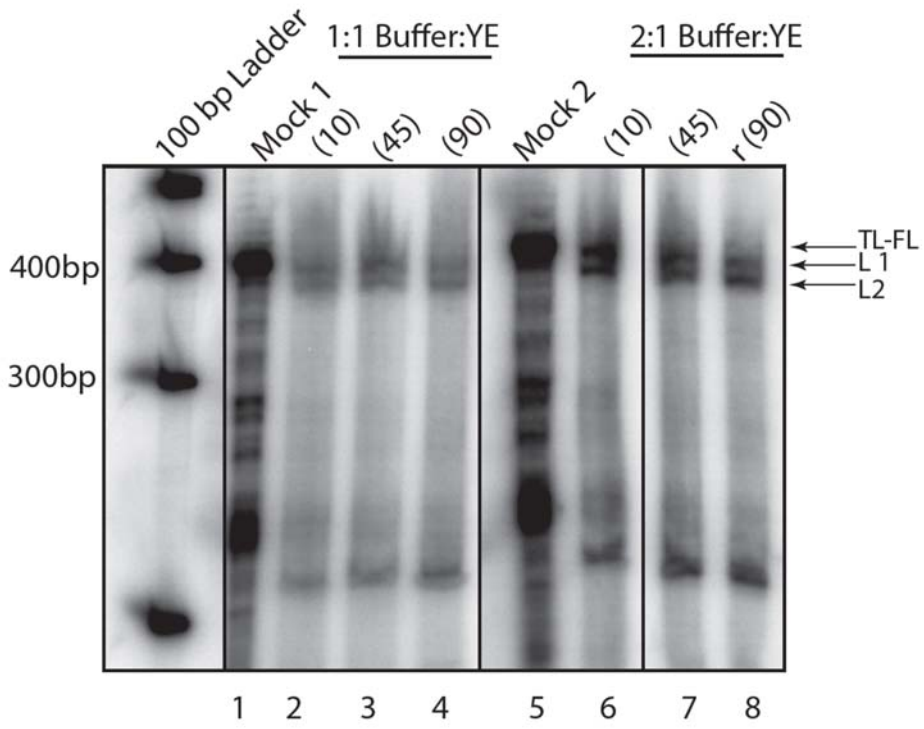

Figure 4.1: Cleavage of TL IVT in yeast whole cell extract

A total of 10^5 cpm of ^{32} P labeled TB110 IVT were used for the reactions. For loading, 10^4 counts of RNA were loaded into each well. Mock represents a reaction in which no yeast whole cell extract (YE) was used. Reaction times are denoted in parenthesis. Lanes (2-4) contain an equal volume of buffer to YE. Lanes (6-8) contain twice as much buffer to YE. The full-length transcript (FL-TL), and the two cleavage products (L1 and L2) are marked by arrows. Sizes were calculated according to Supplemental Table 4.1.

In order to optimize both conditions for cleavage and ligation, levels of YE, incubation times, and reaction conditions were varied (Figure 4.2). Each reaction within the set had an additional 0.4 mM rNTP mix added to ascertain if additional rNTP were necessary for the initial processing step. Additional conditions were tested by adding 10mM KCl, 2 mM ATP, and 3mM $MgCl_2$. These conditions were added to assess optimal buffer ionic strength (KCl), additional energy source for processing enzymes (ATP), and cofactor for optimal processing enzyme

activity ($MgCl_2$). Again, there signs of cleavage in most conditions (lanes 3-18), but still no clear signs of ligation. A reaction containing 20% YE that was incubated for 15 minutes with additional KCl gave the best cleavage signal in this experimental set (Lane 11). The bands within this gel appeared hazy and aberrant likely due to residual protein binding to the RNA. The residual protein would obscure the migration of the RNA.

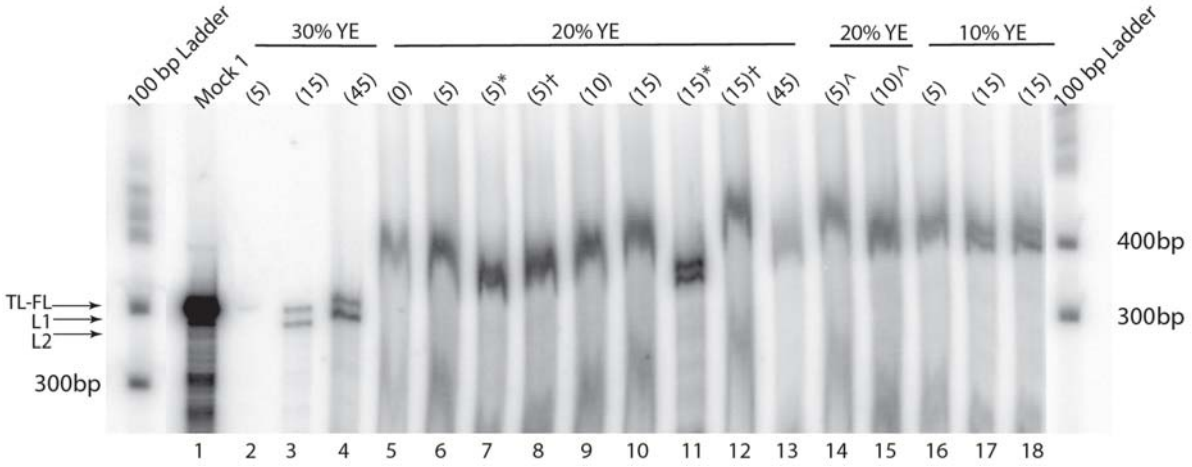

Figure 4.2: Cleavage of TL IVT in YE with varying incubation times and reaction conditions

The amount of spiked transcript and mock reactions are the same as Figure 4.1. A total of 10^4 counts of RNA was loaded into each lane. Lanes (2-5) represent 30% YE used within the reaction and the incubation times increase from 5-45 (min). Lanes (5-13) contain 20% YE with varying incubation times denoted in parenthesis. The asterisks represent a reaction in which 10mM potassium chloride was included. The cross represents the addition of 2mM ATP contained within the reaction. The ^ represents the addition of 3 mM $MgCl_2$ within the reaction. The full-length transcripts and cleavage products are marked according to Figure 4.1. Every reaction contained 0.4mM rNTP mix.

Discussion

As previously stated, the possibility of creating a PSTVd processing assay in yeast whole cell extracts opens the door to rapid screening of PSTVd processing proteins with the full availability of the toolbox of yeast knockouts and ts mutants. Growing and launching PSTVd RNAs in yeast is time consuming and sometimes un-predictable. An *in vitro* system would cut the screening time significantly before moving to an *in vivo* yeast system.

Toward this end, we have demonstrated that a whole cell yeast extract is capable of cleaving PSTVd RNA but not ligation into mature viroid circles or complete cleavage to unit length monomers. Both the lack of potential unit length monomers and circles can be attributed to exoribonucleases present in the yeast whole cell extract. Additionally, the cleavage pattern seemed to be characteristic of the cleavage pattern seen in other *in vitro* processing systems (88).

Our previous work with an *in vivo* yeast system (Chapter 2) indicated that circle formation was a delicate balance of degradation and processing. We were able to show that a knockdown strain of the yeast exoribonuclease (*RAT1*) had a positive effect on the production of primary transcripts and PSTVd circles (Chapter 2 supplemental information). Other studies have shown that another exoribonuclease *XRN1* had a positive effect on ASVBd linear and circle production in yeast (128). The ribonuclease inhibitor used in our assays protects against RNase A, B, and C. The inhibitor is more designed for inhibition of RNases during *in vitro* transcriptions and may not be effective against *RAT1* or *XRN1*.

We have shown conditions that appear to optimize the initial cleavage events, but circles may not be formed because the correct substrate to circularize is being degraded quickly by host

machinery. PSTVd degradation is very host specific and can vary from system to system (111). We believe that yeast is a system with high levels of degradation prior to ligation events.

The next steps will include making yeast whole cell extracts in the xrn1Δ strain and the *RAT1-107* strain and then assaying for circle production with the TL transcript. In addition, the pre-treatment of the transcript was shown to be of importance to the processing. Baumstark *et al*. (88) snap cooled the transcript prior to use. This step would ensure that the RNA is folded correctly for processing to occur. We will conduct these experiments using the initial conditions in Figure 4.1. Only upon clear signs of unit length monomer, can the buffer conditions be optimized. This optimization would allow for maximum circle formation and insights into conditions needed for the host nuclease and ligase.

In conclusion, processing by the yeast whole cell system requires some significant optimization. The RNA degradation machinery within yeast is very active with regard to PSTVd processing. Whole cell extracts contain RNases in both the cytoplasm and nucleus. The use of a nuclear extract instead of the whole cell extract may aide with reduction in RNase activity within yeast.

Supplemental Information

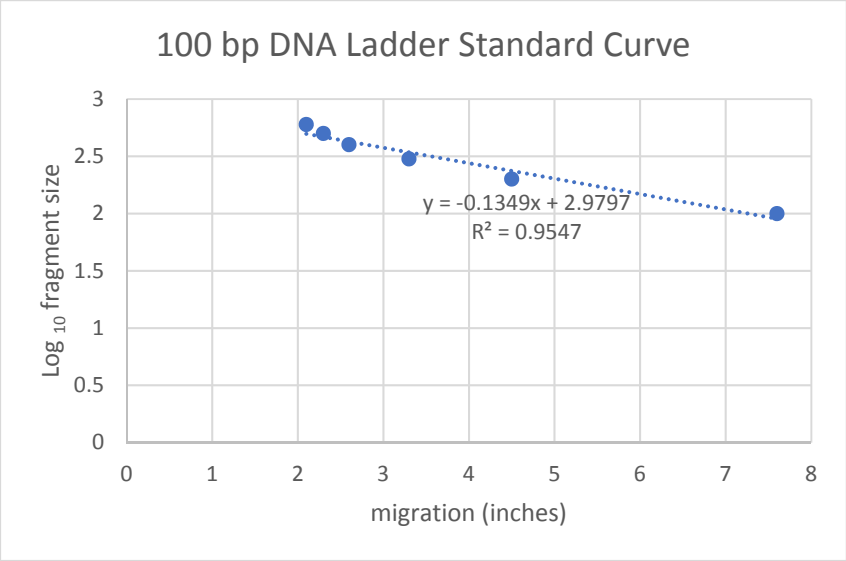

Sample	Cleavage	Migration (inches)	Log 10 frag size	size Kb
Mock 1 (1:1)	FL	2.7	2.60577	403.4316812
10 (1:1)-	L1	2.71	2.604421	402.180491
	L2	2.81	2.590931	389.8800383
45 (1:1)	L1	2.7	2.60577	403.4316812
	L2	2.77	2.596327	394.7544187
90 (1:1)	L1	2.7	2.60577	403.4316812
	L2	2.77	2.596327	394.7544187
Mock 2 (2:1)	FL	2.6	2.61926	416.1596791
10 (2:1)	L1	2.61	2.617911	414.8690148
	L2	2.65	2.612515	409.7462617
45 (2:1)	L1	2.62	2.616562	413.5823533
	L2	2.72	2.603072	400.9331813
90 (2:1)	L1	2.63	2.615213	412.2996822
	L2	2.74	2.600374	398.4501549

Supplemental Table 4.1: Semi-log plot of Band migrations of the bands in Figure 5.

Chapter 5: Cloning of New PSTVd Yeast Expression Systems

Abstract

The available collections of knockout strains and temperature sensitive mutants makes yeast a great model system for studying RNA-protein interactions, including those essential to RNA plant pathogen-host interaction. We have shown that PSTVd can process in yeast, but have been limited to a few yeast strains due to the expression construct that was used. Here we sought to modify this expression construct to allow its use in more yeast strains. The creation of the expression construct has proved challenging, and we have found that not all yeast expression systems may be suited to express PSTVd RNAs. Subtle, and yet uncharacterized, alterations in our new constructs have prevented the expression of RNAs that are processed in yeast. The key elements of our previous expression system that allowed for PSTVd processing in yeast need to be further examined for future research.

Introduction

Yeast is a highly studied, highly characterized and convenient molecular biology tool for *in vivo* and *in vitro* studies (112). Due to extensive genomic studies, knockout strains for every nonessential gene in yeast have been created (115, 116). As for essential genes, knockdown or temperature sensitive (ts) mutant collections have also been created (117). These collections of strains make yeast a very powerful model system to study RNA-protein interactions.

The Ahlquist lab pioneered the use of yeast as a model system to study RNA plant pathogens. They were able to express the brome mosaic virus (BMV) in the yeast strain YPH500

(120, 121). This was followed by a whole series of studies in yeast where replication, localization, and RNA-protein interactions of RNA plant pathogens were determined (212). Yeast has even been used to study processing of viroids (128).

Using yeast as a model system to study viroids is an enticing prospect for viroid-protein interactions. Since 2011, significant progress has been made regarding enzymes and proteins involved in viroid processing. Many of the proteins that have been implicated in viroid processing have analogs in yeast. Nohales *et al*. (96) implicated DNA ligase I as the enzyme involved with ligation of viroid circles using tobacco as a model system. This research can be expanded upon as a DNA ligase I (CDC9) ts mutant exists in yeast and has been well studied for functionality (133, 134). Recently the Dicer-like 4 enzyme in tobacco was suggested to be the enzyme responsible for viroid cleavage (94). The only Dicer-like or RNase III enzyme in yeast is RNT1(213, 214). Again, a gene knockout is available and would allow for quick and directed study of this viroid cleavage in an *in vivo* system. A more recent topic of study for viroid research has been viroid turnover, or decay pathways of replicative intermediates (215). Several studies have shown that yeast mutants of either *XRN* or *RAT1* (exoribonucleases) effect RNA plant pathogen accumulation (128, 179). The genetic research and creation of novel stains in plants has been growing. Many of the viroid studies above to identify proteins have been conducted in Arabidopsis, tobacco, or eggplant; however, this requires the growth of plants that are infected with PSTVd. This can be time consuming and labor intensive. In addition, these systems are not as well characterized as yeast and the yeast systems can provide focused research before moving into plant systems.

We have already shown that in yeast, mutation of *RAT1* to a partial loss-of-function allele does not inhibit PSTVd processing, and may give a slight increase in partially processed

intermediates and circles (Ch2, Supplemental Figure 1). However, the number of RNA metabolism mutants with a Δ*trp* background (needed for selection of the pTBO plasmids) is limited. Thus, to have access to the full toolbox of yeast strains, new PSTVd yeast expression constructs need to be created. The largest collection of yeast knockouts and temperature sensitive mutants exists in the BY4741 background (*MATa his3Δ1 leu2Δ0 met15Δ0 ura3Δ0*). We have attempted to create new PSTVd expression constructs using the pXP722 expression backbone. We have yet to see proper transcription or processing of PSTVd in BY471 (unlike YPH500) using these expression constructs. This finding suggests that not all yeast expression systems are suited for viroid transcription and processing in yeast. The original vector backbone that was created for viroid studied (pB3RQ39) has the correct elements and functionality to launch and process PSTVd in yeast, and this backbone should be used for future studies.

In discussing transcripts produced from our constructs, unprocessed full-length RNAs will be called primary transcripts; RNA from which only the ribozyme has cleaved is called a preliminary transcript. Any RNA on the pathway towards circle formation from the preliminary transcript is a processing intermediate, while those that are no longer capable of making circles are called degraded transcripts.

Materials and Methods

Yeast Strains, cell growth and Transformation

The strains YPH500 (*MAT*α *ura*3-*52 lys2*-801 *ade2-101 trp1*-Δ*63 his3*-Δ *leu2*-Δ*1*), BY4741 (*MATa his3Δ1 leu2Δ0 met15Δ0 ura3Δ0*), xrn1Δ (same as BY4741, but YGL173c: KanMX4) and BMA64 (*MATα ura*3-1; trp1Δ; ade2-1; leu2-3,112; his3-11,15) were used in this study. Yeast cultures were grown at 30˚C in synthetic media containing either 2% glucose or 2% galactose for suppression or stimulation of the *GAL1* promoter. Tryptophan was not added to the media for plasmid maintenance. Transformations were carried out with the Frozen-EZ yeast transformation II kit from Zymo Research (T2001). A *RAT1* mutant strain was also used in this study. The plasmid for creation of the *rat1-107* allele (A661E) was a gift from Dr. Eric Phizicky (181). The plasmid harboring the mutant was digested using *Aat*II and *Bam*H1. The digest was run on an agarose gel and the 5551bp fragment containing the *RAT*1 mutation with the *URA* maker was excised and purified. The excised fragment was transformed into the YPH500 genome and selected against *URA* and *TRP* markers. Additionally, the *BMA64 (RNT1 wt)* was supplied by Dr. Guillaume Chanfrau (216).

Oligonucleotides

Oligonucleotides were obtained from Invitrogen and are listed in Appendix Table 1.

Yeast Expression Plasmid Construction

The existing PSTVd expression plasmids were all cloned into the yeast expression plasmid pB3RQ39 (*trp1*, *CEN4*, *GAL1* promoter; see Appendix). The plasmid also contains a hepatitis delta ribozyme to allow for creation of exact 3’ ends after transcription (180).These

plasmids give us tools for transcribing PSTVd sequences corresponding to the tetraloop (TL), trihelix (triH), dimer, and monomer as described in the Appendix Table 2 .

A new set of plasmids was created using the pXP722 yeast expression plasmid (*ura*3, *CEN*6, *GAL1* promoter) (217). The TL and triH PSTVd sequences from above were placed into the *Spe*1 site of pXP722 using custom gene synthesis (Biomatik Corp., Cambridge, ON, Canada). The only change in PSTVd sequence was that in pTBO TL the 3' GACAU sequence (terminally repeated nt 96 and a four-base vector insert) between nt95 and the delta ribozyme was omitted in the synthesized plasmid. The pXP722 backbone was modified by inserting an *Xba*I site 3' of the *CYC1* terminator. A series of modifications was made to these purchased plasmids and is summarized in Table 5.2. See Appendix Table 2 for descriptions of all plasmids used in this study.

Table 5.2A: Plasmids used in this study

Plasmid Name	Description
pTBO TL	TL forming construct within pB3RQ39 backbone
pTBO triH	triH forming construct within pB3RQ39 backbone
pTL	TL forming construct within pXP722 backbone (original purchase)
ptriH	triH forming construct within pXP722 backbone (original purchase)
pTL#1	TL with *CYC1* terminator removed using *Xba*1
tpriH#14	triH with *CYC1* terminator removed using *Xba*1
pTL2A	pTBO TL was amplified using Delta BstX1 d F and Xho nru bb R. This fragment was digested with *BstX*1 and *Sal*1 and was placed within *BstX*1/*Sal*1 site of TL yielding modified delta ribozyme and 3' vector sequence (31 additional bp past delta)
pTL4B	pTBO TL was amplified using Delta BstX1 d F and Xho nru bb R. This fragment was digested with *BstX*1 and *Xho*1 and was placed within *BstX*1/*Sal*1 site of TL yielding modified delta ribozyme and 3' vector sequence (131 additional bp past delta)
pTL3	pTBO TL was digested with *Age*1 and *Eag*1 and 392 bp fragment was gel purified and inserted into *Age*1/*Eag*1 digest of pTL yielding modified *GAL1* promoter region
ptriH3	The 392 bp pTBO TL *Age*1/*Eag*1 fragment was inserted into *Age*1/*Eag*1 digest of triH yielding modified *GAL1* promoter region

*oligos used are underlined

Table 5.2B: pTL Design

Position	Description
1-464	pXP77
465-466	added to make restriction site
467-468	TBO14-163
468-484	5' CCR duplication
485-843	PSTVd monomer (96-359/1-95)
844-936	delta ribozyme
937-946	Duplicates bases 3' to ribozyme to allow XbaI deletion of *CYC1* transcription terminator without changing ribozyme 3' end
947-5361	pXP77

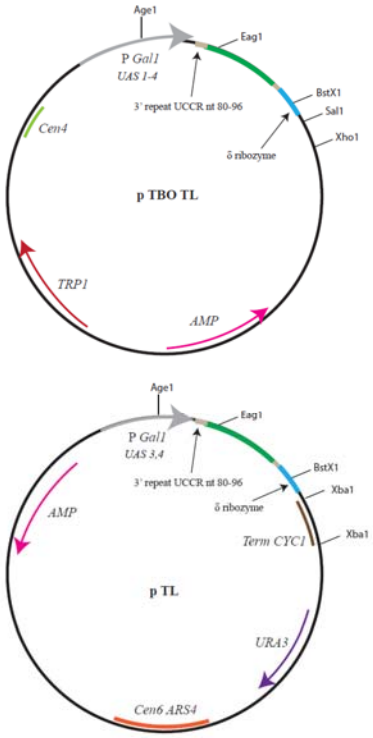

Figure 5.1: Plasmid design for PSTVd yeast expression systems

A. Original pTBO TL plasmid design with TRP marker B. Original design of plasmid TL, a PSTVd momomer with duplication inserted into pXP722. The monomer with a seventeen-nucleotide duplication (16 3' and 1 nt 5'). Key restriction sites as well as selectable markers are noted.

Agarose Gel Extraction

DNA in an agarose gel was visualized using ethidium bromide and gel-extracted by excising and soaking a gel fragment. DNA was purified using a Promega PCR clean up kit.

RNA Extraction

Yeast containing the appropriate plasmid was grown in the selective media to an OD of 0.6-1.0. Total RNA was extracted from 10 OD /mL of cells using the hot phenol extraction method (183), resulting in ethanol precipitated RNA.

Reverse Transcription PCR for Detection of plus-PSTVd and PSTVd Circles

One microgram of total yeast RNA was treated with DNase I (Invitrogen). The RNA was then phenol chloroform extracted and ethanol precipitated. After this, 3 ng of total RNA was subjected to reverse transcription (Invitrogen superscript III) using 20 pmol of the primer 259R (Appendix Table 1) in 10 µl. One tenth of this product was used for PCR amplification. The amplifications were carried out in 12.5 µl of 2x Go Taq (Promega) with 25 pmol of the following primers: 259R/112F for plus-PSTVd and 259R/2F for circles. The following program was run on an Eppendorf thermocycler: 5 mins at 95˚C, 30 cycles of 30s at 95˚C, 40 s at 64˚C, 60s at 72˚C followed by 5 mins at 72˚C and a 4˚C hold. Products were separated on a 5% polyacrylamide-8M urea gel.

RNA Detection by Northern Blotting

Total RNAs (5μg) were separated on a 5% polyacrylamide-8M urea gel and were semi-dry electroblotted to a Hybond N+ membrane (GE Healthcare). The membranes were incubated in UltraHyb solution (Ambion) overnight at 65°F with the appropriate riboprobe. The riboprobes for detection of PSTVd, actin, and ScR1 were generated by *in vitro* transcription of PCR products either obtained from a plasmid (PSTVd) or from genomic DNA from yeast (actin and *SCR1*) (185). The PCR fragments were produced using the primers listed in Table 1. The *in vitro* transcriptions were performed in the in the presence of [α-^{32} P] UTP or CTP. The membranes were washed with 2x SSC (1x SSC is 0.15M NaCl + 0.015M sodium citrate) and 0.1% SDS four times (2x10 minutes and 2x20 minutes) at 65°F. The membranes were exposed to phosphor screens and the signals were measured using a Storm 840 Phosphorimager.

Manganese Chloride Treatment of Total RNA from Yeast to Enrich Small RNAs

For enrichment of viroid linear intermediates, total RNAs from yeast were treated with manganese chloride according to Semancik and Szychowski (186). RNAs at a concentration of 100ng/μL were treated with 50mM $MnCl_2$ in 0.1xTE. After incubation at 4°C, the solution was centrifuged at 15K rcf for 5 minutes. The supernatant containing the small RNA fraction was then ethanol precipitated.

Primer Extension

Oligonucleotide MB1R (Appendix Table 1) binds plus-strand nts 150-133. The primer was 5'-end-labeled with [γ-^{32} P] ATP using T4 polynucleotide kinase (Invitrogen). Approximately 10^6 cpm of this primer was annealed to 6.1 μg of manganese treated RNA from yeast, and to 0.5 pmol of viroid *in vitro* transcript. The extension was conducted using 100 units

of reverse transcriptase (Superscript III kit, Invitrogen). After extension for 90 minutes at 52°C, the reaction was stopped and the products were ethanol precipitated. A DNA sequencing ladder was generated using primer MB1R and PCR fragment encompassing the PSTVd sequence from the plasmid harboring the trihelix sequence. The ladder was formed using Sequitherm cycle sequencing kit (Epicentre Technologies). The products from the primer extension and the ladder were run on 8% (19:1) acrylamide, 8M urea sequencing gels.

Results

In order to utilize the entire tool box of yeast molecular biology and mutant strains to the study of PSTVd RNA processing, we required an expression construct that contained a uracil selectable marker. pTBO TL is a PSTVd expression construct that set up PSTVd for processing in strain YPH500 (see Figure 5.1). We wanted to keep key elements of this construct, but in a new vector backbone with more convenient restriction sites and a *URA3* selection marker, leading us to have pTL created using total gene synthesis. Additional changes included the removal of the insertion GACAU between the PSTVd sequence and the delta ribozyme and the use of a better characterized transnscription terminator 3' to the ribozyme. Apart from the differences detailed above, the PSTVd and ribozyme sequences were identical to those in previous work (Appendix Table 2) . The *GAL1* promtoer is slightly different between the two constructs, as pTL only contains UAS (upstream activating sequences) 3 and 4, while pTBO TL cotains UAS 1-4 (Figure 5.1). The pXP722 series has additional bases 3' to the transcription start site replacing UAS 1-2. Both constructs contain a gene for ampicillin resistance and the CEN6 ARS origin of replication. ptriH is identical to pTL except that the trihelix 3' CCR duplication extends to PSTVd nt 110 5' to the ribozyme.

The PSTVd constructs designed with the pXP722 yeast expression vector backbone did not yield any successful viroid processing, nor did they show signs of high expression of preliminary transcripts in strain BY4147. The only expression constructs to yield preliminary transcripts and viroid circles was the original pTBO TL construct in the strain YPH500. Figure5.2 shows the northern blot giving the first indication of lack of proper viroid transcription and processing. Lane 5 contains the positive-control, pTBO TL in YPH500. We see the preliminary transcript, a shorter processed linear, and the circle, as seen previously (Chapter 2). Lane 8 contains the pTBO triH in YPH500. This construct does not form a circle, but does show two processed linear transcripts, neither long enoughto be the preliminary transcript, consistent with previous studies (Chapter 2). The new pXP722 backbone constructs (TL, triH) do not yeild a preliminary transcript or circle in either strains xrn1Δ or BY4741. There is a viroid product with electrophoretic mobility somewhere between preliminary transcript and viroid circle (Lanes 6-7, 9-10). Both pTL and ptriH gave essentially the same size bands.

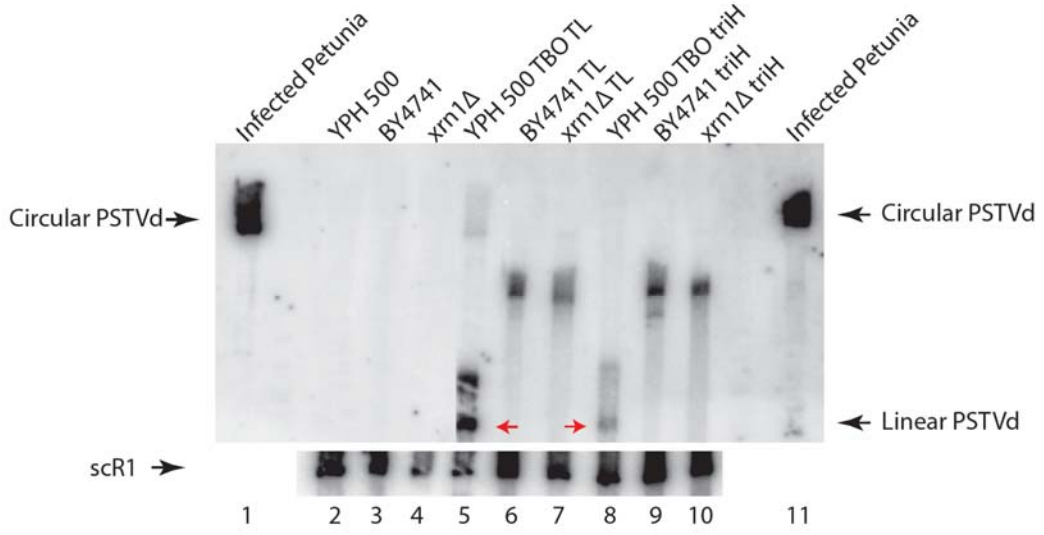

Figure 5.2: Northern blot analysis of total RNA from PSTVd expression constructs in yeast.

Total RNAs from infected petunia (lane 1), empty YPH500 (lane 2), empty BY471 (lane 3), empty xrn1Δ (lane 4), YPH500 transformed with the constructs as indicated (lanes 5,8), BY4741 transformed with constructs as indicated (lanes 6, 9) and xrn1Δ transformed with constructs as indicated (lanes 7, 10) were separated on a 5% PAA and blotted onto positively charged nylon. Yeast were grown under galactose induction or in complete media if not transformed by one of the constructs. Linear and circular PSTVd are marked. For a loading control, the yeast scR1 gene (522 nt) was probed in a second hybridization. Red arrows indicate preliminary transcripts from prior to yeast cleavage/ligation events *in vivo.* The open circle denotes circular products resulting from processing of the TL construct *in vivo* (lane 8), or of circular PSTVd from infected controls (lanes 1, 14). TBO (RQ39 vector backbone) denotes previously used constructs that process (TL) or form preliminary transcripts (triH) in YPH500. The TL, triH are in PXP722 vector backbone (Table 5.2)

Figure 5.2 shows that there is viroid expression, but the product RNAs are not viroid RNAs of normal size. Under these electrophoresis conditions, linear dimers run about even with monomer circles (see Figure 2.3B). Thus, our observed transcripts are longer than TL preliminary transcripts. We postulated that the new transcription terminator did not leave a 3'

end compatible with ribozyme function. Our course of action was to remove the *CYC*1 terminator from the backbone. The terminator was removed from pTL and ptriH by deletion of the small *Xba*I fragment (Figure 5.1). The resulting constructs were designated TL#1 and triH#14 respectively (Table 5.2).

Northern blot analysis (Figure 5.3) indicates that removal of the *CYC*1 terminator did assist in the expression of PSTVd RNAs. Specifically, there was no expression of a preliminary transcript from pTL#1 and for both pTL#1 and ptriH#14, the larger RNAs seen with the terminator disappeared (lanes 7-8, 10-15). However, the migration of several bands might be consistent with circles, these being: BY4741 TL#1 (lane 8), BY4741 triH#14 (lane 11), and xrn1Δ TL#1 and triH#14 (Lanes 13, 15). RT-PCR specific for circles was conducted on these RNAs (Figure 5.4). Unfortunately, the only positive bands for PSTVd circles were detected in the infected petunia (Figure 5.4 lanes 1, 13) and YPH500 transformed with pTBO TL (lane 4) samples.

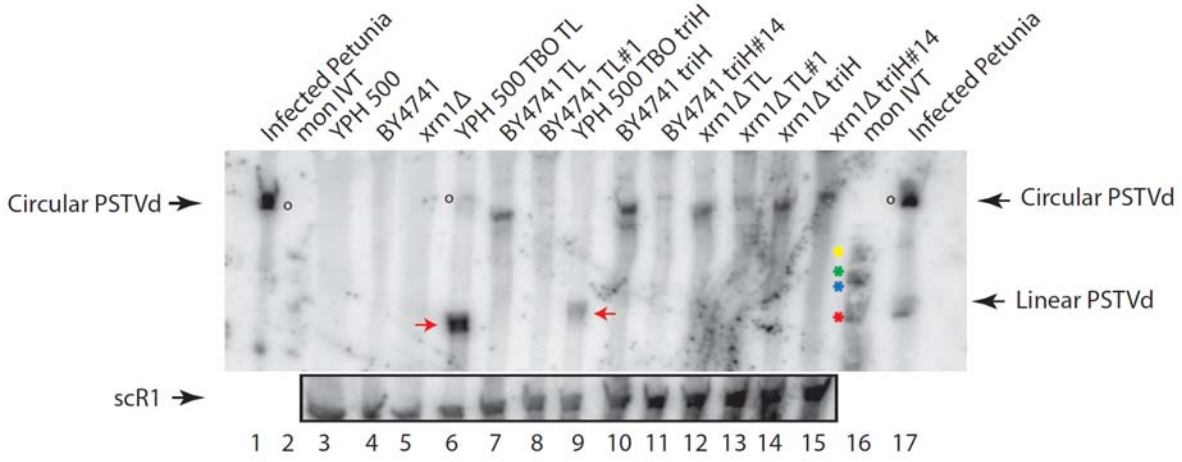

Figure 5.3: Northern blot analysis of total RNA from modified PSTVd expression constructs in yeast.

Total RNAs from infected petunia (lane 1), empty YPH500 (lane 3), empty BY471 (lane 4), empty xrn1Δ (lane 5), YPH500 transformed with the constructs as indicated (lanes 6, 9), BY4741 transformed with constructs as indicated (lanes 7-8, 10-11) and xrn1Δ transformed with constructs as indicated (lanes 12-15) were separated on a 5% PAA and blotted onto positively charged nylon similar to Figure 5.1, as was the probing. Red arrows indicate preliminary transcripts from prior to yeast cleavage/ligation events *in vivo.* The open circle denotes circular products resulting from processing of the TL construct *in vivo* (lane 6), or of circular PSTVd from infected controls (lanes 1, 17). TBO (RQ39 vector backbone) denotes previously used constructs that process (TL) or form preliminary transcripts (triH) in YPH500. The dim, TL, triH are in PXP722 vector backbone. The ribozymes of the monomer IVT (lane 16) did not cleave to completion, resulting in four bands: HH-PSTVd-HP (547 nt, yellow asterisk), PSTVd-HP (482 nt, green asterisk), HH-PSTVd (424 nt, blue asterisk), and linear PSTVd (359nt, red asterisk). This PSTVd transcript was used as an additional loading control. #1 and #14 represent removal of the cyc1 terminator from the original construct (TL and triH) (Table5.2).

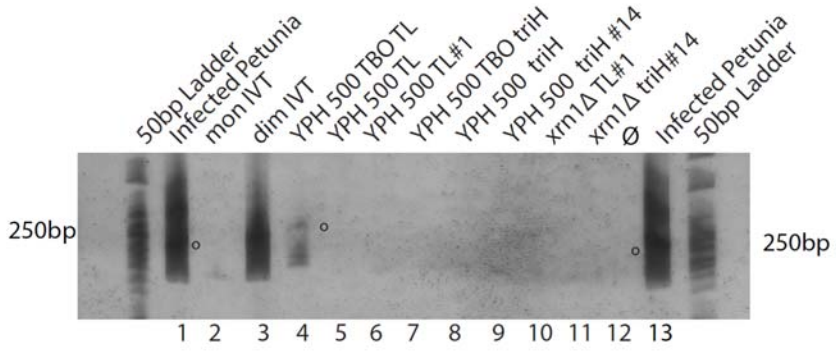

Figure 5.4: RT-PCR for detection of viroid circles in yeast expression constructs

RT-PCR with outward primer set 2F/259R reveals the presence of any PSTVd circles RNA as a DNA fragment of 240bp (Infected petunia) or 248 bp (infected yeast); denoted with a circle. Lanes are: (1, 13) infected petunia, (4-9) RNA from the yeast strain YPH500 transformed with plasmids listed in Table 5.1. Lanes 10-11 are xrn1Δ strains transformed with TL#1 and triH #14. Positive controls were *in vitro* transcripts of monomer (2) and dimer (3). Lane 12 is a transcript-free RT-PCR control. A 50 bp ladder was used as a molecular weight marker.

Since the *CYC*1 terminator was not the culprit for the faulty processing with TL and triH, the focus remained on the prospect of faulty ribozyme cleavage due to interfering 3' RNA. The *BstX*1/*Xho*I fragment of pTL was cut out and replaced with either the *BstX*1/*Sal*I or the *BstX*I/*Xho*I fragment of pTBO TL. This adds either 31 nt (pTL 2A) or 131 nt (pTL 4B) sequence of pTBO TL 3' vector sequence downstream of the delta ribozyme. The modified constructs were confirmed through PCR screening and restriction analysis (data not shown). These new constructs were transformed into BY4741 and YPH500 and analyzed by northern blotting (Figure 5.5). Again, the modifications to the delta ribozyme and 3' sequence past the delta ribozyme did not yield preliminary transcripts or viroid circles in any strain (Lanes 2-3, 6-7).

pTBO triH (lane 5) yielded a processed transcript and pTBO TL (lane 4) yielded a preliminary transcript and a circle.

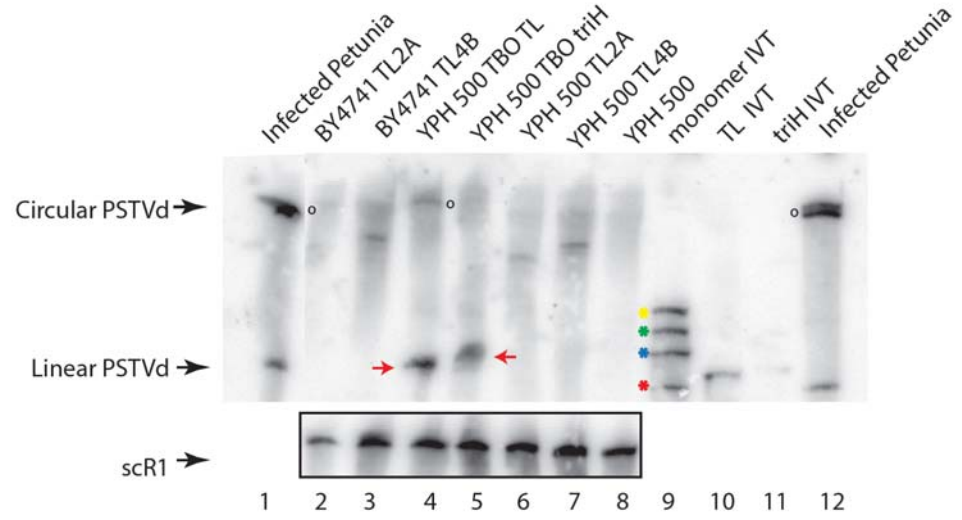

Figure 5.5: Northern blot analysis of total RNA from modified PSTVd expression constructs in yeast.

Total RNAs from infected petunia (lane 1), empty YPH500 (lane 8), YPH500 transformed with the constructs as indicated (lanes 4-7), BY4741 transformed with constructs as indicated (lanes 2-3) were separated on a 5% PAA and blotted onto positively charged nylon similar to Figure 5.1 as was the probing. Red arrows indicate preliminary transcripts from prior to yeast cleavage/ligation events *in vivo.* The open circle denotes circular products resulting from processing of the TL construct *in vivo* (lane 4), or of circular PSTVd from infected controls (lanes 1, 12). TBO (pB3RQ39) denotes previously used constructs that process (TL) or form preliminary transcripts (triH) in YPH500. The ribozymes of the monomer IVT (lane 9) did not cleave to completion, resulting in four bands: HH-PSTVd-HP (547 nt, yellow asterisk), PSTVd-HP (482 nt, green asterisk), HH-PSTVd (424 nt, blue asterisk), and linear PSTVd (359nt, red asterisk). Additional loading controls were TL IVT (lane 10) and triH IVT (lane 11). 2A and 4B represent modifications to the delta ribozyme and 3' end of the original TL and triH constructs (Table 5.2).

After eliminating the variables of *CYC*1 terminator interference and faulty delta cleavage, the focus was then moved towards the 5' end of the gene. Sequence alignment of the pXP722 gal

promoter vs. pTBO TL gal promoter revealed that the pXP722 promoter has 63 additional base pairs between the Pol II TATA box and the transcription start site (TACG) (Figure 5.6).

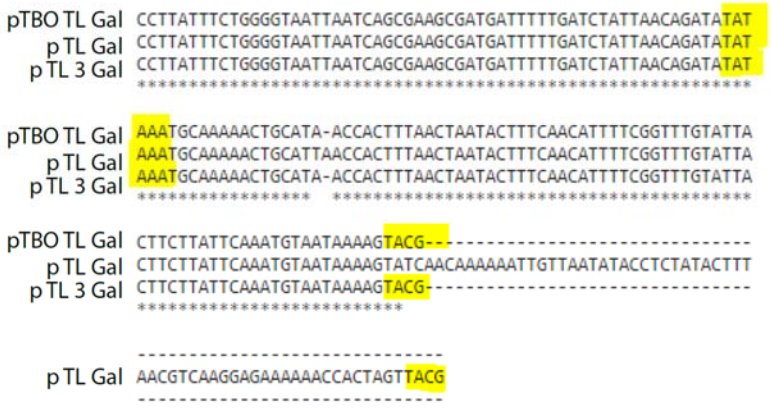

Figure 5.6: Clustal Omega sequence alignment of gal promoter sequences.

Three galactose promoter sequences alignments from pTBO TL (pTBO 163), p TL, and pTL3 (desired). The p TL galactose promoter has an additional 63 bp from TATA box (highlighted yellow) to the TACG transcription start site (also highlighted yellow).

As a fix to this discrepancy, the promoter region of pTL was replaced with that from pTBO TL. The *Age*I/*Eag*I fragment of pTL (455 bp) and p triH (455 bp) were removed and replaced with the *Age*I/*Eag*I fragment from pTBO TL. The promoter and PSTVd 5' ends of pTBO TL and pTBO triH are identical.

Primer extension was performed to map the 5' ends of these transcripts. Total RNA from yeast that was transformed with either pTBO TL, pTL3 or ptrH3 was enriched for PSTVd by $MnCl_2$ precipitation. The primer extension (Figure 5.7) showed that the TL3 and triH3 5' ends

(Lane 4) shared several important bands with TBO TL (Lane 3), including one consistent with the *GAL1* start site (red arrow heads). However, their intensity was much lower. Interestingly all three constructs gave a strong triplet of bands from 91-93, indicative that the 5; end of these RNAs are processed similarly.

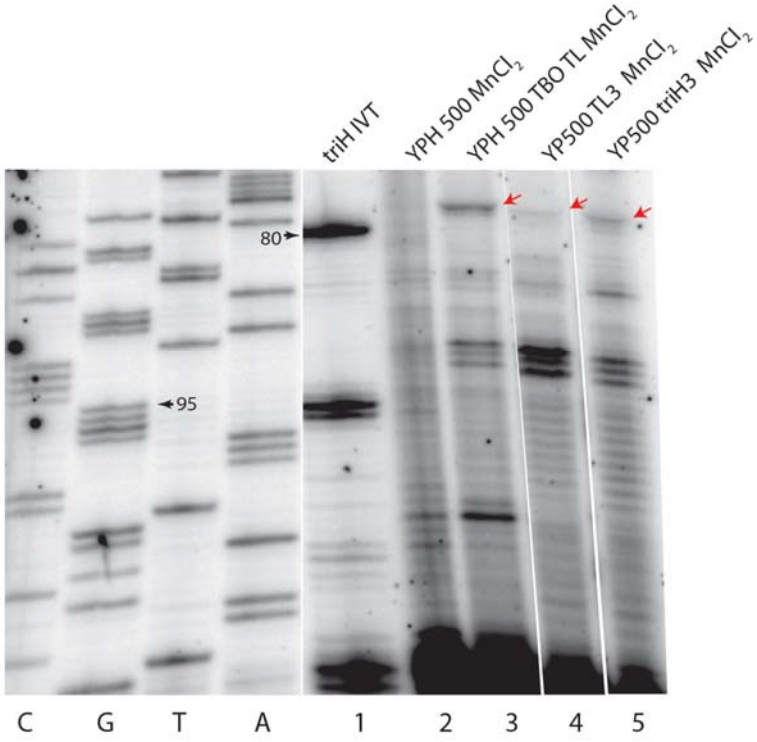

Figure 5.7: Primer extension of PSTVd expression constructs to reveal preliminary transcript.

Total RNA was prepared from YPH500 strain expressing pTBO TL and pTL3 PSTVd RNAs. $MnCl_2$ -treated RNA (6.1µg) to enrich preliminary transcripts was analyzed by primer extension. γ ^{32}P MB1R was used to perform the extension. *In vitro* transcript of triH (Lane 1) was used as a loading control. The 5' end of the triH *in vitro* transcript starts at position G80. Lane 2 is YPH500 with $MnCl_2$ treatment. Lanes 3 and 4 represent pTBO TL and pTL3 transformed YPH500 with $MnCl_2$ treatment. Position -2C (red arrow) marks the yeast transcription start sites in constructs harboring a *GAL1* promoter. Position G80 marks the first PSTVd base. TL3 is a variant of the original TL construct that has a modification of the galactose promoter region (Table 5.2).

Northern blotting was used to probe for preliminary transcripts and circle formation (Figure 5.8). There remains no strong evidence for either being produced. Both pTBO TL and pTBO triH gave their expected bands in YPH500. The RNAs expressed from pTL3 and ptriH3 did not give preliminary transcripts of unit length in YPH500 (lanes 7 and 8, respectively) or in BY4147 (lanes 9 and 10, respectively). As before, a larger RNA is seen, but it does not align properly with the control circles (lanes 5 and 11). The size of this band did not change with respect to the original constructs.

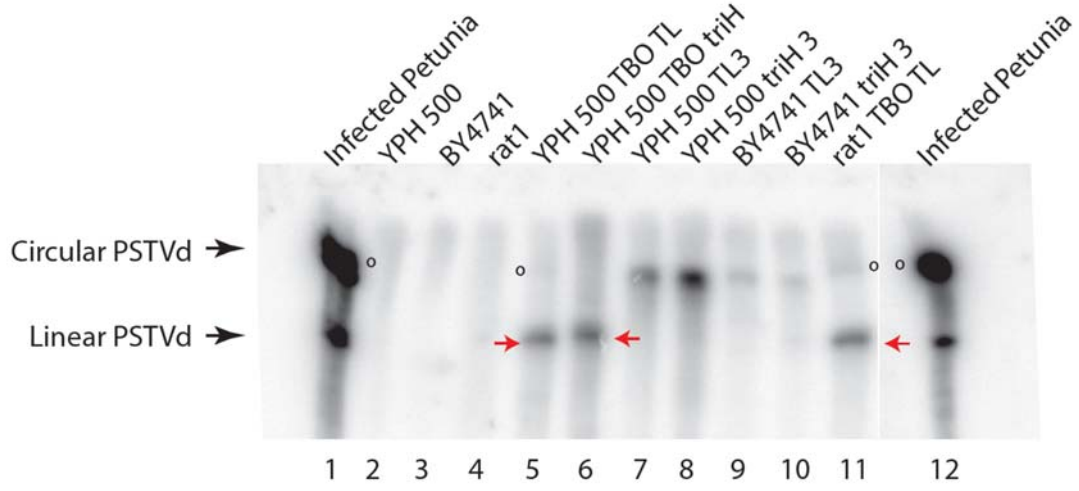

Figure 5.8: Northern blot analysis of total RNA from modified PSTVd expression constructs in yeast.

Total RNAs from infected petunia (lane 1), empty YPH500 (lane 3), empty BY471 (lane 3), empty *RAT1-107* (lane 4), YPH500 transformed with the constructs as indicated (lanes 5-8), BY4741 transformed with constructs as indicated (lanes 9-10) and *RAT1-107* transformed with pTBO TL (lane 11) were separated on a 5% PAA and blotted onto positively charged nylon similar to Figure 5.1 as was the probing. Red arrows indicate preliminary transcripts from prior to yeast cleavage/ligation events *in vivo.* The open circle denotes circular products resulting from processing of the TL construct *in vivo* (lane 5, 11), or of circular PSTVd from infected controls (lanes 1, 12). TBO (RQ39 vector backbone) denotes previously used constructs that process (TL) or form preliminary transcripts (triH) in YPH500. TL3 and triH3 are modified versions of the original TL and triH constructs with a modified gal promoter and modified 3' region containing the delta ribozyme (Table 5.2).

Discussion

Expressing PSTVd RNAs in yeast strains containing gene knockouts and temperature sensitive (ts) knock down proteins is of vital importance to gain insight into proteins used for PSTVd processing. The largest collection of knockout strains and ts mutants reside within the BY yeast strain series (114, 218), with BY4741 being the most used. The constructs that we have previously shown to process in yeast (pTBO) contain a *TRP* marker. However, switching this *TRP* marker to a *URA* maker would allow for transformation into BY4741 and thus allow for access to the deletion and ts mutant strains.

We have attempted to create PSTVd expression plasmids based on the established vector pXP722. Unfortunately, we did not see proper ribozyme cleavage or circle ligation in any of our attempts (Figures 5.2-5.5, 5, 8). Several modifications to both the 3' and 5' end of the PSTVd gene were made, copying these segments from the functional pTBO TL construct. pTL3 and ptriH were capable of producing the 5' end of the primary transcript in yeast as show by primer extension in Figure 5.7 (lanes 4 and 5); however, the production of these transcripts was much lower than that of pTBO TL. Here we consider two possible reasons for this: transcription levels and the ligation substrate.

Three considerations determine the level of RNA transcription from a plasmid: plasmid copy number, transcription efficiency and product degradation. Fang *et al*. (219) show that copy number of the pXP plasmid series is quite stable and it is independent of the transcript load and the promoter. The pXP series is based on *CEN6*, while the pTBO uses *CEN4*; we are unaware of studies comparing the copy number of these origins, but would be surprised if there were a

difference, since yeast chromosomes 4 and 6 have the same copy number.

Modifying the pXP722 *GAL1* promoter or the removal of the *CYC1* terminator did not improve efficiency. We have not yet tried to combine these changes, as either alone had no detectable effect on the RNA product. With similar 5' and 3' ends, it is reasonable to assume that any RNAs transcribed from these plasmids should behave similarly with respect to degradation. Yet, it could be that different strains would utilize different degradative processes on these RNAs. We can also rule out strain affects as pTL and ptriH and their derivatives can be transformed into YPH500, the strain that demonstrated viroid RNA process from pTBO TL transcripts. The resulting RNAs were the same as those directed by pTL and ptriH in BY4741. We have also shown that strain MBA64 transformed with pTBO TL produces the same preliminary RNAs and circles as YPH500 transformed with the plasmid (Supplemental Figure 5.8). MBA64 derives from W303 and is congenic, but not isogenic with YPH500, a derivative of YNN26 (114).

The other possibility that has not yet been addressed is the influence of the deletion of the sequence GACAU between the 3' end of PSTVd and the delta ribozyme on pTL. This sequence was introduced during the cloning of PSTVd into pB3RQ39 in the creation of pTBO TL. This sequence is not present between PSTVd with its triH 3' repeat and the delta ribozyme in pTBO triH. Initially, this insertion was thought to be inconsequential however, it may be significant in the light of learning that the yeast endonuclease involved in circle production cuts at position 92/93 rather than 95/96 (Figure 2.7A). Figure 2.7C shows that the addition of GACAU allows a potential folding of the RNA for ligation to the 3' end created by the delta ribozyme. A similar potential substrate fold for an RNA without the five-nucleotide insertion could not be found. If the RNA cannot ligate to a circle it could be degraded instead, explaining the failure to see circle

formation and a loss of the primary transcript from pTL. However, this is not consistent with the low ratio of circle to preliminary transcript in pTBO TL strains. Neither does it explain why ptriH does not give the same products as pTBO triH.

Clearly, the processing of viroid RNA is highly nuanced. Only slight changes in the cellular environment dictate the degradation versus ligation to circles of these RNAs. The plasmids used to express BMV RNA is yeast seems to have the essential elements to express plant pathogens in yeast (180). The TBO TL/triH constructs utilize the original pB3RQ39 backbone and this backbone should be employed in future studies for the expression of PSTVd in yeast.

Supplemental Information

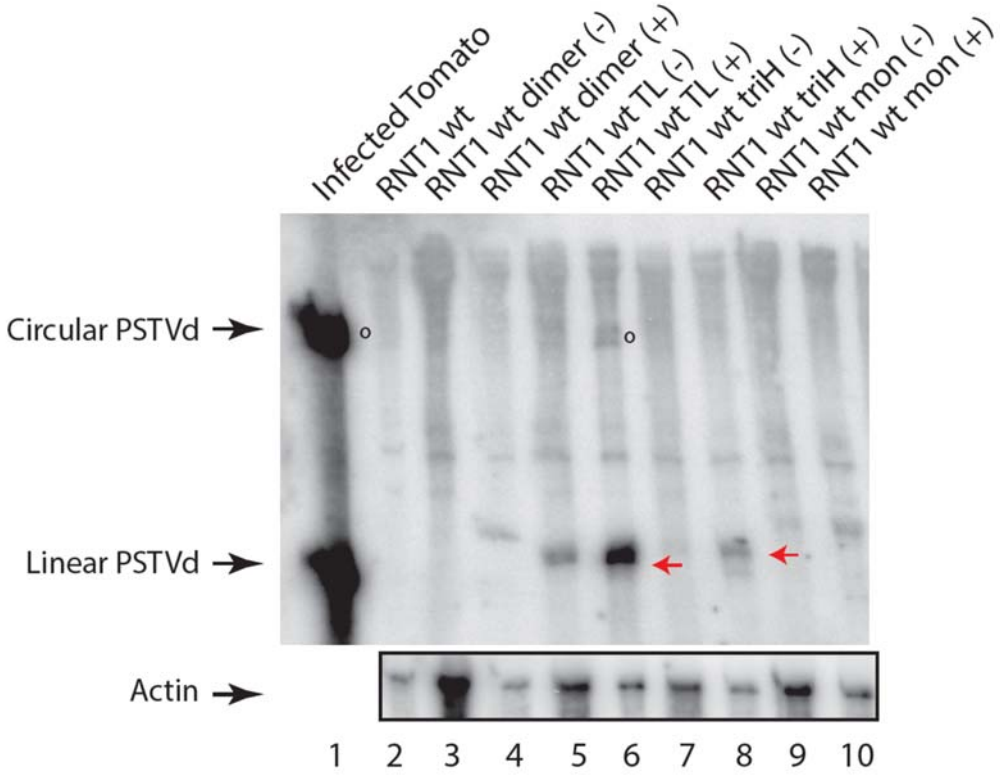

Supplemental Figure 5.1: Northern blot analysis of total RNA from modified PSTVd expression constructs in yeast strain RNT1 wt (BMA64)

Total RNAs from infected tomato (lane 1), empty RNT1wt (lane 2), and RNT1wt transformed with pTBO constructs corresponding to the dimer, monomer, TL and triH (lanes 3-10) were separated on a 5% PAA and blotted onto positively charged nylon similar to Figure 5.1. Induction conditions are represented by dextrose (–) and galactose (+). Red arrows indicate primary transcripts from prior to yeast cleavage/ligation events *in vivo.* The open circle denotes circular products resulting from processing of the TL construct *in vivo* (lane 6), or of circular PSTVd from infected controls (lane 1).

Chapter 6: Summary and Future Prospects

The study of PSTVd processing in yeast is advantageous with regard to yeast being a simple, highly characterized, and well-studied simple eukaryotic system. For RNA biology studies and pathogen-host interactions, the yeast toolbox of knockout strains provides a relatively quick and simple method for studying pathogen-protein interactions. The main overall objective of this research was to establish a PSTVd expression system allowing access to the many benefits yeast can offer for PSTVd-host studies. PSTVd processing has been highly studied through the years, however the details regarding the structure and proteins involved in PSTVd processing are still largely uncharacterized. In Chapter 2, we created a PSTVd expression construct that processes in yeast. This was the first case of *Pospiviroidae* processing in a non-plant system. We gained insight into the structural motifs that dictate cleavage and ligation and discovered that PSTVd processing in yeast is an interplay between ligation and degradation.

The processing of PSTVd in yeast is not a highly efficient process as the PSTVd processing intermediates are either quickly ligated or degraded. In order to study PSTVd primary transcripts produced from yeast, we expanded upon a method of enriching viroids from total RNA by use of $MnCl_2$ (Chapter 3). By use of this method, we showed that small quantities of viroid transcripts in total RNA from yeast can be enriched. This technique allowed detection by primer extension whereas these transcripts undetectable within total RNA that was not enriched using this process. Furthermore, we determined RNA lengths that were more enriched by using $MnCl_2$ enrichment and determined that this enrichment allowed for detection of RNAs of 422nt and below from total RNA from yeast.

Apart from the processing of PSTVd in yeast, the actual transcription of a plant pathogen in a non-host is not an efficient process. To overcome the *in vivo* processing factors and challenges, we have established an *in vitro* processing system in yeast whole cell extracts (Chapter 4). The degradation mechanism still exists in this system; however, the transcription and levels of transcript can be controlled. Thus, the use of an *in vitro* system opens up the screening process and allows for structural analysis that cannot be conducted *in vivo*.

As a corollary of the previous study, we have found that *in vivo* processing of PSTVd in yeast is a very specific with regard to the expression system used (Chapter 5). We have attempted to express PSTVd in using a different expression system described in Chapter 2. The proposed system had all of the elements of being an excellent yeast expression system that would allow for more access to the yeast knockout toolbox with regard to PSTVd processing studies. This system did not express PSTVd at high levels, nor did it show PSTVd processing. This has led us to conclude that the key elements of proper PSTVd expression in yeast reside in the vector backbone described in Chapter 2.

Future Prospects

1. Create a complete monomer construct that has cleavage at 92/93 and assay for PSTVd processing. In addition, modify the *in vivo* monomer construct to contain a 5' phosphate and a 3' OH and test for *in vivo* ligation.
2. To investigate the kinetics of PSTVd degradation in yeast, conduct a time course extracting total RNA at various stages of yeast growth post galactose induction. If a

specific harvest time displays reduced degradation, this would possibly allow for 5'mapping of the PSTVd replication intermediates.

3. Due to degradation concerns, create yeast whole cell extracts that contain a knockout of XRN1 and RAT1. These strains should limit PSTVd RNA degradation and allow us to establish and *in vitro* processing assay that produces complete PSTVd circles. With these constructs in place, we can use double mutant strains to investigate *in vitro* processing prior to *in vivo* assays.
4. Create a yeast expression system containing a URA 3 marker within the pB3RQ39 vector backbone that expresses the tetraloop and trihelix structure. Screen for in *vivo* processing in the cdc9-1 mutant, the rlg1-4 mutant, and rnt1Δ strain.

Appendix

Appendix Table 1: All Oligonucleotides used throughout this study

Oligonucleotide	Sequence (5'-3')
112F[a]	ACTGGCAAAAAGGACGGTGGGGA
259R	GTAGCCGAAGCGACAGCGCAAAGG
2F	CCTGTGGTTCACACCTGACCTCC
MB1R	TCGGCCGCTGGGCACTCC
ActF	GGTATTCTCACCAACTGGGACG
M13 F	GTAAAACGACGGCCAG
M13 R	CAGGAAACAGCTATGAC
T7 prom F	*GAAATTAATACGACTCACTATA*
TB110 down R	AATTCCGGGGATCCCTGAAGCGCTCC
T7 prom F	*GAAATTAATACGACTCACTATA*
TB112 down R	GCCACCTGACGTCTAAGAAACC
T7ActR	*GTAATACGACTCACTATAG*GCGACGTAACATACTTTTTCCT GATGT
SCR1F	TGGCCGAGGAACAAATCCTT
T7ScR1R	*GTAATACGACTCACTATAG*TTAAACCGCCGAAGCGATCA
T7 PSTVd dim F	TAATACGACTCACTATAGGTACGTACTG
PSTVd dim R	GGG ACAGAGGTCCTCAG
Delta BstX1 d F	CGTCGTCCACTCGGATG
Xho nru bb R	GAAAGGCTCGAGTCGCGATCATTAGGCACCCCAGG

[a] Forward primers (ending in F) have the same sequence as the transcribed RNA.

[b]Italicized letters indicate the introduced T7 promoter sequence.

Appendix Table 2: All Plasmids used in this study

plasmid	relevant genotype[a]	construct[b]	RNA	Reference
p13/119		PSTVd monomer	Mon IVT	This work
p15/14		PSTVd dimer	Dim IVT	This work
pTB110		parent pRH701	TL IVT	(88)
pTB112		PSTVd trihelix	triH IVT	This work
pCR2.1_TOPO		HH-PSTVd monomer-HP		(167)
pB3RQ39	*TRP1*, *CEN4*, P_{GAL1}		BMV	(180)
pXP722	*URA3, CYC1*, *CEN6*, $P_{GAL1'}$			(219)
pTBO_TL	*TRP1*, *CEN4*, P_{GAL1}	P_{GAL1}-PSTVd tetraloop-δ	TBO TL	This work
pTL	*URA3, CYC1*, *CEN6*, $P_{GAL1'}$	$P_{GAL1'}$-PSTVd tetraloop-δ-cyc	TL	This work
pTL#1	*URA3*, *CEN6*, $P_{GAL1'}$	$P_{GAL1'}$-PSTVd tetraloop-δ	TL#1	This work
pTL2A	*URA3, CEN6*, $P_{GAL1'}$ δ'	$P_{GAL1'}$-PSTVd tetraloop-δ'	TL2A	This work
pTL4B	*URA3, CEN6*, $P_{GAL1'}$ δ*	$P_{GAL1'}$-PSTVd tetraloop-δ*	TL4B	This work
pTL3	*URA3, CYC1*, *CEN6*, P_{GAL1*}	P_{GAL1*}-PSTVd tetraloop-δ-cyc	TL3	This work
pTBO triH	*TRP1*, *CEN4*, P_{GAL1}	P_{GAL1}-PSTVd trihelix-δ	TBO triH	This work
ptriH	*URA3, CYC1*, *CEN6*, $P_{GAL1'}$	$P_{GAL1'}$-PSTVd trihelix-δ-cyc	triH	This work
ptriH#14	*URA3*, *CEN6*, $P_{GAL1'}$	$P_{GAL1'}$-PSTVd trihelix-	triH	This work
ptriH3	*URA3, CYC1*, *CEN6*, P_{GAL1*}	P_{GAL1*}-PSTVd trihelix-δ-cyc	triH3	This work
pTBO dim	*TRP1*, *CEN4*, P_{GAL1}	P_{GAL1}-PSTVd dimer -δ	TBO dim	This work
pTBO mon	*TRP1*, *CEN4*, P_{GAL1}	P_{GAL1}-HH-PSTVd monomer-HP	TBO mon	This work
pIC115	URA3	*RAT1-107*::*URA3*	*Rat 1*	(181)

[a] *pGAL1*=full *GAL1* promoter; *pGAL1'=GAL1* promoter without *UAS1*. Gal1*= deletion of 61 bp between TATA and transcription start site

[b] δ=delta ribozyme; HH=hammerhead ribozyme; HP=hairpin ribozyme;

δ'= delta ribozyme + 31 bp vector sequence of TBO TL

δ*= delta ribozyme + 131 bp vector sequence of TBO TL

Appendix Table 3: All templates for IVT and riboprobes

RNA	Template	Forward Primer	Reverse Primer
TL IVT	pTB110	T7 prom F	TB110 down R
triH IVT	pTB112	T7 prom F	TB112 down R
Dimer IVT	p14/15	T7 PSTVd dim F	T7 PSTVd dim F
Mon IVT	p13/119	M13 F	M13 R
(-) PSTVd riboprobe	p13/121	M13 F	M13 R
(-) Actin	YPH500 genome	ActF	T7ActR
(–) SCR1	YPH500 genome	SCR1F	T7ScR1R

References

1. **Owens RA.** 2007. Potato spindle tuber viroid: the simplicity paradox resolved? Mol Plant Pathol **8:**549-560.
2. **Schmitz M, Steger G.** 2007. Potato spindle tuber viroid (PSTVd). Plant viruses **1:**106-115.
3. **Kovalskaya N, Hammond RW.** 2014. Molecular biology of viroid-host interactions and disease control strategies. Plant Sci **228:**48-60.
4. **Diener TO.** 1971. Potato spindle tuber "virus". IV. A replicating, low molecular weight RNA. Virology **45:**411-428.
5. **Diener TO.** 1972. Viroids. Adv Virus Res **17:**295-313.
6. **Sogo J, Koller T, Diener T.** 1973. Potato spindle tuber viroid: X. Visualization and size determination by electron microscopy. Virology **55:**70-80.
7. **Davies J, Kaesberg P, Diener T.** 1974. Potato spindle tuber viroid. XII. An investigation of viroid RNA as a messenger for protein synthesis. Virology **61:**281-286.
8. **Hall T, Wepprich R, Davies J, Weathers L, Semancik J.** 1974. Functional distinctions between the ribonucleic acids from citrus exocortis viroid and plant viruses: cell-free translation and aminoacylation reactions. Virology **61:**486-492.
9. **Sanger HL, Klotz G, Riesner D, Gross HJ, Kleinschmidt AK.** 1976. Viroids are single-stranded covalently closed circular RNA molecules existing as highly base-paired rod-like structures. Proceedings of the National Academy of Sciences **73:**3852-3856.
10. **Gross HJ, Domdey H, Lossow C, Jank P, Raba M, Alberty H.** 1978. Nucleotide sequence and secondary structure of potato spindle tuber viroid. Nature **273:**203-208.
11. **Flores R, Hernández C, Alba AEMd, Daròs J-A, Serio FD.** 2005. Viroids and viroid-host interactions. Annu Rev Phytopathol **43:**117-139.
12. **Di Serio F, Flores R, Verhoeven JTJ, Li S-F, Pallás V, Randles J, Sano T, Vidalakis G, Owens R.** 2014. Current status of viroid taxonomy. Archives of virology **159:**3467-3478.
13. **De Bokx J, Piron P.** 1981. Transmission of potato spindle tuber viroid by aphids. European Journal of Plant Pathology **87:**31-34.
14. **Kryczyński S, Paduch-Cichal E, Skrzeczkowski L.** 1988. Transmission of three viroids through seed and pollen of tomato plants. Journal of Phytopathology **121:**51-57.
15. **Hammond RW, Owens RA.** 2006. Viroids: New and continuing risks for horticultural and agricultural crops. APSnet Features.
16. **Rodio M-E, Delgado S, De Stradis A, Gómez M-D, Flores R, Di Serio F.** 2007. A viroid RNA with a specific structural motif inhibits chloroplast development. The Plant Cell **19:**3610-3626.
17. **Di Serio F, De Stradis A, Delgado S, Flores R, Navarro Ramirez B.** 2013. Cytopathic effects incited by viroid RNAs and putative underlying mechanisms. Frontiers in plant science **3:**288.
18. **Hadidi A, Flores R, Randles J, Semancik J.** 2003. Viroids: properties, detection, diseases and their control. Csiro Publishing.
19. **Soliman T.** 2012. Economic impact assessment of invasive plant pests in the European Union.
20. **Protection MP, Smith I.** QUARANTINE PESTS FOR EUROPE.
21. **Singh RP.** 2014. The discovery and eradication of potato spindle tuber viroid in Canada. Virusdisease **25:**415-424.
22. **Singh R, Clark M.** 1971. Infectious low-molecular weight ribonucleic acid from tomato. Biochemical and biophysical research communications **44:**1077-1083.
23. **Owens RA, Diener T.** 1981. Sensitive and rapid diagnosis of potato spindle tuber viroid disease by nucleic acid hybridization. Science **213:**670-672.

24. **Bostan H, Nie X, Singh RP.** 2004. An RT-PCR primer pair for the detection of Pospiviroid and its application in surveying ornamental plants for viroids. Journal of Virological Methods **116:**189-193.
25. **Botermans M, Van de Vossenberg B, Verhoeven JTJ, Roenhorst J, Hooftman M, Dekter R, Meekes E.** 2013. Development and validation of a real-time RT-PCR assay for generic detection of pospiviroids. Journal of virological methods **187:**43-50.
26. **De Boer S, DeHaan T.** 2005. Absence of potato spindle tuber viroid within the Canadian potato industry. Plant Disease **89:**910-910.
27. **Zhang W, Zhang Z, Fan G, Gao Y, Wen J, Bai Y, Qiu C, Zhang S, Shen Y, Meng X.** 2017. Development and application of a universal and simplified multiplex RT-PCR assay to detect five potato viruses. Journal of General Plant Pathology **83:**33-45.
28. **Garnsey S, Whidden R.** Decontamination treatments to reduce the spread of citrus exocortis virus (CEV) by contaminated tools, p 63-67. *In* (ed),
29. **Mackie A, Coutts B, Barbetti M, Rodoni B, McKirdy S, Jones R.** 2015. Potato spindle tuber viroid: stability on common surfaces and inactivation with disinfectants. Plant Disease **99:**770-775.
30. **Paduch-Cichal E, Kryczyński S.** 1987. A low temperature therapy and meristem-tip culture for eliminating four viroids from infected plants. Journal of Phytopathology **118:**341-346.
31. **Postman J, Hadidi A.** Elimination of apple scar skin viroid from pears by in vitro thermo-therapy and apical meristem culture, p 536-543. *In* (ed),
32. **Wang Q, Valkonen JP.** 2009. Cryotherapy of shoot tips: novel pathogen eradication method. Trends in plant science **14:**119-122.
33. **QIU C-l, ZHANG Z-x, LI S-f, BAI Y-j, LIU S-w, FAN G-q, GAO Y-l, ZHANG W, ZHANG S, LÜ W-h.** 2016. Occurrence and molecular characterization of Potato spindle tuber viroid (PSTVd) isolates from potato plants in North China. Journal of Integrative Agriculture **15:**349-363.
34. **Tsagris EM, Martínez de Alba ÁE, Gozmanova M, Kalantidis K.** 2008. Viroids. Cellular microbiology **10:**2168-2179.
35. **Palukaitis P, Hatta T, Alexander DM, Symons RH.** 1979. Characterization of a viroid associated with avocado sunblotch disease. Virology **99:**145-151.
36. **Symons RH.** 1981. Avocado sunblotch viroid: primary sequence and proposed secondary structure. Nucleic Acids Research **9:**6527-6537.
37. **Flores R, Daròs J-A, Hernández C.** 2000. Avsunviroidae family: viroids containing hammerhead ribozymes. Advances in virus research **55:**271-323.
38. **Kolonko N, Bannach O, Aschermann K, Hu K-H, Moors M, Schmitz M, Steger G, Riesner D.** 2006. Transcription of potato spindle tuber viroid by RNA polymerase II starts in the left terminal loop. Virology **347:**392-404.
39. **Giguère T, Adkar-Purushothama CR, Bolduc F, Perreault JP.** 2014. Elucidation of the structures of all members of the Avsunviroidae family. Molecular plant pathology **15:**767-779.
40. **Dubé A, Bolduc F, Bisaillon M, PERREAULT JP.** 2011. Mapping studies of the Peach latent mosaic viroid reveal novel structural features. Molecular plant pathology **12:**688-701.
41. **Flores R, Serra P, Minoia S, Di Serio F, Navarro B.** 2012. Viroids: from genotype to phenotype just relying on RNA sequence and structural motifs. Frontiers in microbiology **3:**217.
42. **Glouzon J-PS, Bolduc F, Wang S, Najmanovich RJ, Perreault J-P.** 2014. Deep-sequencing of the peach latent mosaic viroid reveals new aspects of population heterogeneity. PloS one **9:**e87297.
43. **Bruening G, Gould AR, Murphy PJ, Symons RH.** 1982. Oligomers of avocado sunblotch viroid are found in infected avocado leaves. FEBS Letters **148:**71-78.
44. **Hutchins CJ, Keese P, Visvader JE, Rathjen PD, McInnes JL, Symons RH.** 1985. Comparison of multimeric plus and minus forms of viroids and virusoids. Plant molecular biology **4:**293-304.

45. **Daròs J-A, Marcos JF, Hernandez C, Flores R.** 1994. Replication of avocado sunblotch viroid: evidence for a symmetric pathway with two rolling circles and hammerhead ribozyme processing. Proceedings of the National Academy of Sciences **91:**12813-12817.
46. **Bussière F, Lehoux J, Thompson D, Skrzeczkowski L, Perreault J-P.** 1999. Subcellular localization and rolling circle replication of peach latent mosaic viroid: hallmarks of group A viroids. Journal of virology **73:**6353-6360.
47. **Navarro J-A, Vera A, Flores R.** 2000. A chloroplastic RNA polymerase resistant to tagetitoxin is involved in replication of avocado sunblotch viroid. Virology **268:**218-225.
48. **Hutchins CJ, Rathjen PD, Forster AC, Symons RH.** 1986. Self-cleavage of plus and minus RNA transcripts of avocado sunblotch viroid. Nucleic acids research **14:**3627-3640.
49. **Forster AC, Symons RH.** 1987. Self-cleavage of virusoid RNA is performed by the proposed 55-nucleotide active site. Cell **50:**9-16.
50. **De la Peña M, Navarro B, Flores R.** 1999. Mapping the molecular determinant of pathogenicity in a hammerhead viroid: a tetraloop within the in vivo branched RNA conformation. Proceedings of the National Academy of Sciences **96:**9960-9965.
51. **Gilbert W.** 1986. Origin of life: The RNA world. nature **319**.
52. **Diener T.** 1989. Circular RNAs: relics of precellular evolution? Proceedings of the National Academy of Sciences **86:**9370-9374.
53. **GAGO S, DE LA PEÑA M, FLORES R.** 2005. A kissing-loop interaction in a hammerhead viroid RNA critical for its in vitro folding and in vivo viability. Rna **11:**1073-1083.
54. **Martinez F, Marques J, Salvador ML, Daros J-A.** 2009. Mutational analysis of eggplant latent viroid RNA processing in Chlamydomonas reinhardtii chloroplast. Journal of general virology **90:**3057-3065.
55. **Dubé A, Baumstark T, Bisaillon M, Perreault J-P.** 2010. The RNA strands of the plus and minus polarities of peach latent mosaic viroid fold into different structures. Rna **16:**463-473.
56. **Delan-Forino C, Deforges J, Benard L, Sargueil B, Maurel M-C, Torchet C.** 2014. Structural analyses of Avocado sunblotch viroid reveal differences in the folding of plus and minus RNA strands. Viruses **6:**489-506.
57. **Nohales M-Á, Molina-Serrano D, Flores R, Daròs J-A.** 2012. Involvement of the chloroplastic isoform of tRNA ligase in the replication of viroids belonging to the family Avsunviroidae. Journal of virology **86:**8269-8276.
58. **Dubé A, Bisaillon M, Perreault J-P.** 2009. Identification of proteins from Prunus persica that interact with peach latent mosaic viroid. Journal of virology **83:**12057-12067.
59. **Ding B.** 2010. Viroids: self-replicating, mobile, and fast-evolving noncoding regulatory RNAs. Wiley Interdisciplinary Reviews: RNA **1:**362-375.
60. **Gómez G, Pallas V.** 2012. Studies on Subcellular Compartmentalization of Plant Pathogenic Noncoding RNAs Give New Insights into the Intracellular RNA-Traffic Mechanisms. Plant Physiology **159:**558-564.
61. **Keese P, Symons RH.** 1985. Domains in viroids: evidence of intermolecular RNA rearrangements and their contribution to viroid evolution. Proceedings of the National Academy of Sciences **82:**4582-4586.
62. **Zhong X, Archual AJ, Amin AA, Ding B.** 2008. A genomic map of viroid RNA motifs critical for replication and systemic trafficking. Plant Cell **20:**35-47.
63. **Baumstark T, Schroder AR, Riesner D.** 1997. Viroid processing: switch from cleavage to ligation is driven by a change from a tetraloop to a loop E conformation. EMBO J **16:**599-610.
64. **Gas ME, Hernandez C, Flores R, Daros JA.** 2007. Processing of nuclear viroids in vivo: an interplay between RNA conformations. PLoS Pathog **3:**e182.

65. **Wang Y, Zhong X, Itaya A, Ding B.** 2007. Evidence for the existence of the loop E motif of Potato spindle tuber viroid in vivo. Journal of virology **81:**2074-2077.
66. **Branch AD, Benenfeld BJ, Robertson HD.** 1985. Ultraviolet light-induced crosslinking reveals a unique region of local tertiary structure in potato spindle tuber viroid and HeLa 5S RNA. Proceedings of the National Academy of Sciences **82:**6590-6594.
67. **Havrila M, Réblová K, Zirbel CL, Leontis NB, Šponer J.** 2013. Isosteric And Non-Isosteric Base Pairs In RNA Motifs: Molecular Dynamics And Bioinformatics Study Of The Sarcin-Ricin Internal Loop. The journal of physical chemistry B **117:**14302-14319.
68. **Henco K, Sänger HL, Riesner D.** 1979. Fine structure melting of viroids as studied by kinetic methods. Nucleic acids research **6:**3041-3059.
69. **Loss P, Schmitz M, Steger G, Riesner D.** 1991. Formation of a thermodynamically metastable structure containing hairpin II is critical for infectivity of potato spindle tuber viroid RNA. The EMBO journal **10:**719.
70. **Dingley AJ, Steger G, Esters B, Riesner D, Grzesiek S.** 2003. Structural characterization of the 69 nucleotide potato spindle tuber viroid left-terminal domain by NMR and thermodynamic analysis. Journal of molecular biology **334:**751-767.
71. **Gast F-U, Kempe D, Spieker RL, Sänger HL.** 1996. Secondary structure probing of potato spindle tuber viroid (PSTVd) and sequence comparison with other small pathogenic RNA replicons provides evidence for central non-canonical base-pairs, large A-rich loops, and a terminal branch. Journal of molecular biology **262:**652-670.
72. **Takahashi T, Diener T.** 1975. Potato spindle tuber viroid: XIV. Replication in nuclei isolated from infected leaves. Virology **64:**106-114.
73. **Branch AD, Robertson HD.** 1984. A replication cycle for viroids and other small infectious RNA's. Science **223:**450-456.
74. **Warrilow D, Symons R.** 1999. Citrus exocortis viroid RNA is associated with the largest subunit of RNA polymerase II in tomato in vivo. Archives of virology **144:**2367-2375.
75. **Kolonko N, Bannach O, Aschermann K, Hu KH, Moors M, Schmitz M, Steger G, Riesner D.** 2006. Transcription of potato spindle tuber viroid by RNA polymerase II starts in the left terminal loop. Virology **347:**392-404.
76. **Wassenegger M, Krczal G.** 2006. Nomenclature and functions of RNA-directed RNA polymerases. Trends in plant science **11:**142-151.
77. **Wang Y, Qu J, Ji S, Wallace AJ, Wu J, Li Y, Gopalan V, Ding B.** 2016. A land plant-specific transcription factor directly enhances transcription of a pathogenic noncoding RNA template by DNA-dependent RNA polymerase II. The Plant Cell **28:**1094-1107.
78. **Branch AD, Benenfeld BJ, Robertson HD.** 1988. Evidence for a single rolling circle in the replication of potato spindle tuber viroid. Proc Natl Acad Sci U S A **85:**9128-9132.
79. **Branch AD, Robertson HD.** 1984. A replication cycle for viroids and other small infectious RNA's. Science **223:**450-455.
80. **Cress DE, Kiefer MC, Owens RA.** 1983. Construction of infectious potato spindle tuber viroid cDNA clones. Nucleic acids research **11:**6821-6835.
81. **Tabler M, Sanger HL.** 1984. Cloned single- and double-stranded DNA copies of potato spindle tuber viroid (PSTV) RNA and co-inoculated subgenomic DNA fragments are infectious. EMBO J **3:**3055-3062.
82. **Meshi T, Ishikawa M, Ohno T, Okada Y, Sano T, Ueda I, Shikata E.** 1984. Double-stranded cDNAs of hop stunt viroid are infectious. J Biochem **95:**1521-1524.
83. **Ishikawa M, Meshi T, Ohno T, Okada Y, Sano T, Ueda I, Shikata E.** 1984. A revised replication cycle for viroids: the role of longer than unit length RNA in viroid replication. Mol Gen Genet **196:**421-428.

84. **Candresse T, Diener TO, Owens RA.** 1990. The role of the viroid central conserved region in cDNA infectivity. Virology **175:**232-237.
85. **Rakowski AG, Symons RH.** 1994. Infectivity of linear monomeric transcripts of citrus exocortis viroid: terminal sequence requirements for processing. Virology **203:**328-335.
86. **Diener TO.** 1986. Viroid processing: a model involving the central conserved region and hairpin I. Proc Natl Acad Sci U S A **83:**58-62.
87. **Steger G, Baumstark T, Mörchen M, Tabler M, Tsagris M, Sänger H, Riesner D.** 1992. Structural requirements for viroid processing by RNase T1. Journal of molecular biology **227:**719-737.
88. **Baumstark T, Riesner D.** 1995. Only one of four possible secondary structures of the central conserved region of potato spindle tuber viroid is a substrate for processing in a potato nuclear extract. Nucleic Acids Res **23:**4246-4254.
89. **Schrader O, Baumstark T, Riesner D.** 2003. A mini-RNA containing the tetraloop, wobble-pair and loop E motifs of the central conserved region of potato spindle tuber viroid is processed into a minicircle. Nucleic Acids Res **31:**988-998.
90. **Flores R, Gas M-E, Molina-Serrano D, Nohales M-Á, Carbonell A, Gago S, De la Peña M, Daròs J-A.** 2009. Viroid replication: rolling-circles, enzymes and ribozymes. Viruses **1:**317-334.
91. **Owens RA, Baumstark T.** 2007. Structural differences within the loop E motif imply alternative mechanisms of viroid processing. RNA **13:**824-834.
92. **Flores R, Minoia S, Carbonell A, Gisel A, Delgado S, López-Carrasco A, Navarro B, Di Serio F.** 2015. Viroids, the simplest RNA replicons: how they manipulate their hosts for being propagated and how their hosts react for containing the infection. Virus research **209:**136-145.
93. **Gas M-E, Molina-Serrano D, Hernández C, Flores R, Daròs J-A.** 2008. Monomeric linear RNA of citrus exocortis viroid resulting from processing in vivo has 5'-phosphomonoester and 3'-hydroxyl termini: implications for the RNase and RNA ligase involved in replication. Journal of virology **82:**10321-10325.
94. **Dadami E, Boutla A, Vrettos N, Tzortzakaki S, Karakasilioti I, Kalantidis K.** 2013. DICER-LIKE 4 but not DICER-LIKE 2 may have a positive effect on potato spindle tuber viroid accumulation in Nicotiana benthamiana. Molecular plant **6:**232-234.
95. **Katsarou K, Mavrothalassiti E, Dermauw W, Van Leeuwen T, Kalantidis K.** 2016. Combined Activity of DCL2 and DCL3 Is Crucial in the Defense against Potato Spindle Tuber Viroid. PLOS Pathogens **12:**e1005936.
96. **Nohales MA, Flores R, Daros JA.** 2012. Viroid RNA redirects host DNA ligase 1 to act as an RNA ligase. Proc Natl Acad Sci U S A **109:**13805-13810.
97. **Katsarou K, Rao A, Tsagris M, Kalantidis K.** 2015. Infectious long non-coding RNAs. Biochimie **117:**37-47.
98. **Ding B, Kwon MO, Hammond R, Owens R.** 1997. Cell-to-cell movement of potato spindle tuber viroid. The plant journal **12:**931-936.
99. **Palukaitis P.** 1987. Potato spindle tuber viroid: investigation of the long-distance, intra-plant transport route. Virology **158:**239-241.
100. **Zhu Y, Qi Y, Xun Y, Owens R, Ding B.** 2002. Movement of potato spindle tuber viroid reveals regulatory points of phloem-mediated RNA traffic. Plant Physiology **130:**138-146.
101. **Ding B, Itaya A.** 2007. Viroid: a useful model for studying the basic principles of infection and RNA biology. Molecular plant-microbe interactions **20:**7-20.
102. **Jiang D, Wang M, Li S.** 2017. Functional analysis of a viroid RNA motif mediating cell-to-cell movement in Nicotiana benthamiana. Journal of General Virology **98:**121-125.
103. **Ding S-W.** 2010. RNA-based antiviral immunity. Nature Reviews Immunology **10:**632-644.
104. **Qi Y, Denli AM, Hannon GJ.** 2005. Biochemical specialization within Arabidopsis RNA silencing pathways. Molecular cell **19:**421-428.

105. **Axtell MJ.** 2013. Classification and comparison of small RNAs from plants. Annual review of plant biology **64:**137-159.
106. **Mallory A, Vaucheret H.** 2010. Form, function, and regulation of ARGONAUTE proteins. The Plant Cell **22:**3879-3889.
107. **Wassenegger M, Heimes S, Riedel L, Sänger HL.** 1994. RNA-directed de novo methylation of genomic sequences in plants. Cell **76:**567-576.
108. **Navarro B, Gisel A, Rodio ME, Delgado S, Flores R, Di Serio F.** 2012. Small RNAs containing the pathogenic determinant of a chloroplast-replicating viroid guide the degradation of a host mRNA as predicted by RNA silencing. The Plant Journal **70:**991-1003.
109. **Adkar-Purushothama CR, Brosseau C, Giguère T, Sano T, Moffett P, Perreault J-P.** 2015. Small RNA derived from the virulence modulating region of the potato spindle tuber viroid silences callose synthase genes of tomato plants. The Plant Cell **27:**2178-2194.
110. **Li W, Zhao Y, Liu C, Yao G, Wu S, Hou C, Zhang M, Wang D.** 2012. Callose deposition at plasmodesmata is a critical factor in restricting the cell-to-cell movement of Soybean mosaic virus. Plant cell reports **31:**905-916.
111. **Minoia S, Navarro B, Delgado S, Di Serio F, Flores R.** 2015. Viroid RNA turnover: characterization of the subgenomic RNAs of potato spindle tuber viroid accumulating in infected tissues provides insights into decay pathways operating in vivo. Nucleic Acids Res **43:**2313-2325.
112. **Botstein D, Fink GR.** 1988. Yeast: an experimental organism for modern biology. Science **240:**1439-1443.
113. **Dujon B.** 2010. Yeast evolutionary genomics. Nature Reviews Genetics **11:**512-524.
114. **Louis EJ.** 2016. Historical Evolution of Laboratory Strains of Saccharomyces cerevisiae. Cold Spring Harbor Protocols **2016:**pdb. top077750.
115. **Tong AHY, Evangelista M, Parsons AB, Xu H, Bader GD, Page N, Robinson M, Raghibizadeh S, Hogue CW, Bussey H.** 2001. Systematic genetic analysis with ordered arrays of yeast deletion mutants. Science **294:**2364-2368.
116. **Winzeler EA, Shoemaker DD, Astromoff A, Liang H, Anderson K, Andre B, Bangham R, Benito R, Boeke JD, Bussey H.** 1999. Functional characterization of the S. cerevisiae genome by gene deletion and parallel analysis. science **285:**901-906.
117. **Li Z, Vizeacoumar FJ, Bahr S, Li J, Warringer J, Vizeacoumar FS, Min R, VanderSluis B, Bellay J, DeVit M.** 2011. Systematic exploration of essential yeast gene function with temperature-sensitive mutants. Nature biotechnology **29:**361-367.
118. **Kuzmin E, Sharifpoor S, Baryshnikova A, Costanzo M, Myers CL, Andrews BJ, Boone C.** 2014. Synthetic genetic array analysis for global mapping of genetic networks in yeast. Yeast Genetics: Methods and Protocols**:**143-168.
119. **Nagy PD.** 2008. Yeast as a model host to explore plant virus-host interactions. Annu Rev Phytopathol **46:**217-242.
120. **Quadt R, Ishikawa M, Janda M, Ahlquist P.** 1995. Formation of brome mosaic virus RNA-dependent RNA polymerase in yeast requires coexpression of viral proteins and viral RNA. Proceedings of the National Academy of Sciences **92:**4892-4896.
121. **Janda M, Ahlquist P.** 1993. RNA-dependent replication, transcription, and persistence of brome mosaic virus RNA replicons in S. cerevisiae. Cell **72:**961-970.
122. **Ishikawa M, Díez J, Restrepo-Hartwig M, Ahlquist P.** 1997. Yeast mutations in multiple complementation groups inhibit brome mosaic virus RNA replication and transcription and perturb regulated expression of the viral polymerase-like gene. Proceedings of the National Academy of Sciences **94:**13810-13815.
123. **Ahlquist P, Noueiry AO, Lee W-M, Kushner DB, Dye BT.** 2003. Host factors in positive-strand RNA virus genome replication. Journal of virology **77:**8181-8186.

124. **Diaz A, Zhang J, Ollwerther A, Wang X, Ahlquist P.** 2015. Host ESCRT proteins are required for bromovirus RNA replication compartment assembly and function. PLoS Pathog **11:**e1004742.
125. **Nawaz-ul-Rehman MS, Prasanth KR, Baker J, Nagy PD.** 2013. Yeast screens for host factors in positive-strand RNA virus replication based on a library of temperature-sensitive mutants. Methods **59:**207-216.
126. **Prasanth KR, Kovalev N, de Castro Martín IF, Baker J, Nagy PD.** 2016. Screening a yeast library of temperature-sensitive mutants reveals a role for actin in tombusvirus RNA recombination. Virology **489:**233-242.
127. **Nagata K, Kawaguchi A, Naito T.** 2008. Host factors for replication and transcription of the influenza virus genome. Reviews in medical virology **18:**247-260.
128. **Delan-Forino C, Maurel MC, Torchet C.** 2011. Replication of avocado sunblotch viroid in the yeast Saccharomyces cerevisiae. J Virol **85:**3229-3238.
129. **Daròs J-A, Flores R.** 2004. Arabidopsis thaliana has the enzymatic machinery for replicating representative viroid species of the family Pospiviroidae. Proceedings of the National Academy of Sciences of the United States of America **101:**6792-6797.
130. **Phizicky E, Consaul S, Nehrke K, Abelson J.** 1992. Yeast tRNA ligase mutants are nonviable and accumulate tRNA splicing intermediates. Journal of Biological Chemistry **267:**4577-4582.
131. **Wang LK, SHUMAN S.** 2005. Structure–function analysis of yeast tRNA ligase. Rna **11:**966-975.
132. **Wu J, Hopper AK.** 2014. Healing for destruction: tRNA intron degradation in yeast is a two-step cytoplasmic process catalyzed by tRNA ligase Rlg1 and 5′-to-3′ exonuclease Xrn1. Genes & development **28:**1556-1561.
133. **Willer M, Rainey M, Pullen T, Stirling C.** 1999. The yeast CDC9 gene encodes both a nuclear and a mitochondrial form of DNA ligase I. Current biology **9:**1085-S1081.
134. **Nguyen HD, Becker J, Thu YM, Costanzo M, Koch EN, Smith S, Myung K, Myers CL, Boone C, Bielinsky A-K.** 2013. Unligated Okazaki fragments induce PCNA ubiquitination and a requirement for Rad59-dependent replication fork progression. PloS one **8:**e66379.
135. **Chanfreau G, Buckle M, Jacquier A.** 2000. Recognition of a conserved class of RNA tetraloops by Saccharomyces cerevisiae RNase III. Proceedings of the National Academy of Sciences **97:**3142-3147.
136. **Wu H, Yang PK, Butcher SE, Kang S, Chanfreau G, Feigon J.** 2001. A novel family of RNA tetraloop structure forms the recognition site for Saccharomyces cerevisiae RNase III. The EMBO journal **20:**7240-7249.
137. **Leslie E O.** 2004. Prebiotic chemistry and the origin of the RNA world. Critical reviews in biochemistry and molecular biology **39:**99-123.
138. **Kruger K, Grabowski PJ, Zaug AJ, Sands J, Gottschling DE, Cech TR.** 1982. Self-splicing RNA: autoexcision and autocyclization of the ribosomal RNA intervening sequence of Tetrahymena. cell **31:**147-157.
139. **Flores R, Gago-Zachert S, Serra P, Sanjuán R, Elena SF.** 2014. Viroids: survivors from the RNA world? Annual review of microbiology **68:**395-414.
140. **Margulis L.** 1993. Symbiosis in cell evolution: microbial communities in the Archean and Proterozoic eons.
141. **Latifi A, Bernard C, da Silva L, Andéol Y, Elleuch A, Risoul V, Vergne J, Maurel C.** 2016. Replication of Avocado Sunblotch Viroid in the Cyanobacterium Nostoc Sp. PCC 7120. J Plant Pathol Microbiol **7:**341.
142. **Gago S, Elena SF, Flores R, Sanjuán R.** 2009. Extremely high mutation rate of a hammerhead viroid. Science **323:**1308-1308.
143. **Wilusz JE, Sharp PA.** 2013. A circuitous route to noncoding RNA. Science **340:**440-441.

144. **Kapranov P, Willingham AT, Gingeras TR.** 2007. Genome-wide transcription and the implications for genomic organization. Nature Reviews Genetics **8:**413-423.
145. **Luco RF.** 2013. The non-coding genome: a universe in expansion for fine-tuning the coding world. Genome biology **14:**314.
146. **Lasda E, Parker R.** 2014. Circular RNAs: diversity of form and function. Rna **20:**1829-1842.
147. **Shimura H, Masuta C.** 2016. Plant subviral RNAs as a long noncoding RNA (lncRNA): Analogy with animal lncRNAs in host–virus interactions. Virus research **212:**25-29.
148. **Zhang Z, Qi S, Tang N, Zhang X, Chen S, Zhu P, Ma L, Cheng J, Xu Y, Lu M.** 2014. Discovery of replicating circular RNAs by RNA-seq and computational algorithms. PLoS Pathog **10:**e1004553.
149. **Fischer JW, Leung AK.** 2017. CircRNAs: a regulator of cellular stress. Critical reviews in biochemistry and molecular biology **52:**220-233.
150. **Hansen TB, Kjems J, Damgaard CK.** 2013. Circular RNA and miR-7 in cancer. Cancer research **73:**5609-5612.
151. **Roy G, Mercure S, Beuvon F, Perreault J-P.** 1997. Characterization of stable RNAs from the resected intestinal tissues of individuals with either Crohn's disease or ulcerative colitis. Biochemistry and cell biology **75:**789-794.
152. **Pogue AI, Hill JM, Lukiw WJ.** 2014. MicroRNA (miRNA): sequence and stability, viroid-like properties, and disease association in the CNS. Brain research **1584:**73-79.
153. **Diener TO.** 1974. Viroids: the smallest known agents of infectious disease. Annu Rev Microbiol **28:**23-39.
154. **Tsagris EM, Martinez de Alba AE, Gozmanova M, Kalantidis K.** 2008. Viroids. Cell Microbiol **10:**2168-2179.
155. **Flores R, Minoia S, Carbonell A, Gisel A, Delgado S, Lopez-Carrasco A, Navarro B, Di Serio F.** 2015. Viroids, the simplest RNA replicons: How they manipulate their hosts for being propagated and how their hosts react for containing the infection. Virus Res **209:**136-145.
156. **Owens RA, Hammond RW.** 2009. Viroid pathogenicity: one process, many faces. Viruses **1:**298-316.
157. **Gago S, Elena SF, Flores R, Sanjuan R.** 2009. Extremely high mutation rate of a hammerhead viroid. Science **323:**1308.
158. **Ding B.** 2010. Viroids: self-replicating, mobile, and fast-evolving noncoding regulatory RNAs. Wiley Interdiscip Rev RNA **1:**362-375.
159. **Navarro JA, Vera A, Flores R.** 2000. A chloroplastic RNA polymerase resistant to tagetitoxin is involved in replication of avocado sunblotch viroid. Virology **268:**218-225.
160. **Flores R, Serra P, Minoia S, Di Serio F, Navarro B.** 2012. Viroids: from genotype to phenotype just relying on RNA sequence and structural motifs. Front Microbiol **3:**217.
161. **Hutchins CJ, Rathjen PD, Forster AC, Symons RH.** 1986. Self-cleavage of plus and minus RNA transcripts of avocado sunblotch viroid. Nucleic Acids Res **14:**3627-3640.
162. **Daros JA, Marcos JF, Hernandez C, Flores R.** 1994. Replication of avocado sunblotch viroid: evidence for a symmetric pathway with two rolling circles and hammerhead ribozyme processing. Proc Natl Acad Sci U S A **91:**12813-12817.
163. **Flores R, Daros JA, Hernandez C.** 2000. Avsunviroidae family: viroids containing hammerhead ribozymes. Adv Virus Res **55:**271-323.
164. **Nohales MA, Molina-Serrano D, Flores R, Daros JA.** 2012. Involvement of the chloroplastic isoform of tRNA ligase in the replication of viroids belonging to the family Avsunviroidae. J Virol **86:**8269-8276.
165. **Goodman TC, Nagel L, Rappold W, Klotz G, Riesner D.** 1984. Viroid replication: equilibrium association constant and comparative activity measurements for the viroid-polymerase interaction. Nucleic Acids Res **12:**6231-6246.

166. **Tsagris M, Tabler M, Sanger HL.** 1987. Oligomeric potato spindle tuber viroid (PSTV) RNA does not process autocatalytically under conditions where other RNAs do. Virology **157:**227-231.
167. **Feldstein PA, Hu Y, Owens RA.** 1998. Precisely full length, circularizable, complementary RNA: an infectious form of potato spindle tuber viroid. Proc Natl Acad Sci U S A **95:**6560-6565.
168. **Flores R, Gas ME, Molina-Serrano D, Nohales MA, Carbonell A, Gago S, De la Pena M, Daros JA.** 2009. Viroid replication: rolling-circles, enzymes and ribozymes. Viruses **1:**317-334.
169. **Gross HJ, Domdey H, Lossow C, Jank P, Raba M, Alberty H, Sanger HL.** 1978. Nucleotide sequence and secondary structure of potato spindle tuber viroid. Nature **273:**203-208.
170. **Keese P, Symons RH.** 1985. Domains in viroids: evidence of intermolecular RNA rearrangements and their contribution to viroid evolution. Proc Natl Acad Sci U S A **82:**4582-4586.
171. **Tabler M, Sanger HL.** 1985. Infectivity studies on different potato spindle tuber viroid (PSTV) RNAs synthesized in vitro with the SP6 transcription system. EMBO J **4:**2191-2199.
172. **Henco K, Sanger HL, Riesner D.** 1979. Fine structure melting of viroids as studied by kinetic methods. Nucleic Acids Res **6:**3041-3059.
173. **Visvader JE, Forster AC, Symons RH.** 1985. Infectivity and in vitro mutagenesis of monomeric cDNA clones of citrus exocortis viroid indicates the site of processing of viroid precursors. Nucleic Acids Res **13:**5843-5856.
174. **Steger G, Tabler M, Bruggemann W, Colpan M, Klotz G, Sanger HL, Riesner D.** 1986. Structure of viroid replicative intermediates: physico-chemical studies on SP6 transcripts of cloned oligomeric potato spindle tuber viroid. Nucleic Acids Res **14:**9613-9630.
175. **Gast FU, Kempe D, Sanger HL.** 1998. The dimerization domain of potato spindle tuber viroid, a possible hallmark for infectious RNA. Biochemistry **37:**14098-14107.
176. **Steger G, Baumstark T, Morchen M, Tabler M, Tsagris M, Sanger HL, Riesner D.** 1992. Structural requirements for viroid processing by RNase T1. J Mol Biol **227:**719-737.
177. **Ding B.** 2009. The biology of viroid-host interactions. Annu Rev Phytopathol **47:**105-131.
178. **Johnston JR.** 1994. Molecular genetics of yeast: a practical approach. The Practical approach series (USA).
179. **Garcia-Ruiz H, Ahlquist P.** 2006. Inducible yeast system for Viral RNA recombination reveals requirement for an RNA replication signal on both parental RNAs. J Virol **80:**8316-8328.
180. **Quadt R, Ishikawa M, Janda M, Ahlquist P.** 1995. Formation of brome mosaic virus RNA-dependent RNA polymerase in yeast requires coexpression of viral proteins and viral RNA. Proc Natl Acad Sci U S A **92:**4892-4896.
181. **Chernyakov I, Whipple JM, Kotelawala L, Grayhack EJ, Phizicky EM.** 2008. Degradation of several hypomodified mature tRNA species in Saccharomyces cerevisiae is mediated by Met22 and the 5'-3' exonucleases Rat1 and Xrn1. Genes Dev **22:**1369-1380.
182. **Ishikawa M, Janda M, Krol MA, Ahlquist P.** 1997. In vivo DNA expression of functional brome mosaic virus RNA replicons in Saccharomyces cerevisiae. J Virol **71:**7781-7790.
183. **Köhrer K, Domdey H.** 1991. [27] Preparation of high molecular weight RNA. Methods in Enzymology **194:**398-405.
184. **Chevallet M, Luche S, Rabilloud T.** 2006. Silver staining of proteins in polyacrylamide gels. Nature Protocols **1:**1852-1858.
185. **Maderazo AB, Belk JP, He F, Jacobson A.** 2003. Nonsense-containing mRNAs that accumulate in the absence of a functional nonsense-mediated mRNA decay pathway are destabilized rapidly upon its restitution. Mol Cell Biol **23:**842-851.
186. **Semancik JS, Szychowski J.** 1983. Enhanced detection of viroid-RNA after selective divalent cation fractionation. Anal Biochem **135:**275-279.
187. **Gas ME, Molina-Serrano D, Hernandez C, Flores R, Daros JA.** 2008. Monomeric linear RNA of citrus exocortis viroid resulting from processing in vivo has 5'-phosphomonoester and 3'-

hydroxyl termini: implications for the RNase and RNA ligase involved in replication. J Virol **82:**10321-10325.
188. **Diener TO.** 2016. Viroids:"living fossils" of primordial RNAs? Biology direct **11:**15.
189. **Daros JA, Flores R.** 2004. Arabidopsis thaliana has the enzymatic machinery for replicating representative viroid species of the family Pospiviroidae. Proc Natl Acad Sci U S A **101:**6792-6797.
190. **Hecker R, Wang ZM, Steger G, Riesner D.** 1988. Analysis of RNA structures by temperature-gradient gel electrophoresis: viroid replication and processing. Gene **72:**59-74.
191. **Glow D, Nowacka M, Skowronek KJ, Bujnicki JM.** 2016. Sequence-specific endoribonucleases. Postepy Biochem **62:**303-314.
192. **Conrad C, Rauhut R.** 2002. Ribonuclease III: new sense from nuisance. The international journal of biochemistry & cell biology **34:**116-129.
193. **Gagnon J, Lavoie M, Catala M, Malenfant F, Elela SA.** 2015. Transcriptome wide annotation of eukaryotic RNase III reactivity and degradation signals. PLoS Genet **11:**e1005000.
194. **MacRae IJ, Zhou K, Doudna JA.** 2007. Structural determinants of RNA recognition and cleavage by Dicer. Nature structural & molecular biology **14:**934-940.
195. **Nagel R, Ares M.** 2000. Substrate recognition by a eukaryotic RNase III: the double-stranded RNA-binding domain of Rnt1p selectively binds RNA containing a 5'-AGNN-3'tetraloop. Rna **6:**1142-1156.
196. **Lamontagne B, Elela SA.** 2004. Evaluation of the RNA determinants for bacterial and yeast RNase III binding and cleavage. Journal of Biological Chemistry **279:**2231-2241.
197. **Wang Z, Hartman E, Roy K, Chanfreau G, Feigon J.** 2011. Structure of a yeast RNase III dsRBD complex with a noncanonical RNA substrate provides new insights into binding specificity of dsRBDs. Structure **19:**999-1010.
198. **Popow J, Schleiffer A, Martinez J.** 2012. Diversity and roles of (t) RNA ligases. Cellular and Molecular Life Sciences **69:**2657-2670.
199. **Abelson J, Trotta CR, Li H.** 1998. tRNA splicing. Journal of Biological Chemistry **273:**12685-12688.
200. **Hammann C, Steger G.** 2012. Viroid-specific small RNA in plant disease. RNA Biol **9:**809-819.
201. **Sambrook J, Russell DW.** 2006. Purification of nucleic acids by extraction with phenol: chloroform. Cold Spring Harbor Protocols **2006:**pdb. prot4455.
202. **Schmitz A, Riesner D.** 2006. Purification of nucleic acids by selective precipitation with polyethylene glycol 6000. Analytical biochemistry **354:**311-313.
203. **Chillón I, Marcia M, Legiewicz M, Liu F, Somarowthu S, Pyle AM.** 2015. Chapter One-Native Purification and Analysis of Long RNAs. Methods in enzymology **558:**3-37.
204. **Kumar N, Lin M, Zhao X, Ott S, Santana-Cruz I, Daugherty S, Rikihisa Y, Sadzewicz L, Tallon LJ, Fraser CM.** 2016. Efficient Enrichment of Bacterial mRNA from Host-Bacteria Total RNA Samples. Scientific Reports **6**.
205. **Dickman MJ, Hornby DP.** 2006. Enrichment and analysis of RNA centered on ion pair reverse phase methodology. Rna **12:**691-696.
206. **Sentenac A, Hall B.** 1982. Yeast nuclear RNA polymerases and their role in transcription. Cold Spring Harbor Monograph Archive **11:**561-606.
207. **Lin R, Newman A, Cheng S-C, Abelson J.** 1985. Yeast mRNA splicing in vitro. Journal of Biological Chemistry **260:**14780-14792.
208. **Kovalev N, Pogany J, Nagy PD.** 2014. Template role of double-stranded RNA in tombusvirus replication. Journal of virology **88:**5638-5651.
209. **Umen JG, Guthrie C.** 1995. A novel role for a U5 snRNP protein in 3'splice site selection. Genes & Development **9:**855-868.

210. **Ding Y, Kwok CK, Tang Y, Bevilacqua PC, Assmann SM.** 2015. Genome-wide profiling of in vivo RNA structure at single-nucleotide resolution using structure-seq. Nat Protocols **10:**1050-1066.
211. **Spitale RC, Flynn RA, Zhang QC, Crisalli P, Lee B, Jung J-W, Kuchelmeister HY, Batista PJ, Torre EA, Kool ET.** 2015. Structural imprints in vivo decode RNA regulatory mechanisms. Nature **519:**486-490.
212. **Nagy PD, Pogany J, Lin J-Y.** 2014. How yeast can be used as a genetic platform to explore virus–host interactions: from 'omics' to functional studies. Trends in microbiology **22:**309-316.
213. **Bernstein DA, Vyas VK, Fink GR.** 2012. Genes come and go: the evolutionarily plastic path of budding yeast RNase III enzymes. RNA biology **9:**1123-1128.
214. **Chanfreau G, Rotondo G, Legrain P, Jacquier A.** 1998. Processing of a dicistronic small nucleolar RNA precursor by the RNA endonuclease Rnt1. The EMBO Journal **17:**3726-3737.
215. **Minoia S, Navarro B, Delgado S, Di Serio F, Flores R.** 2015. Viroid RNA turnover: characterization of the subgenomic RNAs of potato spindle tuber viroid accumulating in infected tissues provides insights into decay pathways operating in vivo. Nucleic acids research**:**gkv034.
216. **EGECIOGLU DE, HENRAS AK, CHANFREAU GF.** 2006. Contributions of Trf4p-and Trf5p-dependent polyadenylation to the processing and degradative functions of the yeast nuclear exosome. Rna **12:**26-32.
217. **Shen MW, Fang F, Sandmeyer S, Da Silva NA.** 2012. Development and characterization of a vector set with regulated promoters for systematic metabolic engineering in Saccharomyces cerevisiae. Yeast **29:**495-503.
218. **Brachmann CB, Davies A, Cost GJ, Caputo E, Li J, Hieter P, Boeke JD.** 1998. Designer deletion strains derived from Saccharomyces cerevisiae S288C: a useful set of strains and plasmids for PCR-mediated gene disruption and other applications. YEAST-CHICHESTER- **14:**115-132.
219. **Fang F, Salmon K, Shen MW, Aeling KA, Ito E, Irwin B, Tran UPC, Hatfield G, Da Silva NA, Sandmeyer S.** 2011. A vector set for systematic metabolic engineering in Saccharomyces cerevisiae. Yeast **28:**123-136.